STATIC ANALYSIS OF PLANE COUPLED SHEAR WALLS

STATIC ANALYSIS OF PLANE COUPLED SHEAR WALLS

BY

I. A. S. ELKHOLY

A THESIS

SUBMITTED TO THE SCHOOL OF GRADUATE STUDIES

IN PARTIAL FULFILMENT OF THE REQUIREMENTS

FOR THE DEGREE

MASTER OF ENGINEERING

McMASTER UNIVERSITY

December 1971

MASTER OF ENGINEERING (1972) McMASTER UNIVERSITY

Civil Engineering and Engineering Mechanics Hamilton, Ontario.

TITLE: STATIC ANALYSIS OF PLANE COUPLED SHEAR WALLS

AUTHOR: Ismail Abdel Salam Elkholy, B.Sc.,
Cairo University, Egypt, 1968.

SUPERVISOR: Dr. H. Robinson

NUMBER OF PAGES: xv, 158

SCOPE AND CONTENTS:

The aim of this thesis is to present a finite difference method, for analysing coupled shear walls with constant or variable cross-section, resting on rigid or elastic foundations and with elastic or inelastic connecting beams. It is also intended to compare the finite difference method with the continuous connection method, which can be developed using Rosman's approach or Newmark's concept for analysing composite beams or the energy approach, and with the finite element method. An analysis of coupled shear walls with multiple piers is presented.

ACKNOWLEDGMENTS

This thesis was prepared under the direction of Dr. H. Robinson, Associate Professor of Civil Engineering. The author wishes to express his gratitude and sincere appreciation for the guidance and helpful advice received during every stage of the progress of the thesis. The author also wishes to express his thanks to Dr. W. K. Tso, Dr. A. C. Heidebrecht and Dr. M. Levinson for their valuable suggestions during this work.

The numerical work was carried out using the CDC 6400 Computer system of McMaster University.

I am very grateful to the National Research Council of Canada and to the Department of Civil Engineering and Engineering Mechanics, McMaster University for the financial assistance for the present work.

My thanks are due to Mrs. Anne MacIntosh who made this thesis presentable.

TABLE OF CONTENTS

LIST OF FIGURES

LIST OF TABLES

LIST OF REFERENCES

1. SIESS, C. P., VIEST, I. M., and NEWMARK, N. M., "Small-scale Tests of Shear Connectors and Composite T-Beams", Bulletin No. 396, Experiment Station, University of Illinois, Urbana, Illinois, 1952.

2. STÜSSI, F., "Profilträger, Kambiniert mit Beton Oder Eisenbeton, auf Beigung Beanspruch", Final Report, First Congress (Paris), International Association of Bridge and Structural Engineering, pp. 579 - 595, 1932.

3. STÜSSI, F., "Zusammengesetzte Vollwandträger", Publications, International Association of Bridge and Structural Engineering, Vol. VIII, pp. 249 - 269, 1947.

4. THIRUVENGADAM, T. R., "A Method for Inelastic Analysis of Single-span Composite Beams", Ph.D. Thesis, University of Illinois, Urbana, Illinois, 1969.

5. BECK, H.,"Contribution to the Analysis of Coupled Shear Walls", ACI Journal, pp. 1055-1070, 1962.

6. ROSMAN, R., "Approximate Analysis of Shear Walls Subjected to Lateral Loads", ACI Journal, pp. 717-733, 1964.

7. TRAUM, E., "Multistorey Pierced Shear Walls of Variable Cross-section", Proceeding of a Symposium on Tall Buildings, University of Southampton, April 1966, Pergamon Press, pp. 333-356.

8. COULL, A., PURI, R. D., "Analysis of Coupled Shear Walls of Variable Cross-section", Build. Science Vol. 2, pp. 313 - 320, Pergamon Press 1968.

9. PISANTY, A., TRAUM, E., "Simplified Analysis of Coupled Shear Walls of Variable Cross-Sections", Build. Science Vol. 5, pp. 11 - 20, Pergamon Press, 1970.

10. PAULAY, T., "The Coupling of Shear Walls", Vol. I and II, Ph.D. Thesis, University of Canterbury, at Christchurch, New Zealand, 1969.

11. GIRIJAVALLABHAN, C. V., "Analysis of Shear Walls with Openings", Journal of the Structural Division, ASCE, Vol. 95, No. ST10, October, 1969, pp. 2093 - 2103.

12. GURFINKEL, German, "Simple Method of Analysis of Vierendeel Structures", Journal of the Structural Division, ASCE, Vol. 93, No. ST3, Proc. Paper 5296. June, 1967, pp. 273 - 285.

13. COULL, A., "Interaction of Coupled Shear Walls with Elastic Foundations", ACI Journal, Proceedings V.68, No. 1, June 1971, pp. 456 - 461.

14. ZIENKIEWICZ, O.C., "The Finite Element Method", McGraw-Hill, 1967.

15. HOFF, N. J., "The Analysis of Structures", John Wiley & Sons, 1956.

16. BROWN, E. H., "Structural Analysis, Volume"1", John Wiley & Sons, 1967.

CHAPTER 1

INTRODUCTION

1.1 General

In multistorey buildings, particularly of reinforced concrete, shear walls are one of the more economical means of providing lateral stability against wind or earthquake loading. Such walls are often pierced by vertical bands of openings for doors, windows and corridors, yielding highly redundant structures from the point of view of stress analysis.

Shear walls with uniform cross-section over the full height of the building have been treated by assuming that the uniformly spaced discrete set of connecting beams may be replaced by an equivalent continuous medium. By assuming that the cross-beams deflect with a point of contraflexure at mid-span, but do not deform axially, the behaviour of the system may be expressed as a single second order differential equation, enabling a general closed solution of the problem to be obtained.

Very often shear walls, pierced by one or more rows of openings, have an abrupt change of cross-section at one or several levels. The horizontal loading, to which such walls

are subjected, may also vary along the height of the building. This problem has been treated using the continuous connection method (7, 8, 9)*. Also, coupled shear walls with elastic foundations have been treated by Coull (13).

The aim of this thesis is to present a finite difference method, for analysing coupled shear walls with constant or variable cross-section, resting on rigid or elastic foundations and with elastic or inelastic connecting beams. It is also intended to compare the finite difference method with the continuous connection method, which can be developed using Rosman's (6) approach or Newmark's (1) concept for analysing composite beams or the energy approach, and with the finite element method.

1.2 Object and Scope

The object of this study is to treat the problem of coupled shear walls, with constant cross-section and with variable cross-section resting on rigid or elastic foundations, by:

1. A continuous solution based on the concept of Newmark's (1) solution for composite beams. This yields the well-known governing differential equation for coupled shear walls.

2. A finite difference solution based on the concept of Stussi's (2, 3) solution for composite beams. The advantage of this method, over the continuous connection method, is that

---

* Number in parantheses refers to entries in the list of references.

unusual configurations of the coupled shear walls can be analysed. This method treats the coupled shear walls as two piers connected together by discrete connecting beams.

3. Using the energy method. A solution of the problem was achieved. The principles of the minimum of the total potential furnishes all the necessary and sufficient conditions of equilibrium in the form of differential equations as well as boundary conditions.

4. The finite element method. The coupled shear wall was approximated as a plane stress boundary value problem and solved using the finite element method. Different configurations of moderately high coupled shear walls were treated by the finite element and the finite difference methods. The ratios between the height of the shear walls, the width of the piers and the span and stiffness of the connecting beams were varied to study the agreement between the two methods.

An approximate analysis of coupled shear walls with multiple piers, assuming that the cross-beams deflect with a point of contraflexure at mid-span, is presented here.

1.3 Notation

A_1, A_2, A_{j1}, A_{j2}	cross-sectional area of piers 1 and 2 in Zone (j)
d_1, d_2, d_{j1}, d_{j2}	depth of piers 1 and 2 in Zone (j)
d_b, b, b'	depth, span and width of the connecting beam
h, $h_{(i)}$, h_j	storey height
H_j	height of Zone (j)
H	height of the coupled shear wall
I_1, I_2, I_{j1}, I_{j2}	moments of inertia of piers 1 and 2 in Zone (j)
γ, γ_i	vertical displacement between the two ends of the connecting beams (slip)
ε_1, ε_2	bottom fiber strain and top fiber strain at the point of contraflexure
ε	strain
c_{j1}, c_{j2}	distance between the centroidal axis of piers 1 and 2 and the point of contraflexure
ℓ, ℓ_j	distance between the centroids of the two piers $= c_{j1} + c_{j2}$
I_p, A_b, A_b^*	moment of inertia, area and reduced cross-sectional area of the connecting beam
n	number of storeys
E_1, E_2, E_{j1}, E_{j2}	modulus of elasticity of piers 1 and 2
q, q_1, q_2	shear force intensity in substitute connecting medium
Q, Q_i	shear force in a connecting beam i

M_1, M_2	bending moments in the piers
T, $T_{(j)}$, $T_{(i)}$	axial force in the piers
M	external bending moment at an arbitrary cross-section
ϕ	curvature of the piers
k_i	modulus of the connecting beams
αH	interaction coefficient
u_1, u_2, u_{j1}, u_{j2}	extensional deformation for piers 1 and 2 in Zone (j)
v_1, v_2	horizontal deformation for Zone (1) and Zone (2)
M_0, Q_0, N_0	external forces acting at the free end of a prismatic coupled shear wall
M_2, Q_2, N_2, Q_1, N_1	external forces acting on Zone (1) and Zone (2) at both ends

CHAPTER 2

PRISMATIC COUPLED SHEAR WALL

2.1 General

A similarity was found between the equations governing the behaviour of coupled shear walls and composite beams. Two solutions are presented:

1) A continuous solution based on Newmark's (1) solution for composite beams; which yields the same differential equation as that for the coupled shear walls.

2) A finite difference solution based on Stussi's (2, 3) solution for composite beams. This method yields the same forces and deformations as the continuous solution for the typical shear wall treated by the continuous method. The advantage of this method is that it can take into account different configurations of the shear wall, as will be clear later.

Fig. (2.1) shows the shear wall schemes with single or double bands of openings.

2.2 Continuous Solution

2.2.1 Basic Assumptions

1) The upper end beam has one half the cross-section and one half the moment of inertia of an interior connecting beam.

2) The connecting beams are replaced by continuous elastic lamella.

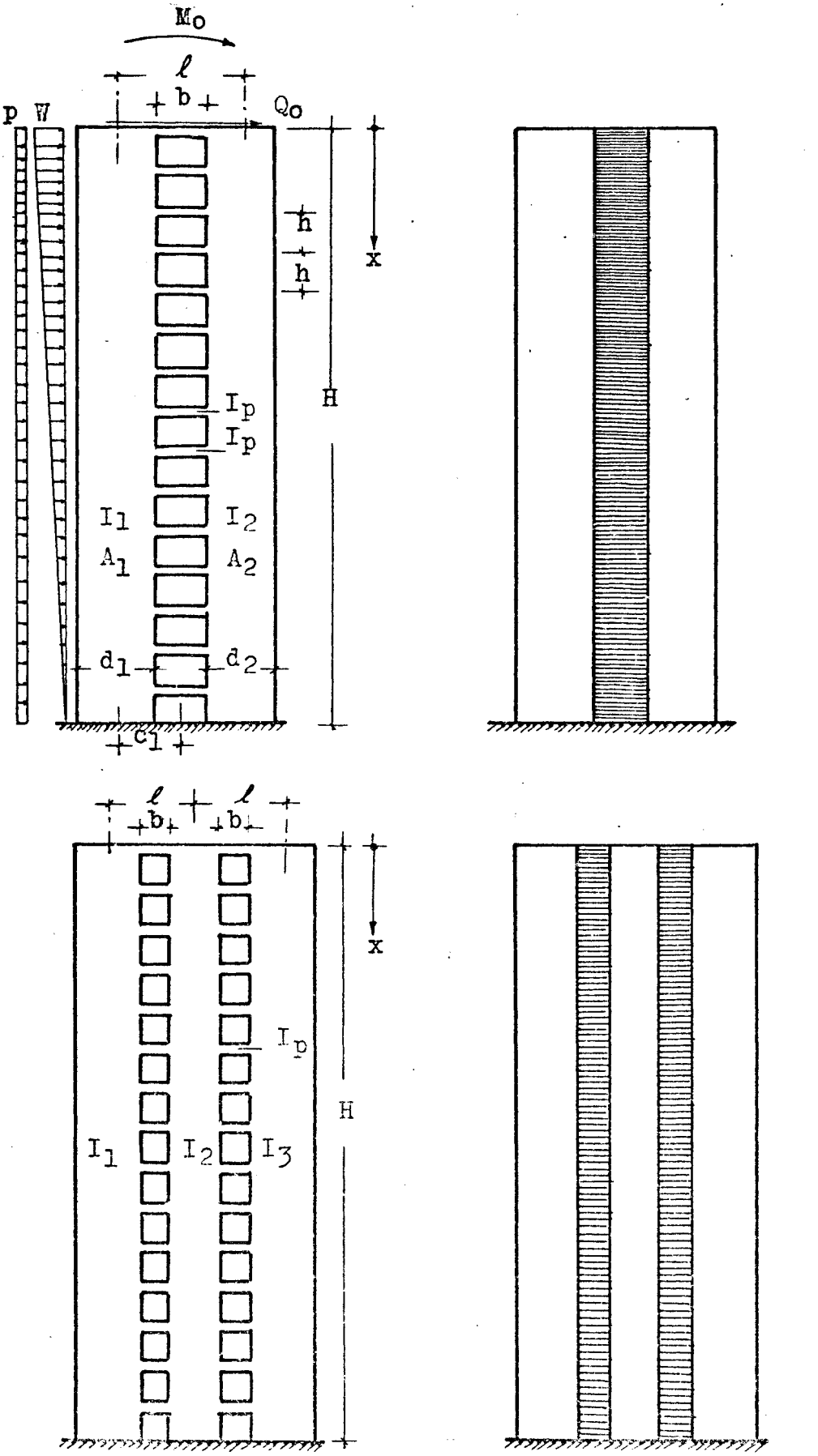

a) Real Structure

b) Substitute System, Continucus Method

FIG. 2.1 SHEAR WALL SCHEMES

3) The points of contraflexure are assumed to be at the mid-span of the connecting beams, since the cross-sections of the pers are much greater than the cross-sections of the connecting beams.

4) The values H, b, ℓ, A_1, I_1, A_2, I_2 and I_p are constant throughout the whole height H.

5) The two piers have equal curvatures at any section.

2.2.2 Formulation of the Problem for One Band of Openings

The equilibrium and compatibility conditions can be written as, Fig. (2.2),

$$M(x) = M_1 + M_2 + T.\ell \qquad (2.1)$$

$$h_{(i)} + \int_{h_{(i)}} \varepsilon_2 \, dx + \gamma_{i+1} = \gamma_i + h_{(i)} + \int_{h_{(i)}} \varepsilon_1 \, dx \qquad (2.2.1)$$

i.e. $$\gamma_{i+1} - \gamma_i = \int_{h_{(i)}} (\varepsilon_1 - \varepsilon_2) \, dx \qquad (2.2.2)$$

i.e. $$\frac{d\gamma}{dx} = \varepsilon_1 - \varepsilon_2 \qquad (2.2.3)$$ ✓

If the amount of slip (γ) permitted by the connecting beams is directly proportional to the load transmitted,

i.e. $$Q = k.\gamma \qquad (2.3.1)$$

also $$Q = q.h \qquad (2.3.2)$$

where k is the modulus of the connecting beams, the force required to produce unit displacement between the two ends of the connecting beam.

The displacement (γ) can be found as,

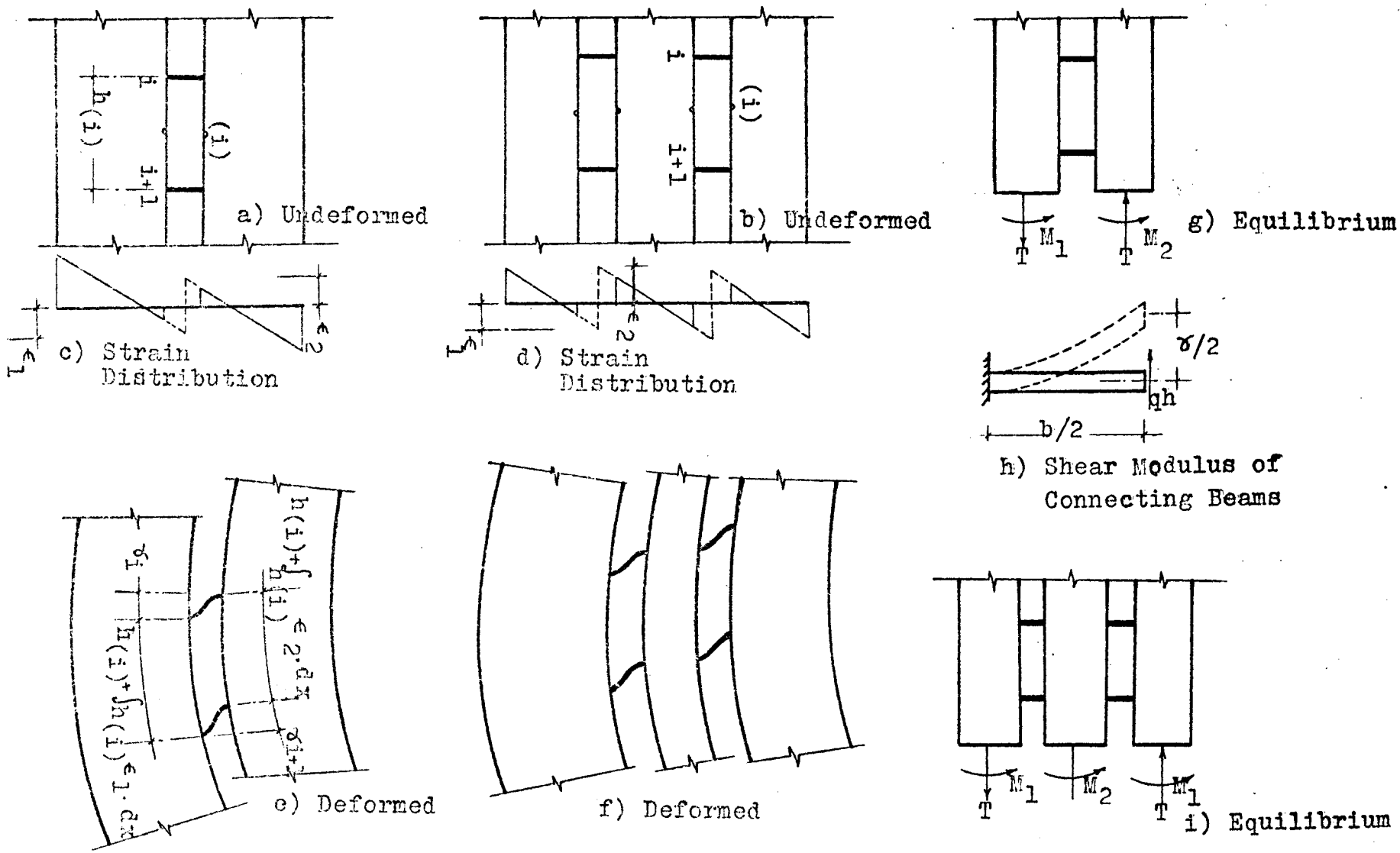

FIG. 2.2 EQUILIBRIUM AND COMPATIBILITY CONDITIONS

$$\gamma = \left(\frac{b^3}{12EI_p} + \frac{b}{GA_b^*}\right) Q \qquad (2.3.3)$$

Substitution of Eqs. (2.3.1), (2.3.2) in Eq. (2.3.3) yields

$$\gamma = \left(\frac{hb^3}{12EI_p} + \frac{hb}{GA_b^*}\right) q \qquad (2.4.1)$$

Differentiating once gives

$$\frac{d\gamma}{dx} = \left(\frac{hb^3}{12EI_p} + \frac{hb}{GA_b^*}\right) \frac{d^2T}{dx^2} \qquad (2.4.2)$$

The strains ε_1 and ε_2 can be found as

$$\varepsilon_1 = + \frac{T}{E_1 A_1} - \frac{M_1 c_1}{E_1 I_1} \qquad (2.5.1)$$

$$\varepsilon_2 = - \frac{T}{E_2 A_2} + \frac{M_2 c_2}{E_2 I_2} \qquad (2.5.2)$$

The assumption of equal curvatures of the two piers yields

$$\frac{M_1}{E_1 I_1} = \frac{M_2}{E_2 I_2} = \frac{M_1 + M_2}{E_1 I_1 + E_2 I_2} \qquad (2.6.1)$$

Substitution of Eq. (2.1) in Eq. (2.6.1) yields

$$\frac{M_1}{E_1 I_1} = \frac{M_2}{E_2 I_2} = \frac{M - T\,\ell}{E_1 I_1 + E_2 I_2} \qquad (2.6.2)$$

Substitution of Eqs. (2.4.2), (2.5.1), (2.5.2), (2.6.2) in Eq. (2.2.3) yields

$$\frac{d^2T}{dx^2} - \acute{\alpha}\ T = -R.M(x) \qquad (2.7.1)$$

where

$$\acute{\alpha} = \left[\frac{1}{E_1 A_1} + \frac{1}{E_2 A_2} + \frac{\ell^2}{EI_1 + EI_2}\right] / \left[\frac{hb^3}{12EI_p} + \frac{hb}{GA_b^*}\right] \qquad (2.7.2)$$

$$R = \left[\frac{\ell}{E_1 I_1 + E_2 I_2} \right] / \left[\frac{hb^3}{12EI_p} + \frac{hb}{GA_b^*} \right] \qquad (2.7.3)$$

or

$$\acute{\alpha} = \frac{k}{h} \frac{\overline{EI}}{\overline{EA}.\ \Sigma EI} \qquad (2.7.4)$$

$$R = \frac{k}{h} \frac{\ell}{\Sigma EI} \qquad (2.7.5)$$

$$k = 1 / \left[\frac{b^3}{12EI_p} + \frac{b}{GA_b^*} \right] \qquad (2.7.6)$$

$$\Sigma EI = E_1 I_1 + E_2 I_2 \qquad (2.7.7)$$

$$\frac{1}{\overline{EA}} = \frac{1}{E_1 A_1} + \frac{1}{E_2 A_2} \qquad (2.7.8)$$

$$\overline{EI} = \Sigma EI + \overline{EI}.\ell^2 \qquad (2.7.9)$$

$$\frac{1}{c} = \frac{k}{h} \frac{\overline{EI}}{\overline{EA}.\ \Sigma EI} \frac{H^2}{\pi^2} \qquad (2.7.10)$$

Eq. (2.7.1) is the governing differential equation for a coupled shear wall.

If the external applied bending moment, M(x), is expressed as

$$M(x) = + \frac{px^2}{2} + Q_0 x + M_0 + \frac{wx^2}{2} - \frac{wx^3}{6H} \qquad (2.8)$$

The solution of the differential equation for the axial forces in the piers and shearing forces in the connecting medium can be found as

$$T(x) = c_1 \cosh x\sqrt{\alpha} + c_2 \sinh x\sqrt{\alpha} + \frac{R}{\alpha} \left(\frac{px^2}{2} + Q_0 x + M_0 + \frac{wx^2}{2} - \frac{wx^3}{6H} \right) + \frac{R}{\alpha^2} \left(p + w - \frac{wx}{H} \right) \qquad (2.9.1)$$

$$q(x) = c_1 \sqrt{\alpha} \sinh x\sqrt{\alpha} + c_2 \sqrt{\alpha} \cosh x\sqrt{\alpha} + \frac{R}{\alpha} \left(px + Q_0 + wx - \frac{wx^2}{2H} \right) - \frac{R}{\alpha^2} \frac{w}{H} \qquad (2.9.2)$$

The boundary conditions are

at x = 0 $\quad T = 0$ (2.9.3)

at x = H $\quad q = 0$ (2.9.4)

The internal bending moments of the piers can be determined from

$$M_i(x) = E_i I_i \left[\frac{M(x) - T(x).\ell}{\Sigma EI}\right] \qquad i = 1,2 \qquad (2.10)$$

where the curvature of the piers is

$$\phi(x) = \frac{M(x) - T(x).\ell}{\Sigma EI} \qquad (2.11)$$

The deflection can be determined by numerical integration of the curvature.

2.2.3 Formulation of the Problem for Two Bands of Openings

The equilibrium and compatibility conditions are, Fig. (2.2),

$$M(x) = 2M_1 + M_2 + T_1.2\ell \qquad (2.12.1)$$

$$\frac{d\gamma}{dx} = \varepsilon_1 - \varepsilon_2 \qquad (2.12.2)$$

$$\frac{M_1}{E_1 I_1} = \frac{M_2}{E_2 I_2} = \frac{M - 2T\ell}{2E_1 I_1 + E_2 I_2} \qquad (2.12.3)$$

The strains can be found as

$$\varepsilon_1 = + \frac{T_1}{E_1 A_1} - \frac{M_1 c}{E_1 I_1} \qquad (2.13.1)$$

$$\varepsilon_2 = + \frac{M_2 c}{E_2 I_2} \qquad (2.13.2)$$

Hence, the governing differential equation may be found as

$$\frac{d^2 T_1}{dx^2} - \alpha T = - R M(x) \qquad (2.14.1)$$

where

$$\acute{\alpha} = \frac{k}{h}\left(\frac{1}{E_1 A_1} + \frac{2\ell^2}{\Sigma EI}\right) \qquad (2.14.2)$$

$$R = \frac{k}{h}\,\frac{2\ell}{\Sigma EI} \qquad (2.14.3)$$

$$\Sigma EI = 2E_1 I_1 + E_2 I_2 \qquad (2.14.4)$$

The differential equation has similar form to that obtained for the coupled shear walls with single band of openings.

2.3 Finite Difference Solution

2.3.1 Basic Assumptions

1) The two piers deflect equally at all points along their lengths; they thus have equal curvature at all points.

2) The points of contraflexure in the connecting beams are assumed to be at midspan.

3) The shear connection between the two piers is provided by connecting beams placed at discrete points along the span of the beam.

4) The strain distribution in the two piers is linear but in general is not continuous across the whole width of the structure.

2.3.2 Formulation of the problem for One Band of Openings

Consider a section of the shear wall in the vicinity of two connecting beams identified as the i th and i + 1 th connecting beams. The space between the connecting beams is identified as the (i) th space of magnitude $h_{(i)}$, Fig. (2.3).

The equilibrium and compatibility conditions are:

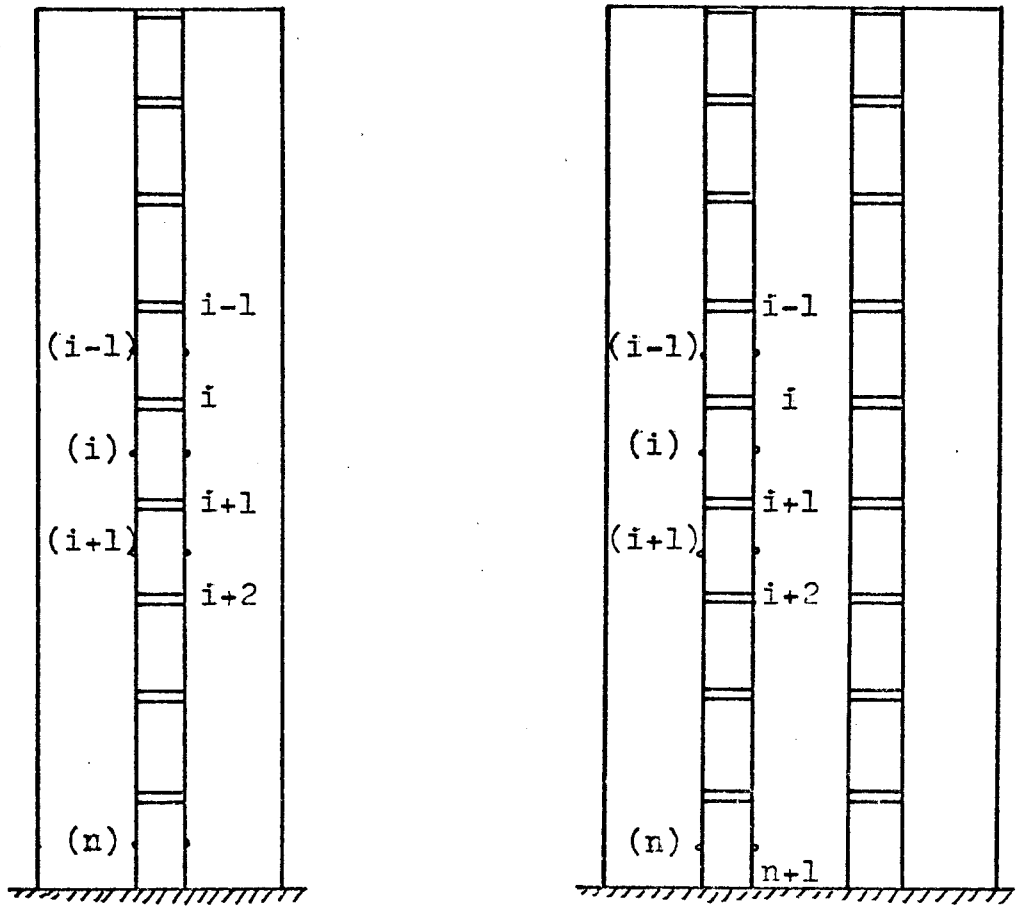

a) Substiute System of Actual Structure,
Finite Difference Method

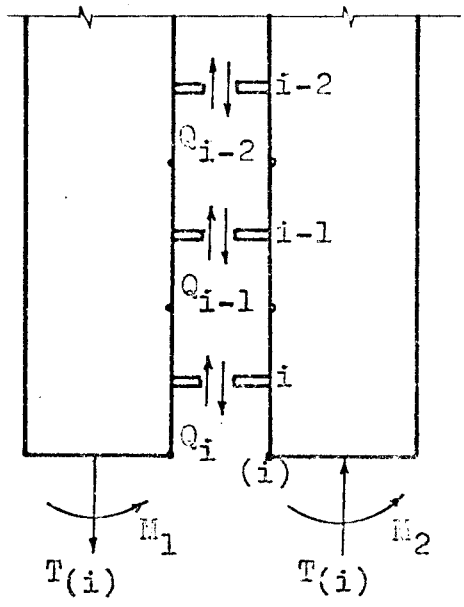

b) Free Body Diagram

FIG. 2.3 FINITE DIFFERENCE METHOD

$$M_{(i)} = M_1(i) + M_2(i) + T_{(i)} \cdot \ell \tag{2.15.1}$$

$$\gamma_{i+1} - \gamma_i = \int_{h(i)} (\varepsilon_1 - \varepsilon_2)\, dx \tag{2.15.2}$$

$$\frac{M_1(i)}{E_1 I_1} = \frac{M_2(i)}{E_2 I_2} = \frac{M(i) - T(i) \cdot \ell}{\Sigma EI} \tag{2.15.3}$$

also

$$Q_i = k_i \gamma_i \tag{2.15.4}$$

The strains ε_1 and ε_2 are

$$\varepsilon_1 = + \frac{T(i)}{E_1 A_1} - \frac{M_1(i) \cdot c_1}{E_1 I_1} \tag{2.16.1}$$

$$\varepsilon_2 = - \frac{T(i)}{E_2 A_2} + \frac{M_2(i) \cdot c_2}{E_2 I_2} \tag{2.16.2}$$

The equilibrium of horizontal forces gives

$$Q_i = T_{(i)} - T_{(i-1)} \tag{2.17}$$

Substitution of Eqs. (2.15.4), (2.17) in Eq. (2.15.2) yields

$$\frac{Q_{i+1}}{k_{i+1}} - \frac{Q_i}{k_i} = \int_{h(i)} (\varepsilon_1 - \varepsilon_2)\, dx \tag{2.18}$$

$$\frac{T_{(i-1)}}{k_i} - \left(\frac{1}{k_i} + \frac{1}{k_{i+1}}\right) T_{(i)} + \frac{T_{(i+1)}}{k_{i+1}} = \int_{h(i)} (\varepsilon_1 - \varepsilon_2)\, dx \tag{2.18.1}$$

Substitution of Eqs. (2.16.1), (2.16.2) in Eq. (2.18.1) yields

$$\frac{T_{(i-1)}}{k_i} - \left(\frac{1}{k_i} + \frac{1}{k_{i+1}} + \psi_{(i)} \cdot h_{(i)}\right) T_{(i)} + \frac{T_{(i+1)}}{k_{i+1}} = -\int_{h(i)} \zeta\, M\, dx \tag{2.18.2}$$

where

$$k_i = 1 \Big/ \left[\frac{b^3}{12EI_p} + \frac{b}{GA_b^*}\right]_i \qquad (2.18.3)$$

$$\psi_{(i)} = \left[\frac{1}{E_1A_1} + \frac{1}{E_2A_2} + \frac{\ell^2}{\Sigma EI}\right]_{(i)}$$

$$= \left[\frac{\overline{EI}}{\overline{EA}.\ \Sigma EI}\right]_{(i)} \qquad (2.18.4)$$

$$\zeta = \frac{\ell}{\Sigma EI} \qquad (2.18.5)$$

Equation (2.18.2) represents a typical equation for panel length (i). For a coupled shear wall having n panels, n storeys, there are n such equations resulting in a set of n simultaneous equations. The n <u>th</u> equation is different. Assuming a connecting beam at the fixed end denoted as n+1, equation n for panel (n) will be

$$\frac{T(n-1)}{k_n} - \left(\frac{1}{k_n}\right) T_{(n)} = \int_{h(n)} (\varepsilon_1 - \varepsilon_2)\, dx \qquad (2.19.1)$$

or

$$\frac{T_{(n-1)}}{k_n} - \left(\frac{1}{k_n} + \psi_{(n)} h_{(n)}\right) T_{(n)} = -\int_{h(n)} \zeta\, M\, dx \qquad (2.19.2)$$

as $Q_{n+1} = 0$

Now, the n simultaneous equations are:

$$-\left(\frac{1}{k_1} + \frac{1}{k_2} + \psi_{(1)}\, h_{(1)}\right) T_{(1)} + \frac{T_{(2)}}{k_2} = -\int_{h_{(1)}} \zeta\, M\, dx \ \ldots.$$

$$\frac{T_{(1)}}{k_2} - \left(\frac{1}{k_2} + \frac{1}{k_3} + \psi_{(2)}\, h_{(2)}\right) T_{(2)} + \frac{T_{(3)}}{k_3} = -\int_{h_{(2)}} \zeta\, M\, dx$$

....

$$\frac{T_{(i-1)}}{k_1} - \left(\frac{1}{k_1} + \frac{1}{k_{i+1}} + \psi_{(i)}\, h_{(i)}\right) T_{(i)} + \frac{T_{(i+1)}}{k_{i+1}} = -\int_{h_{(i)}} \zeta\, M\, dx$$

.... (2.20)

$$\frac{T(n-1)}{k_n} - \left(\frac{1}{k_n} + \psi_{(n)}\, h_{(n)}\right) T_{(n)} = -\int_{h_{(n)}} \zeta\, M\, dx$$

The boundary conditions are

$$F_{(0)} = 0 \quad \& \quad Q_{n+1} = 0 \tag{2.20.1}$$

This can be written in matrix notation as

$$[B]\,\{T\} = \{A\} \tag{2.20.2}$$

[B] is a symetric band matrix with half band width two, these terms are:

$$B_{11} = -\left(\frac{1}{k_1} + \frac{1}{k_2} + \psi_{(1)}\, h_{(1)}\right) \;\&\; B_{n(n-1)} = \frac{1}{k_n}$$

$$B_{12} = \frac{1}{k_2} \;\&\; B_{nn} = -\left(\frac{1}{k_n} + \psi_{(n)}\, h_{(n)}\right)$$

for $1 < i < n$

$$B_{i(i-1)} = \frac{1}{k_i}$$

$$B_{ii} = -\left(\frac{1}{k_i} + \frac{1}{k_{i+1}} + \psi_{(i)}\, h_{(i)}\right) \tag{2.20.3}$$

$$B_{i(i+1)} = \frac{1}{k_{i+1}}$$

all other $B_{ij} = 0$

{T} is a vector whose i th term is $T_{(i)}$

{A} is a vector whose i th term, $A_{(i)}$, is

$$A_{(i)} = -\int_{h_{(i)}} \zeta\, M\, dx$$

Having obtained the axial forces in the piers by solving the n simultaneous equations, the internal bending moments in the piers, the shearing force in the connecting beams and the strain distribution can be obtained from Eqs. (2.15.3), 2.17), (2.16.1),(2.16.2) respectively. The deflection can be obtained by numerical integration of the curvature.

2.3.3 Formulation of the Problem for Two Bands of Openings

Proceeding the same way, as in the formulation of coupled shear wall with one band of openings, it can be shown that for panel (i) the finite difference equation is

$$\frac{T_{(i-1)}}{k_i} - \left(\frac{1}{k_i} + \frac{1}{k_{i+1}} + \psi_{(i)}\, h_{(i)}\right) T_{(i)} + \frac{T_{(i+1)}}{k_{i+1}} = - \int_{h_{(i)}} \zeta\, M\, dx \qquad (2.21)$$

where $$\psi_{(i)} = \left[\frac{1}{E_1 A_1} + \frac{2\ell^2}{\Sigma EI}\right]_{(i)} \qquad (2.21.1)$$

$$\zeta = \frac{2\ell}{\Sigma EI} \qquad (2.21.2)$$

This gives n simultaneous equations which can be solved for the axial forces in the piers. The internal forces and deflections can be determined as before.

2.3.4 Coupled Shear Wall with an "Infinitely" Rigid Diaphragm at the Top

This situation arises when two shear walls are interconnected by an "infinitely" rigid diaphragm at the top of the structure. In that case the boundary conditions may be defined as follows:

a) Because of the presence of an infinitely rigid diaphragm at the top of the structure, the topmost beam cannot deform, i.e.

$$\text{at } x = 0, \quad \gamma_1 = 0 \tag{2.22}$$

b) At the base, the boundary condition is

$$\text{at } x = H, \quad \gamma_{n+1} = 0 \tag{2.23}$$

The n simultaneous finite difference equations become,

$$-\left(\frac{1}{k_2} + \psi_{(1)}\, h_{(1)}\right)T_{(1)} + \frac{T_{(2)}}{k_2} = -\int_{h_{(1)}} \zeta\, M\, dx$$

$$\frac{T_{(1)}}{k_2} - \left(\frac{1}{k_2}+\frac{1}{k_3} + \psi_{(2)}\, h_{(2)}\right)T_{(2)} + \frac{T_{(3)}}{k_3} = -\int_{h_{(2)}} \zeta\, M\, dx$$

.... (2.24)

$$\frac{T_{(i-1)}}{k_i} - \left(\frac{1}{k_i} + \frac{1}{k_{i+1}} + \psi_{(i)} h_{(i)}\right) T_{(i)} + \frac{T_{(i+1)}}{k_{i+1}} = -\int_{h_{(i)}} \zeta\, M\, dx$$

....

$$\frac{T_{(n-1)}}{k_n} - \left(\frac{1}{k_n} + \psi_{(n)}\, h_{(n)}\right) T_{(n)} = -\int_{h_{(n)}} \zeta\, M\, dx$$

2.4 Numerical Example

A 20 storey coupled shear wall was solved by the continuous solution and the finite difference solution. The properties of the model are the same as those of Rosman (6), namely, H = 196.9 ft., h = 9.845 ft., $A_1 = A_2$ = 23.2 sq. ft., $I_1 = I_2$ = 1040 ft.^{4}, I_p = 0.625 ft.^{4}, b = 5.254, ℓ = 28.45 ft., E = 443000 kips/ft.^{2} and Q_2 = 132 kips. Three examples were solved:

i) The stiffness of the topmost beam is the same as the interior connecting beams.

ii) The stiffness of the topmost beam is half that of the interior connecting beams.

iii) The topmost beam cannot deform, i.e. infinitely stiff.

Figs. (2.4), (2.5) and (2.6) show the distribution of the axial forces, the shearing forces and the bending moments in the piers over all the height of the shear wall. We can come to the following conclusions:

1) The continuous and the finite difference solutions give the same forces in the piers. The two solutions are consistent, however, the finite difference method can treat examples which cannot be treated by the continuous method.

2) The stiffness of the topmost beam has a local effect on the forces in the piers at the free end. It has no effect on the forces in the piers at the fixed end. This effect can be demonstrated only by the finite difference method since the continuous solution cannot take into account variations in the stiffness of the upper most connecting beam.

4) When the two shear walls are inter-connected by an infinitely rigid diaghragm at the top of the structure, this has a local effect over about 30 per cent of the height of the structure. The difference of the deflection at the free end for this case and the usual case was within 2 per-cent. There was no significant difference in the stresses at

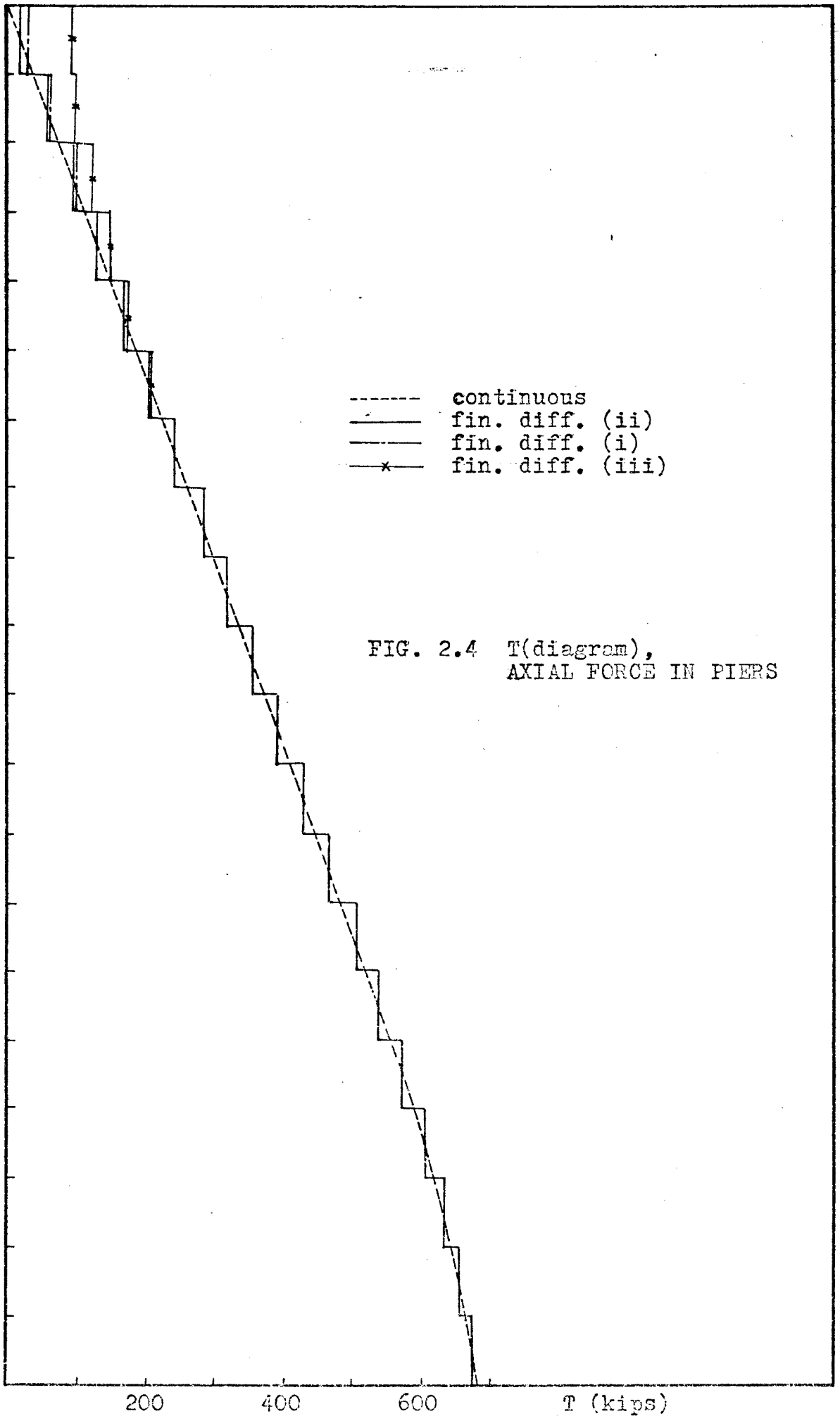

FIG. 2.4 T(diagram), AXIAL FORCE IN PIERS

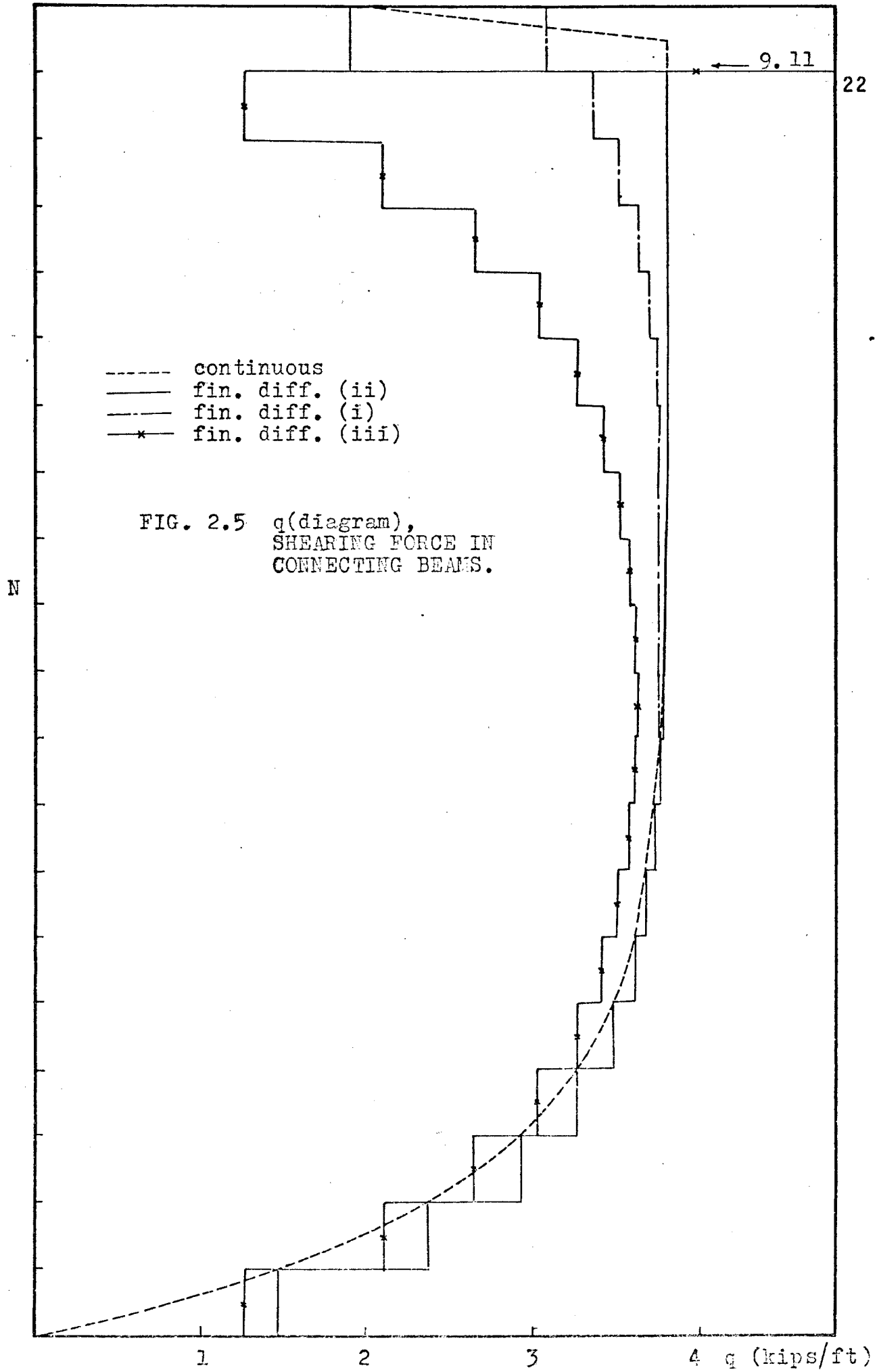

FIG. 2.5 q(diagram), SHEARING FORCE IN CONNECTING BEAMS.

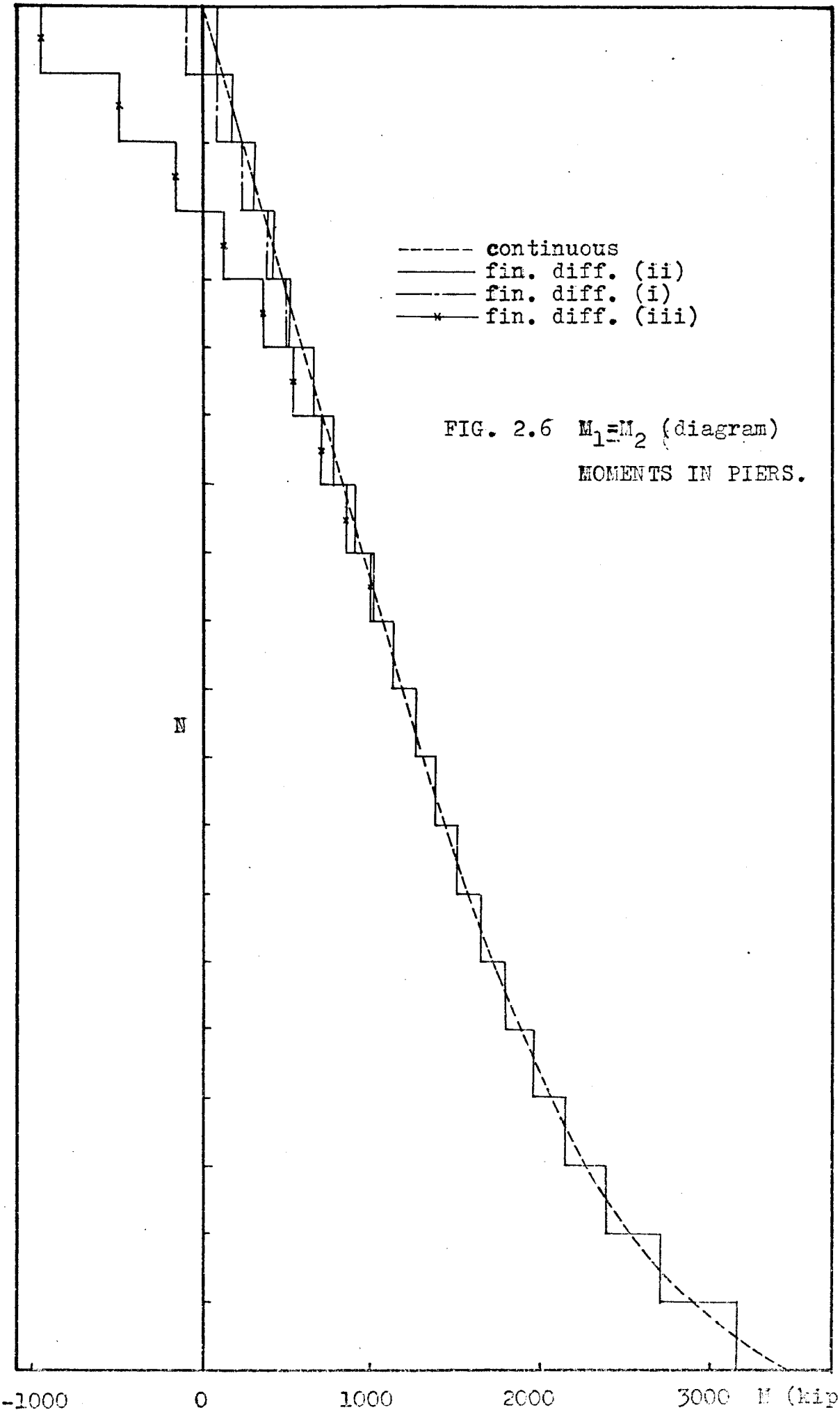

FIG. 2.6 $M_1=M_2$ (diagram)
MOMENTS IN PIERS.

the base which is the critical location for design.

5) From the above conclusions we may see that the lower parts of the wall, which usually become critical in design, are not affected by the type of connection which may exist at the top of the structure.

2.5 Coupled Shear Walls with Inelastic Connecting Beams

2.5.1 Finite Difference Equations

In deriving Eq. (2.18.1) it was assumed that the connecting beam load-slip relationship is linear, Fig. (2.7a); thus

$$\gamma = \frac{Q}{k} \tag{2.25}$$

However, if the load-slip curve is non-linear, then the load-slip relationship is expressed in the following modified form, (Fig. 2.7b),

$$\gamma = \frac{Q}{k} + f \tag{2.26}$$

where k is the slope of the tangent at a point corresponding to Q and γ, and f is the intercept of the tangent on the axis representing slip. The compatibility condition is the same as before:

$$\gamma_{i+1} - \gamma_i = \int_{h(i)} (\varepsilon_1 - \varepsilon_2)\, dx \tag{2.27}$$

Substitution of Eq. (2.26) in Eq. (2.27) yields

$$\left[\frac{Q_{i+1}}{k_{i+1}} + f_{i+1}\right] - \left[\frac{Q_i}{k_i} + f_i\right] = \int_{h(i)} (\varepsilon_1 - \varepsilon_2)\, dx \tag{2.28}$$

or

$$\frac{Q_{i+1}}{k_{i+1}} - \frac{Q_i}{k_i} = \int_{h(i)} (\varepsilon_1 - \varepsilon_2)\, dx + (f_i - f_{i+1}) \tag{2.29}$$

Thus, the finite difference equations can be written in matrix notation as

$$[B]\{T\} = \{A\} + \{F\} \tag{2.30}$$

where $F_{(i)} = f_i - f_{i+1}$

2.5.2 Load-Slip Characteristic of the Connecting Beam

If the connecting beam is reinforced as a doubly reinforced beam and its span to depth ratio such that its behaviour is not like a deep beam, the moment-curvature relation as well as the load-slip relation of the connecting beam can be determined as follows:

Consider a doubly reinforced beam of dimensions b' and d_b, Fig. (2.8). The stress-strain curve for steel is elastic perfectly plastic. The stress-strain curve for concrete in compression can be simplified into a single formula to relate stress and strain from $\varepsilon = 0$ to $\varepsilon = \varepsilon_f$, Fig. (2.9). Adopting a parabolic form (16)

$$\frac{\sigma}{\sigma_u} = 2\frac{\varepsilon}{\varepsilon_u} - \left(\frac{\varepsilon}{\varepsilon_u}\right)^2 \tag{2.31.1}$$

the initial slope of the curve is given by

$$E_0 = \left(\frac{d\sigma}{d\varepsilon}\right)_{\varepsilon=0} = 2\frac{\sigma_u}{\varepsilon_u} \tag{2.31.2}$$

There will be two stages in the beam's behaviour: stage I when the steel obeys Hooke's law, and stage II when the steel yields and $\sigma_s = \sigma_y$.

The distribution of stress over the depth of the cross-section is shown in Fig. (2.10.1). The total compressive force on the concrete is

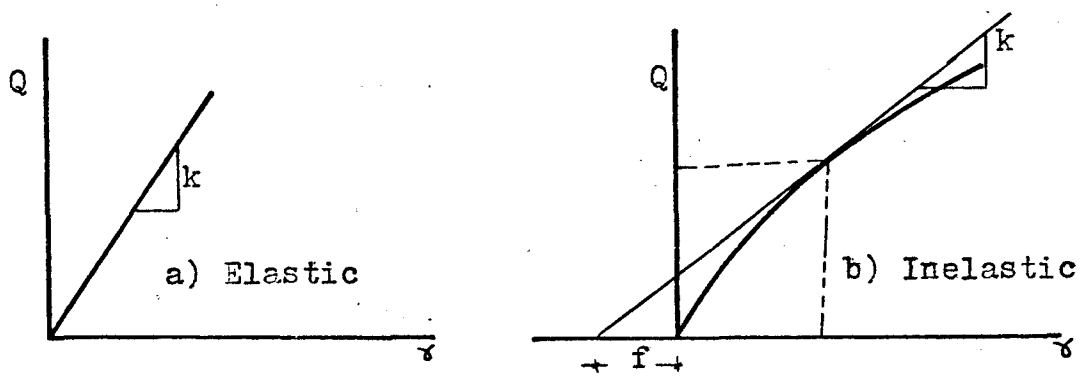

FIG. 2.7 LOAD SLIP CURVE FOR A CONNECTING BEAM.

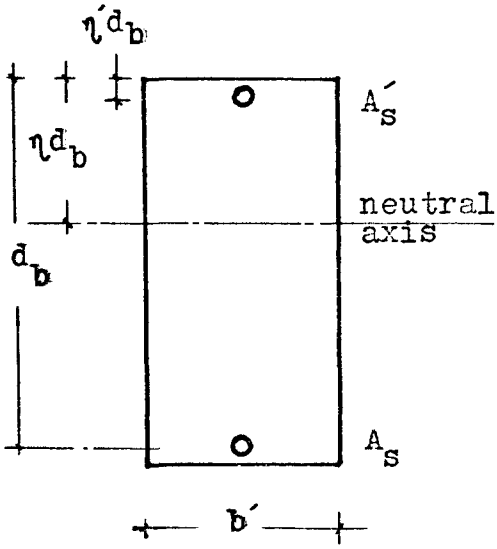

FIG. 2.8 DOUBLY REINFORCED CROSS SECTION

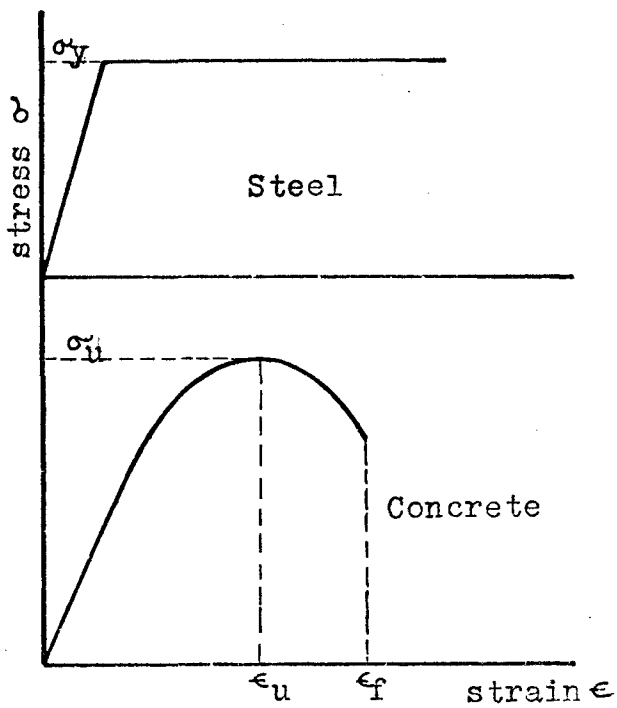

FIG. 2.9 STRESS STRAIN CURVES.

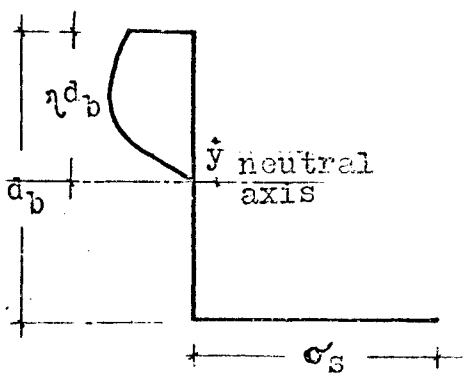

FIG. 2.10.1

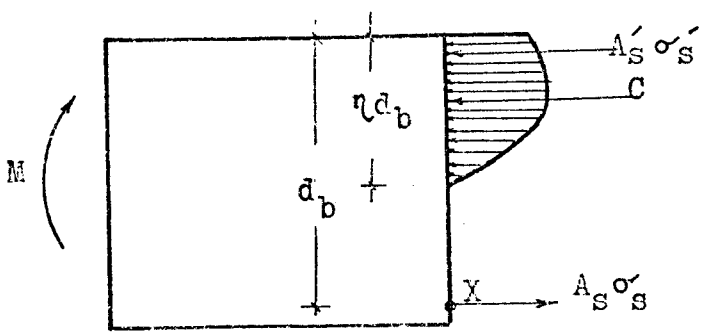

FIG. 2.10.2

$$C = \int_0^{\eta d} \sigma\, b'\, dy \qquad (2.32.1)$$

but $$\varepsilon = y\,\phi \qquad (2.32.2)$$

substitution of Eqs. (2.32.2) and (2.31.1) in Eq. (2.32.1) yields

$$C = \sigma_u\, b' \int_0^{\eta d} \left(2\,\frac{\phi}{\varepsilon_u}\, y - \frac{\phi^2}{\varepsilon_u^2}\, y^2\right) dy$$

$$= \frac{\sigma_u\, \phi\, b'\, d_b^2}{\varepsilon_u}\, \eta^2 \left(1 - \frac{\phi\, d_b}{3\varepsilon_u}\, \eta\right)$$

let

$$\frac{\phi\, d_b}{\varepsilon_u} = \bar{\phi}$$

$$C = \sigma_u\, b'\, d_b\, \bar{\phi}\, \eta^2 \left(1 - \frac{\bar{\phi}}{3}\, \eta\right) \qquad (2.32.3)$$

Equilibrium of moments about point X, Fig. (2.10.2), gives

$$M = \int_0^{\eta d} \sigma b' \{y + (1 - \eta) d_b\}\, dy + A_s'\, \sigma_s' \,(d_b - \eta' d_b)$$

$$= \sigma_u\, b'\, d_b^2\, \bar{\phi}\, \eta^3 \left(\frac{2}{3} - \frac{\bar{\phi}\eta}{4}\right) + \sigma_u\, b'\, d_b^2\, \bar{\phi}\, \eta^2\, (1-\eta)\left(1 - \frac{\bar{\phi}\eta}{3}\right)$$

$$+ A_s'\, \sigma_s' \,(d_b - \eta' d_b)$$

let $\bar{M} = \dfrac{M}{\sigma_u b'\, d_b^2}$

$$x = \frac{\varepsilon_c}{\varepsilon_u} = \frac{\eta\, d_b\, \phi}{\varepsilon_u} = \eta\, \bar{\phi} \quad (\varepsilon_c \text{ is the maximum compressive strain})$$

$$\bar{M} = x\eta \left\{1 - \frac{x}{3} - \frac{\eta}{3}\left(1 - \frac{x}{4}\right)\right\} + A_s'\, \sigma_s' (d_b - \eta' d_b)/\sigma_u b' d_b^2$$

(2.33)

Stage I:

The stresses in the steel, as long as Hooke's law holds, are

$$\sigma_s = E_s(1 - \eta)\, d_b\, \phi$$
$$\sigma_s' = E_s(\eta - \eta')\, d_b\, \phi \qquad (2.34)$$

let

$$m_0 = \frac{E_s}{E_0} = \frac{E_s\, \varepsilon_u}{2\sigma_u}$$

$$p = A_s/b\, d_b \qquad p' = A_s' \left(1 - \frac{1}{m_0}\right)/b\, d_b$$

Equilibrium of horizontal forces gives

$$A_s\, \sigma_s = C + A_s'\, \sigma_s' \left(1 - \frac{1}{m_0}\right) \qquad (2.35)$$

i.e.

$$A_s E_s(1-\eta) d_b \phi = \sigma_u\, b d_b\, \bar{\phi}\, \eta^2 \left(1 - \frac{\bar{\phi}\eta}{3}\right) + A_s' E_s(\eta - \eta') d_b \phi \left(1 - \frac{1}{m_0}\right)$$

i.e.

$$2pm_0(1-\eta)\, \bar{\phi} = \bar{\phi}\, \eta^2 \left(1 - \frac{x}{3}\right) + 2\, p'\, m_0(\eta - \eta')\, \bar{\phi}$$

i.e.

$$\eta^2 + \frac{2(p + p')m_0}{1 - \frac{x}{3}}\, \eta - \frac{2m_0}{1 - \frac{x}{3}}(p + \eta' p') = 0 \qquad (2.36)$$

$$\bar{M} = x\, \eta \left\{1 - \frac{x}{3} - \frac{\eta}{3}\left(1 - \frac{x}{4}\right)\right\} + p'\, d_b E_s(\eta - \eta')(1 - \eta')\phi/\sigma_u \qquad (2.37)$$

$$\phi = \frac{\varepsilon_u}{d_b} \cdot \frac{x}{\eta} = \frac{\varepsilon_u}{d_b}\, \bar{\phi} \qquad (2.38)$$

For a given beam and some chosen value of x, the values η, ϕ, $\bar{M}$ and $\bar{\phi}$ can be determined from Eqs. (2.36), (2.38) and (2.37). By taking a series of values of x it is possible to construct a cuve of $\bar{M}$ against $\bar{\phi}$.

Stage II.

The steel now yields and $\sigma_s = \sigma_y$

Equilibrium of longitudinal forces, Eq. (2.35), yields

$$p\frac{\sigma_y}{\sigma_u} = \eta\, x\left(1 - \frac{x}{3}\right) + 2\acute{p}\, m_0 (\eta - \acute{\eta})\frac{x}{\eta}$$

$$\eta^2 + \frac{2\acute{p} m_0 x - p\frac{\sigma_y}{\sigma_u}}{x\left(1 - \frac{x}{3}\right)}\eta - \frac{2\acute{p} m_0 \acute{\eta}\, x}{x\left(1 - \frac{x}{3}\right)} = 0 \qquad (2.39)$$

For a given beam and some chosen value of x, the values η, ϕ, $\bar{M}$ and $\bar{\phi}$ can be determined from Eqs. (2.39), (2.38) and (2.37). By taking a series of values of x it is possible to construct a curve of $\bar{M}$ against $\bar{\phi}$.

The complete moment-curvature curve will consist of both stage I and stage II. For a given beam the complete curve starts at stage I and changes to stage II at the point where the two curves intersect.

The load-slip curve of the connecting beam can be determined by numerical integration of the curvature over the span of the connecting beam, Fig. (2.11).

As an example, consider a beam with the properties, $p = \acute{p} = 0.01$, $\sigma_u = 3000$ lb/in^2, $\varepsilon_u = .002$, $\sigma_y = 40{,}000$ lb/in^2, $E_s = 30 \times 10^6$ lb/in^2, $\acute{b} = 12$ in, $d_b = 22$ in and $b = 72$ in. Two cases are considered:

i) the beam as doubly reinforced concrete beam.

ii) the beam as homogeneous beam of concrete only, i.e. the gross area and moment of inertia are considered as the properties of the cross-section of the uncracked beam.

Fig. (2.12) shows the moment-curvature curve for the connecting beam. The moment carrying capacity of the cracked beam is about 45 % of that for the uncracked beam.

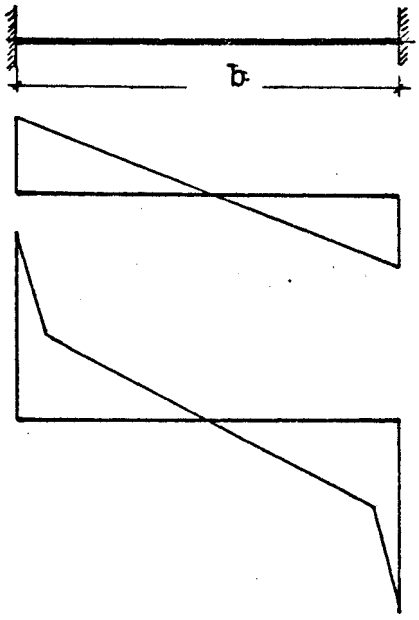

FIG. 2.11 SLIP CALCULATION

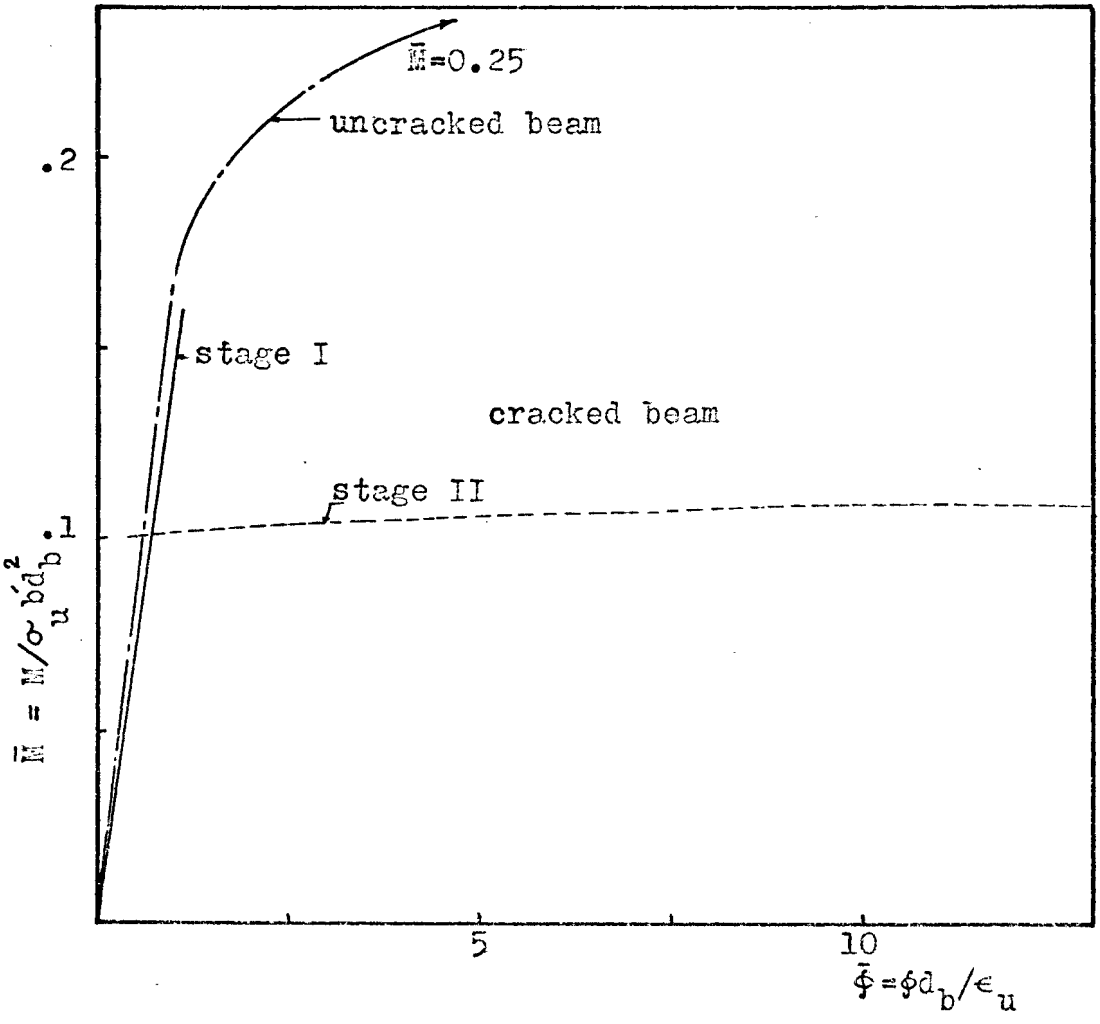

FIG. 2.12 MOMENT CURVATURE CURVE

Fig. (2.13) shows the load-slip curve for the connecting beam. The load-slip curve for the cracked beam is approximated by three linear parts, to be used later in analysing an example of a coupled shear wall, and in which the slope of the third part was given a value 0.1% of the slope of the first part. The shear modulus, k, of the cracked beam is about 90% of that for the uncracked beam.

2.5.3 Numerical Example

To illustrate the behaviour of coupled shear walls with inelastic connecting beams, an example of a twenty storey building with the following properties is used; H = 200 ft., h = 10 ft., d = 24 ft., t = 1 ft., b = 6 ft. and d_b = 2 ft. The coupling beams are assumed to have cracked, while the cracking of the piers is not taken into account.

The history of the structure's behaviour may be followed through stages of incremental loading till first yielding of the piers occurs. A uniformly distributed load is applied to the structure in increments, different stages of loading of the structure are considered:

Stage I

Onset of yielding in the connecting beams. The critical connecting beam is situated at x = 0.75 H. This stage terminates the linear elastic behaviour of the structure.

Stage 2

75% of the connecting beams have yielded. At the end of this load increment yielding has occurred over 75%

of the height of the structure. The maximum ductility ratio at this stage is 3.5, occurring at the level, x = 0.7H, Fig. (2.14c). The over-all ductility factor of the structure, i.e. the deflection at the free end of the shear wall at the end of stage 2 to that at the end of stage 1, is 1.8, Fig. (2.14a).

Stage 3

Yielding of all the connecting beams. The ductility ratio in the critically situated connecting beam, at x = 0.65H, is 7.0. The overall ductility factor in terms of the deflection of the structure is 2.5. Fifty-five per cent of the connecting beams over the range x = 0.35H to x = 0.90H have a ductility ratio greater than 4.0. A ductility ratio of 4.0 is suggested as a maximum ductility capacity for the connecting beams.

Stage 4

All connecting beams are in part three of load-slip curve, Fig. (2.13), i.e. the shear modulus of all the connecting beams is the same and equal to that of part three of the load-slip curve.

Stage 5

Onset of yielding in piers. At the end of this load stage, the strains in the piers reach the specified elastic yield strain for the concrete (.001). The maximum ductility ratio for the connecting beams is 42.0, at a level x = 0.35H, and the overall ductility factor is 11.0. It should be

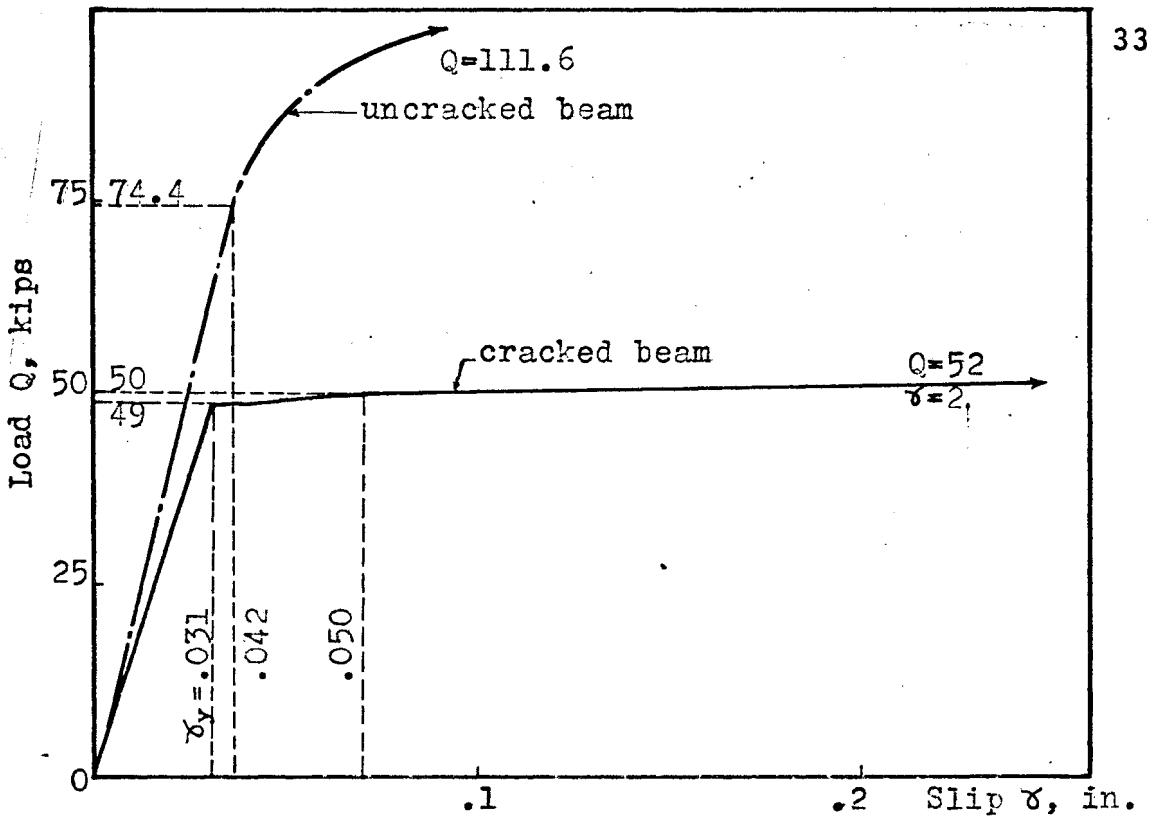

FIG. 2.13 LOAD SLIP CURVE FOR THE CONNECTING BEAM

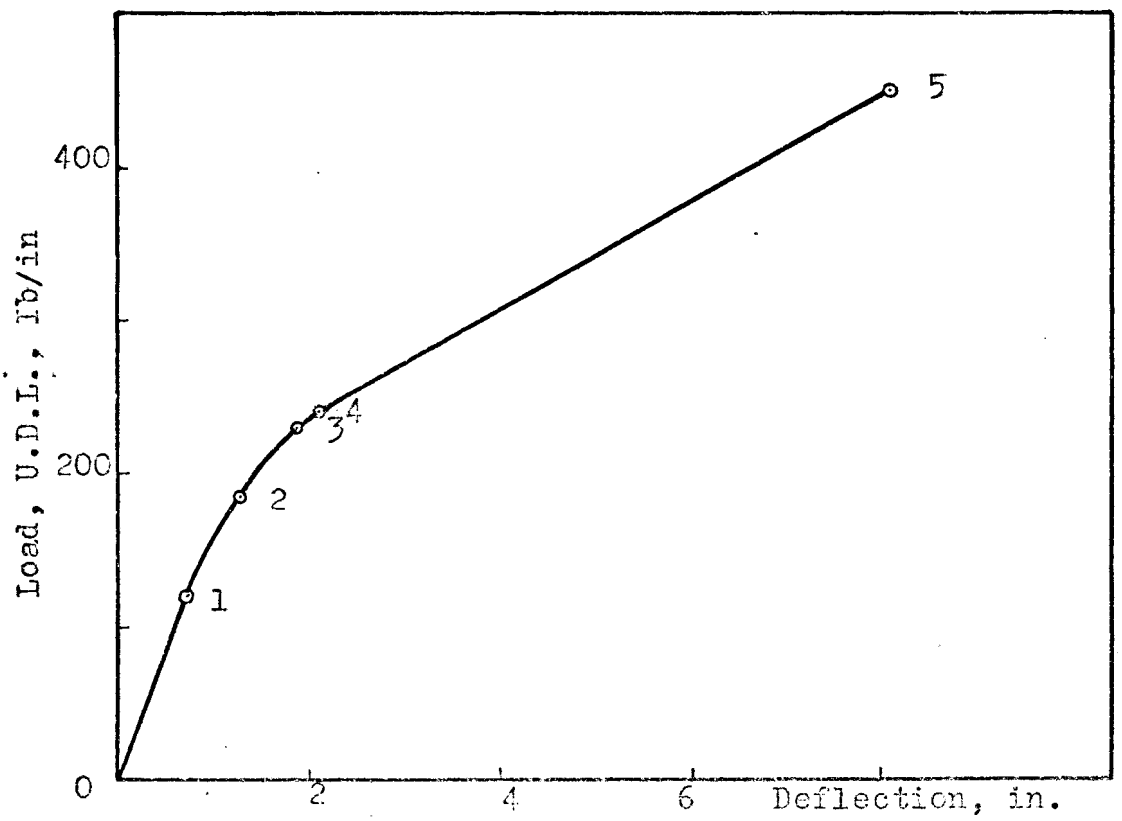

FIG. 2.14a LOAD DEFLECTION CURVE FOR THE TOP OF THE SHEAR WALL.

1 Onset of yielding in the connecting beams,
2 75% of the connecting beams have yielded,
3 Yielding of all the connecting beams,
4 All connecting beams are in part three of load slip curve,
5 Onset of yielding in piers.

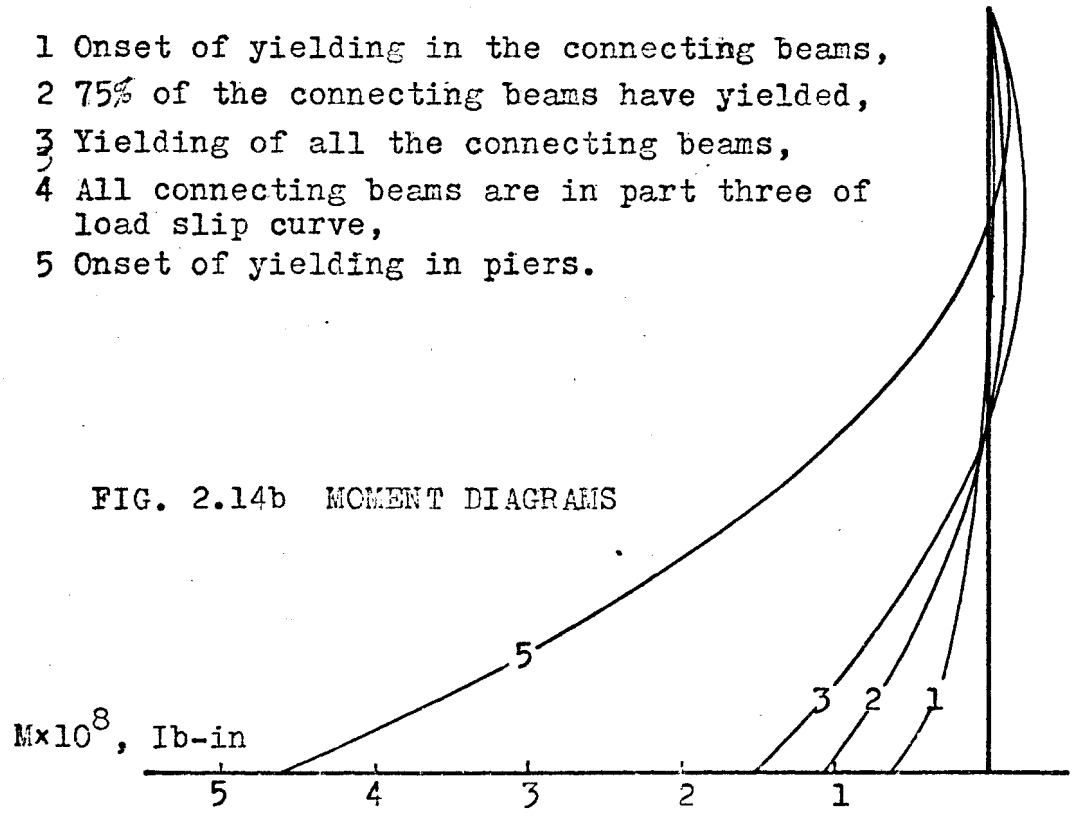

FIG. 2.14b MOMENT DIAGRAMS

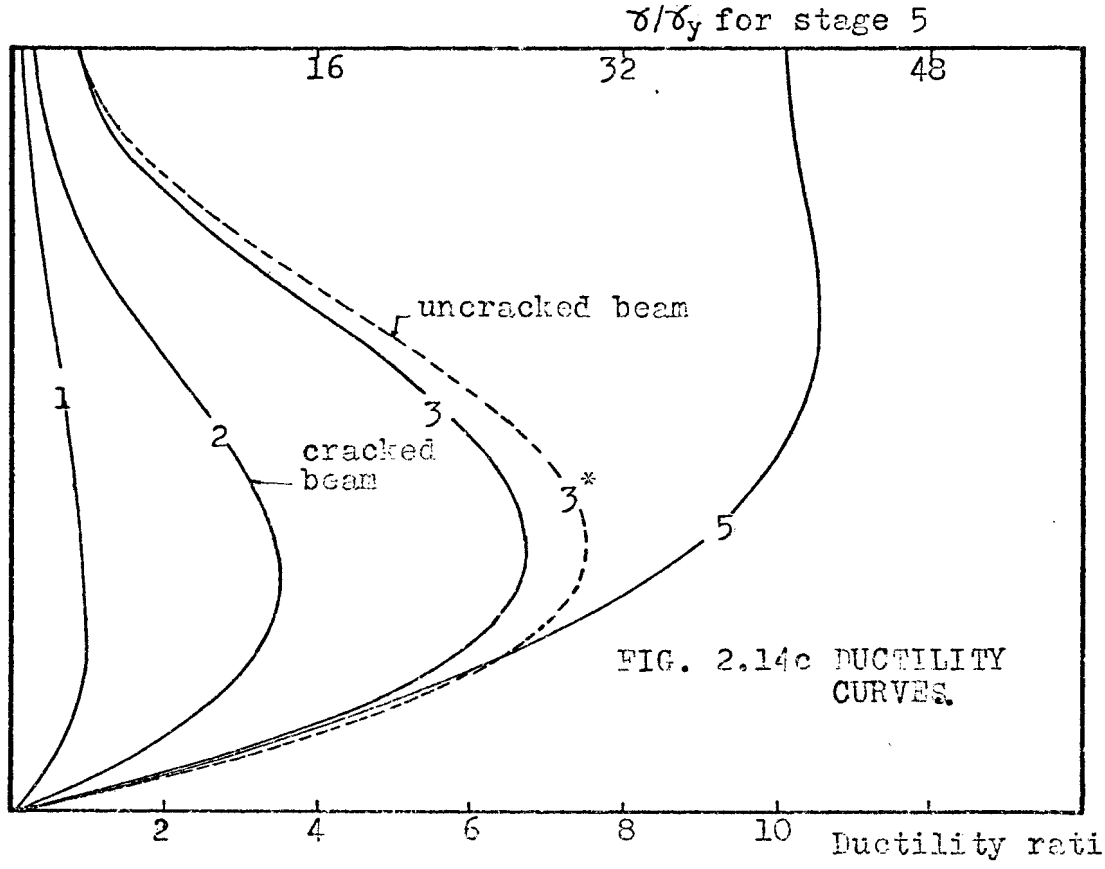

FIG. 2.14c DUCTILITY CURVES.

FIG. 2.14 RESULTS OF THE COUPLED SHEAR WALL WITH INELASTIC CRACKED CONNECTING BEAMS.

mentioned that for actual shear walls of reinforced concrete, the effect of cracking of the piers will affect to a great extent the behaviour of the structure from stage 4 to stage 5. The first yielding of the piers will start earlier than stage 5; the load-deflection curve is expected to be asymptotic to the ultimate load capacity of the structure and the demands for ductility of the connecting beams will be less.

Thus we can say:

1. the finite difference method can be extended to study the behaviour of reinforced concrete coupled shear walls taking into account the cracking of the piers as well as the connecting beams.

2. the ductility of the coupling system as well as the overall structure need further study. In reality the coupling beams will withstand a ductility ratio of about 4.0 beyond which a reduction in capacity will occur.

3. the ductility is affected by the relative stiffness of the coupled shear walls. For a coupled shear wall, the lower the shear modulus of the connecting beams, the lower are the demands for ductility. To demonstrate this point, the coupled shear wall example was solved for the uncracked connecting beams, i.e. for larger shear modulus of the connecting beams, and the ductility ratio distribution was plotted, Fig. (2.14c), when all the connecting beams had reached first yield. The maximum ductility ratio was 7.5, compared to 6.7 for the connecting beams with lower shear modulus.

CHAPTER 3

ANALYSIS OF COUPLED SHEAR WALLS OF VARIABLE CROSS-SECTION

3.1 General

In modern multi-storey buildings, shear walls are normally used as an economic means of providing lateral stability against wind or earthquake loading. If the building is very tall, it may become economical to reduce the width of the shear walls at the upper levels.

The problem of coupled shear walls with abrupt changes of cross-section was first treated by Traum in 1966 (7) and by Coull and Puri in 1968 (8) and then by Traum and Pisanty in 1970 (9). The continuous connection method, to analyse a symetrical coupled shear wall structure containing one band of openings with one discontinuity in the depth of the walls, was used.

Coull and Puri (8) present a solution for this problem by obtaining solutions for the two segments of the shear wall and considering the equilibrium and compatibility relationships at the junction between the upper and lower segments, a complete solution for the entire structure was achieved.

The results obtained by Coull and Puri are consistant with one of the solutions presented here for this problem. Coull and Puri stated that, "Traum in 1966, in his analysis, ignored the fact that the centroids of the wall segments undergo a relative vertical deformation at the junction where the change in width occurs, due to the rotation of the cross-section under bending. In addition an error was made in the derivation of the governing differential equation for the upper wall segment".

Traum and Pisanty in their recent paper in 1970 (9) made the same error mentioned by Coull and Puri above. Another error was made in the compatibility condition at the change of cross-section. They assume the same slope at the change of cross section which is correct but then they differentiate once before substitution. This means that they assume the same value of curvature at the change of cross-section for the upper and lower segment which is not correct.

Herein, simpler methods are developed for the analysis of coupled shear walls of variable cross-section. Two methods of analysis are presented:

1) a continuous solution based on Newmark's solution for composite beams.

2) a finite difference solution based on Stussi's solution for composite beams.

Fig. (3.1) shows the shear wall model considered in the analysis.

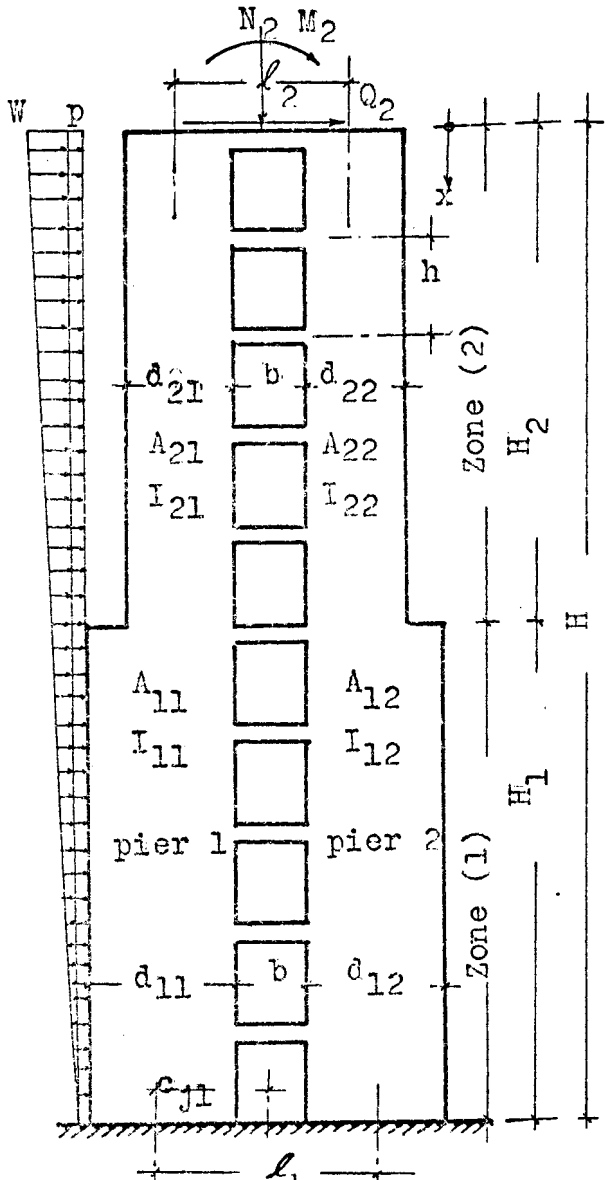

a) Real Structure

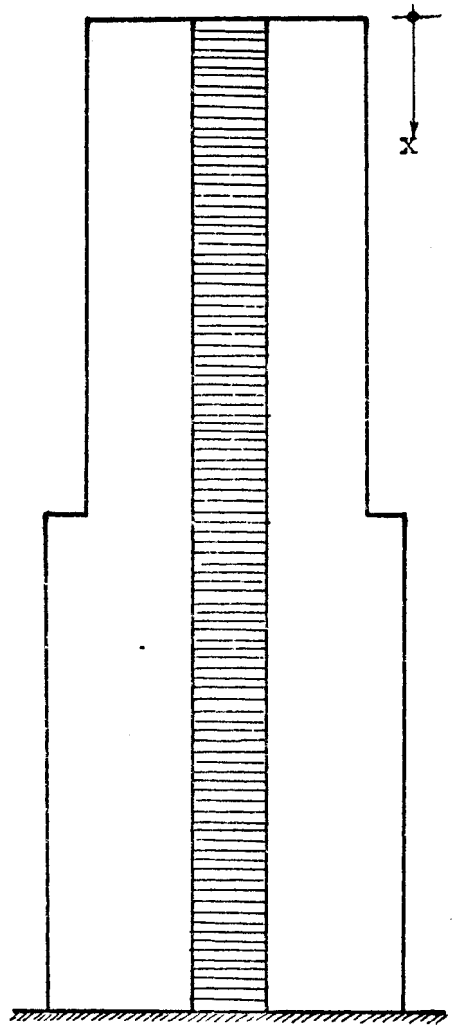

b) Substitute System, continuous solution.

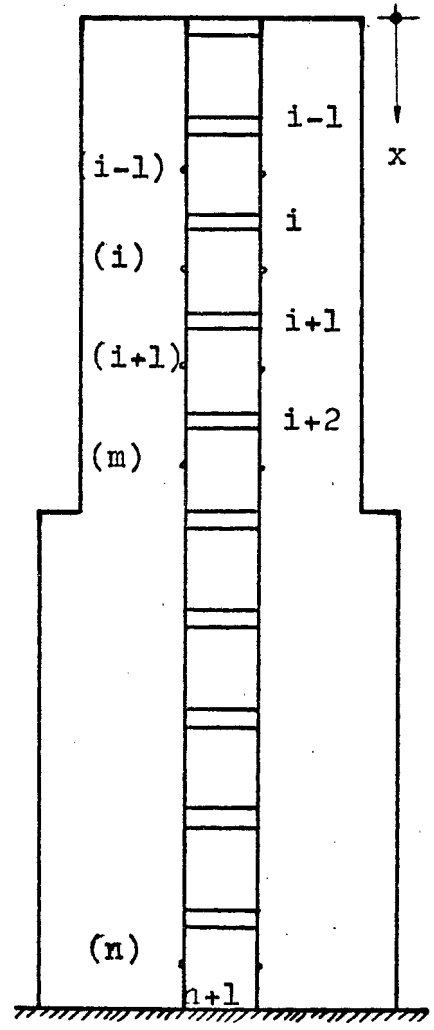

c) Substitute System, Finite Difference Method.

FIG. 3.1 SHEAR WALL WITH VARIABLE CROSS SECTION.

3.2 Continuous Solution

3.2.1 Basic Assumptions

We may make the same assumptions mentioned in the analysis of prismatic coupled shear walls except that there is an abrupt change in cross-section of the piers.

3.2.2 Formulation of the Problem

For zone (j), $j = 1,2$, the differential equation can be derived as follows:

The compatibility and equilibrium conditions can be written as

$$\gamma_{i+1} - \gamma_i = \int_{h_{(i)}} (\varepsilon_1 - \varepsilon_2)\, dx \qquad (3.1.1)$$

$$\frac{d\gamma}{dx} = \varepsilon_1 - \varepsilon_2 \qquad (3.1.2)$$

$$M(x) = M_{j1} + M_{j2} + T_{(j)} \cdot \ell_j \qquad (3.1.3)$$

The strain can be found as

$$\varepsilon_2 = -\frac{T_{(j)}}{E_1 A_{j1}} + \frac{M_{j1} \cdot c_{j1}}{E_1 I_{j1}} \qquad (3.2.1)$$

$$\varepsilon_1 = \frac{T_{(j)}}{E_2 A_{j2}} - \frac{M_{j2} \cdot c_{j2}}{E_2 I_{j2}} \qquad (3.2.2)$$

we may prove that

$$\frac{d\gamma}{dx} = \left(\frac{hb^3}{12EI_p} + \frac{hb}{GA^*_b}\right) \frac{d^2T_{(j)}}{dx^2}$$

$$= \frac{h}{k} \frac{d^2T_{(j)}}{dx^2} \qquad (3.3)$$

The piers, having equal curvatures, yield

$$\frac{M_{j1}}{E_1 I_{j1}} = \frac{M_{j2}}{E_2 I_{j2}} = \frac{M - T_{(j)} \cdot \ell_j}{E_1 I_{j1} + E_2 I_{j2}} \qquad (3.4)$$

Substitution of Eqs. (3.4), (3.3), (3.2.2), (3.2.1) in Eq. (3.1.2) yields

$$\frac{d^2T_{(j)}}{dx^2} - \acute{\alpha}_j T_{(j)} = - R_j M(x) \qquad (3.5.1)$$

where

$$\acute{\alpha}_j = \frac{k}{h} \frac{\overline{EI}}{\overline{EA}.\Sigma EI} \qquad (3.5.2)$$

$$R_j = \frac{k}{h} \frac{\ell_j}{\Sigma EI} \qquad (3.5.3)$$

$$\Sigma EI = E_1 I_{j1} + E_2 I_{j2} \qquad (3.5.4)$$

$$\frac{1}{\overline{EA}} = \frac{1}{E_1 A_{j1}} + \frac{1}{E_2 A_{j2}} \qquad (3.5.5)$$

$$\overline{EI} = \Sigma EI + \overline{EA}. \ell_j^2 \qquad (3.5.6)$$

Thus, the governing differential equation for the two wall segments can be written as:

Zone (1) $H_2 \leq x \leq H$ Lower segment of walls

$$\frac{d^2T_{(1)}}{dx^2} - \acute{\alpha}_1 T_{(1)} = - R_1 M(x) \qquad (3.6)$$

Zone (2) $0 \leq x \leq H_2$ Upper segment of walls.

$$\frac{d^2T_{(2)}}{dx^2} - \acute{\alpha}_2 T_{(2)} = - R_2 M(x) \qquad (3.7)$$

If the shear wall is subjected to a uniformly distributed load of intensity p, a concentrated load Q_2 at the free end, a moment M_2 at the free end, and a triangular load of maximum intensity ω, the external applied bending moment can be expressed as

$$M(x) = + \frac{px^2}{2} + Q_2 x + M_2 + \frac{\omega x^2}{2} - \frac{\omega x^3}{6H} \qquad (3.8)$$

The solution of the governing differential equations (3.5) and (3.7) can be found as

$$T_{(2)} = C_1 \cosh x\sqrt{\alpha_2} + C_2 \sinh x\sqrt{\alpha_2} + \frac{R_2}{\alpha_2}\left(\frac{px^2}{2} + Q_2 x + M_2 + \frac{\omega x^2}{2} - \frac{\omega x^3}{6H}\right) + \frac{R_2}{\alpha_2^2}\left(p + \omega - \frac{\omega x}{H}\right) \qquad (3.9.1)$$

$$T_{(1)} = C_3 \cosh x\sqrt{\alpha_1} + C_4 \sinh x\sqrt{\alpha_1} + \frac{R_1}{\alpha_1}\left(\frac{px^2}{2} + Q_2 x + M_2 + \frac{\omega x^2}{2} - \frac{\omega x^3}{6H}\right) + \frac{R_1}{\alpha_1^2}\left(p + \omega - \frac{\omega x}{H}\right) \qquad (3.9.2)$$

Differentiating once yields

$$q_{(2)} = C_1 \sqrt{\alpha_2} \sinh x\sqrt{\alpha_2} + C_2 \sqrt{\alpha_2} \cosh x\sqrt{\alpha_2} + \frac{R_2}{\alpha_2}\left(px + Q_2 + \omega x - \frac{wx^2}{2H}\right) - \frac{R_2}{\alpha^2}\frac{\omega}{H} \qquad (3.10.1)$$

$$q_{(1)} = C_3 \sqrt{\alpha_1} \sinh x\sqrt{\alpha_1} + C_4 \sqrt{\alpha_1} \cosh x\sqrt{\alpha_1}^2 + \frac{R_1}{\alpha_1}\left(px + Q_2 + \omega x - \frac{\omega x^2}{2H}\right) - \frac{R_1}{\alpha_1^2}\frac{\omega}{H} \qquad (3.10.2)$$

The following boundary conditions will serve to determine the four constants C_1 to C_4

1) at $x = 0$ $\quad T_{(2)} = 0$ (3.11.1)

2) at $x = H$ $\quad q_{(1)} = 0$ (3.11.2)

at $x = H_2$ one of the two following sets of boundary conditions may be considered

I at $x = H_2$ $\quad T_{(1)} = T_{(2)}$ (3.12.1)

$$\text{at } x = H_2 \qquad \frac{d\,T_{(1)}}{dx} = \frac{d\,T_{(2)}}{dx} \tag{3.12.2}$$

or II

$$\text{at } x = H_2 \qquad \frac{d^2T_{(1)}}{dx^2} = \frac{d^2T_{(2)}}{dx^2} \tag{3.13.1}$$

$$\text{at } x = H_2 \qquad \frac{d\,T_{(1)}}{dx} = \frac{d\,T_{(2)}}{dx} \tag{3.13.2}$$

We may have two possible solutions, denoted as solution (I) and solution (II) corresponding to the two sets of boundary conditions, I and II respectively. We may mention here that it will be proved in Chapters 4 and 5 that solution (I) is the correct one by using the principles of minimal potential energy and the finite element method. However, solution (II) was based on a supposition that there may be only one value of the rate of change of slip at the change of cross-section, Eq. (3.3).

Applying compatibility conditions (I) we get:

$$\begin{bmatrix} 1.0 & 0 & 0 & 0 \\ \cosh H_2\sqrt{\alpha_2'} & \sinh H_2\sqrt{\alpha_2'} & -\cosh H_2\sqrt{\alpha_1'} & -\sinh H_2\sqrt{\alpha_1'} \\ \sqrt{\alpha_1'}\sinh H_2\sqrt{\alpha_2'} & \sqrt{\alpha_2'}\cosh H_2\sqrt{\alpha_2'} & -\sqrt{\alpha_1'}\sinh H_2\sqrt{\alpha_1'} & -\sqrt{\alpha_1'}\cosh H_2\sqrt{\alpha_1'} \\ 0 & 0 & \sqrt{\alpha_1'}\sinh H\sqrt{\alpha_1'} & \sqrt{\alpha_1'}\cosh H\sqrt{\alpha_1'} \end{bmatrix} \begin{bmatrix} C_1 \\ C_2 \\ C_3 \\ C_4 \end{bmatrix} =$$

$$\begin{bmatrix} \frac{R_2}{\alpha_2'^2}(p+\omega) + \frac{R_2}{\alpha_2'} M_2 \\ \frac{pH_2^2}{2} + Q_2 H_2 + M_2 + \frac{\omega H_2^2}{2} - \frac{\omega H_2^3}{6H})(\frac{R_2}{\alpha_2'} - \frac{R_1}{\alpha_1'}) + (\frac{R_2}{\alpha_2'^2} - \frac{R_1}{\alpha_1'^2})(p+\omega - \frac{\omega H_2}{H}) \\ (pH_2 + Q_2 + \omega H_2 - \frac{\omega H_2^2}{2H})(\frac{R_2}{\alpha_2'} - \frac{R_1}{\alpha_1'}) - (\frac{R_2}{\alpha_2'^2} - \frac{R_1}{\alpha_1'^2}) \frac{\omega}{H} \\ (pH + Q_2 + \frac{\omega H}{2}) \frac{R_1}{\alpha_1'} - \frac{R_1}{\alpha_1'^2} \frac{\omega}{H} \end{bmatrix} \quad (3.14$$

Applying compatibility conditions (II) we get:

$$\begin{bmatrix} 1.0 & 0 & 0 & 0 \\ \alpha_2' \cosh H_2\sqrt{\alpha_2'} & \alpha_2' \sinh H_2\sqrt{\alpha_2'} & -\alpha_1' \cosh H_2\sqrt{\alpha_1'} & -\alpha_1' \sinh H_2\sqrt{\alpha_1'} \\ \sqrt{\alpha_2'} \sinh H_2\sqrt{\alpha_2'} & \sqrt{\alpha_2'} \cosh H_2\sqrt{\alpha_2'} & -\sqrt{\alpha_1'} \sinh H_2\sqrt{\alpha_1'} & -\sqrt{\alpha_1'} \cosh H_2\sqrt{\alpha_1'} \\ 0 & 0 & \sqrt{\alpha_1'} \sinh H\sqrt{\alpha_1'} & \sqrt{\alpha_1'} \cosh H\sqrt{\alpha_1'} \end{bmatrix} \begin{bmatrix} C_1 \\ C_2 \\ C_3 \\ C_4 \end{bmatrix}$$

$$\begin{bmatrix} \frac{R_2}{\alpha_2'^2}(p+\omega) + \frac{R_2}{\alpha_2'} M_2 \\ (\frac{R_2}{\alpha_2'} - \frac{R_1}{\alpha_1'})(p+\omega - \frac{\omega H_2}{H}) \\ (p H_2 + Q_2 + \omega H_2 - \frac{\omega H_2^2}{2H})(\frac{R_2}{\alpha_2'} - \frac{R_1}{\alpha_1'}) - (\frac{R_2}{\alpha_2'^2} - \frac{R_1}{\alpha_1'^2}) \frac{\omega}{H} \\ (pH + Q_2 + \frac{\omega H}{2}) \frac{R_1}{\alpha_1'} - \frac{R_1}{\alpha_1'^2} \frac{\omega}{H} \end{bmatrix} \quad (3.15)$$

Obtaining the constants C_1 to C_4 the axial forces and the shearing forces in the piers can be determined from Eqs. (3.4), (3.9.1), (3.9.2), (3.10.1) and (3.10.2).

The curvature of the wall segments and the internal moments M_{j1}, M_{j2} can be determined from Eq. (3.4).

The strain distribution can be determined from Eqs. (3.2.1), (3.2.2).

The deflection of the shear wall can be determined by numerical integration of the curvature.

The shearing force $Q_i(x)$ in the connecting beam at floor level x can be determined from

$$Q_i(x) = \int_{x-\frac{h}{2}}^{x+\frac{h}{2}} q(x)\, dx \qquad (3.16)$$

3.3 Finite Difference Solution

3.3.1 Basic Assumptions

We may make the same assumptions as those mentioned in the analysis of prismatic coupled shear walls.

3.3.2 Formulation of the Problem

Proceeding as in the analysis of prismatic coupled shear walls, and imposing the condition that the axial force and shearing force at the change of cross-section are continuous, we get:

$$\frac{T_{(i-1)}}{k_i} - \left(\frac{1}{k_i} + \frac{1}{k_{i+1}}\right) T_{(i)} + \frac{T_{(i+1)}}{k_{i+1}} = \int_{h_{(i)}} (\varepsilon_1 - \varepsilon_2)\, dx \qquad (3.17.1)$$

or

$$\frac{T_{(i-1)}}{k_i} - \left(\frac{1}{k_i} + \frac{1}{k_{i+1}} + \psi_{(i)}\, h_{(i)}\right) T_{(i)} + \frac{T_{(i+1)}}{k_{i+1}} = -\int_{h_{(i)}} \zeta\, M\, dx \qquad (3.17.2)$$

where

$$\psi_{(i)} = \frac{1}{E_1 A_{j1}} + \frac{1}{E_2 A_{j2}} + \frac{\ell^2_j}{\Sigma EI}$$

$$= \frac{EI}{EA.\Sigma EI} \qquad (3.17.3)$$

$$\zeta = \frac{\ell_j}{\Sigma EI} \tag{3.17.4}$$

Eq. (3.17.2) represents a typical equation for panel (i). For a coupled shear wall with variable cross-section having n stories (panels) there are n such equations resulting in a set of n simultaneous equations.

The boundary conditions are

$$T(0) = 0 \quad \text{and} \quad Q_{n+1} = 0 \tag{3.17.5}$$

and at the change of cross-section the axial force and the shearing force are continuous, similar to solution (I) in the continuous solution.

The n simultaneous equations can be written in matrix notation as

$$[B]\{T\} = \{A\} \tag{3.17.6}$$

whose terms are defined before in Eqs. (2.20) and (2.20.3).

To get a finite difference solution, similar to the continuous solution with compatibility conditions (II), we proceed as below:

Assume two values of axial forces at $x = H_2$, at panel (m), say $T_{(m)L}$, $T_{(m)R}$. The boundary condition we may impose is

$$\frac{d^2T_{(m)L}}{dx^2} = \frac{d^2T_{(m)R}}{dx^2} \qquad \text{at } x = H_2 \tag{3.18.1}$$

Substitution of Eqs. (3.6), (3.7) in Eq. (3.18.1) yields

$$T_{(m)L} - \frac{\alpha_1'}{\alpha_2'} T_{(m)R} = \frac{R_2 - R_1}{\alpha_2'} M(H_2) \tag{3.18.2}$$

$$\text{i.e.} \quad T_{(m)L} - \frac{\psi_{(m+1)}}{\psi_{(m)}} T_{(m)R} = \frac{\zeta_{(m+1)} - \zeta_{(m)}}{\psi_{(m)}} M(H_2) \quad (3.18.3)$$

So, for a coupled shear wall having (n) panels, where the change of cross section occurs at panel (m), there are (n+1) simultaneous equations given below

$$-\left(\frac{1}{k_1} + \frac{1}{k_2} + \psi_{(1)}h_{(1)}\right) T_{(1)} + \frac{T_{(2)}}{k_2} = -\int_{h(1)} \zeta M dx$$

$$\frac{T_{(1)}}{k_2} - \left(\frac{1}{k_2} + \frac{1}{k_1} + \psi_{(2)}h_{(2)}\right)T_{(2)} + T_{(2)} + \frac{T_{(3)}}{k_3} = -\int_{h(2)} \zeta M dx$$

$$\frac{T_{(i-1)}}{k_i} - \left(\frac{1}{k_i} + \frac{1}{k_{i+1}} + \psi_{(1)}h_{(i)}\right) T_{(i)} + \frac{T_{(i+1)}}{k_{i+1}} = -\int_{h_{(i)}} \zeta M dx$$

$$\frac{T_{(m-2)}}{k_{m-1}} - \left(\frac{1}{k_{m-1}} + \frac{1}{k_m} + \psi_{(m-1)}h_{(m-1)}\right)T_{(m-1)} + \frac{T_{(m)L}}{k_m} = -\int_{h(m-1)} \zeta M dx \quad (3.19.1)$$

$$\frac{T_{(m-2)}}{k_m} - \left(\frac{1}{km} + \psi_{(m)}h_{(m)}\right) T_{(m)L} - \frac{T_{(m)R}}{k_{m+1}} + \frac{T_{m+1}}{k_{m+1}} = -\int_{h_{(m)}} \zeta M dx$$

$$T_{(m)L} - \frac{\psi_{(m+1)}}{\psi_{(m)}} T_{(m)R} = \frac{\zeta_{m+1} - \zeta_m}{\psi_{(m)}} M(H_2)$$

$$\frac{T_{(m)R}}{k_{m+1}} - \left(\frac{1}{k_{m+1}} + \frac{1}{k_{m+2}} + \psi_{(m+1)}h_{(m+1)}\right) T_{(m+1)} + \frac{T_{(m+2)}}{k_{m+2}} = -\int_{h_{(m+1)}} \zeta M dx$$

$$\frac{T_{(i-1)}}{k_i} - \left(\frac{1}{k_i} + \frac{1}{k_{i+1}} + \psi_{(i)}h_{(i)}\right) T_{(i)} + \frac{T_{(i+1)}}{k_{i+1}} = -\int_{h(i)} \zeta M dx$$

$$\frac{T_{(n-1)}}{k_n} - \left(\frac{1}{k_n} + \psi_{(n)} h_{(n)}\right) T_{(n)} = - \int_{h_{(n)}} \zeta M \, dx$$

This can be written in matrix notation as

$$[B] \{T\} = \{A\} \qquad (3.19.2)$$

[B] is a symmetric band matrix, with half band width three, and {A} is a vector, whose terms are,

$$B_{11} = - \left(\frac{1}{k_1} + \frac{1}{k_2} + \psi_{(1)} h_{(1)}\right) \qquad B_{12} = \frac{1}{k_2}$$

$$A_1 = \int_{h(1)} \zeta M \, dx$$

for $1 < i < m$

$$B_{i(i+1)} = \frac{1}{k_i}$$

$$B_{(i)} = - \left(\frac{1}{k_i} + \frac{1}{k_{i+1}} + \psi_{(i)} h_{(i)}\right)$$

$$B_{i(i+1)} = \frac{1}{k_{i+1}} \qquad A_i = \int_{h_{(i)}} \zeta M \, dx$$

$$B_{m(m)} = - \left(\frac{1}{k_m} + \psi_{(m)} h_{(m)}\right) \qquad B_{m(m+1)} = - \left(\frac{1}{k_{m+1}}\right) = -B_{m(m+2)}$$

$$B_{(m+1)(m+1)} = 1 \qquad B_{(m+1)(m+2)} = - \frac{\psi_{(m+1)}}{\psi_{(m)}}$$

$$A_m = \int_{h_{(m)}} \zeta M \, dx \qquad A_{m+1} = \frac{\zeta_{m+1} - \zeta_m}{\psi_{(m)}} M(H_2) \qquad (3.19.3)$$

for $(m+1) < i < (n+1)$

$$B_{i(i-1)} = \frac{1}{k_{i-1}}$$

$$B_{ii} = - \left(\frac{1}{k_{i-1}} + \frac{1}{k_i} + \psi_{(i-1)} h_{(i-1)}\right)$$

$$B_{i(i+1)} = \frac{1}{k_i} \qquad A_i = \int_{h_{(i-1)}} \zeta \, M dx$$

$$B_{(n+1)n} = \frac{1}{k_n} \qquad B_{(n+1)(n+1)} = -\left(\frac{1}{k_n} + \psi_{(n)} h_{(n)}\right)$$

$$A_{n+1} = \int_{h(n)} \zeta M \, dx$$

Having obtained the axial forces, we may get the shearing force per connecting beam Q_i from

for $1 < i < (m+1)$

$$Q_i = T_{(i)} - T_{(i-1)} \qquad (3.20.1)$$

for $m < i < n + 1$

$$Q_i = T_{(i+1)} - T_{(i)} \qquad (3.20.2)$$

The curvature, strain, internal moment and deflection of the shear wall can be determined as mentioned before.

3.4 Numerical Example

A 20 storey coupled shear wall with abrupt change of cross-section after the tenth floor, was solved using both the continuous and finite difference methods, solutions (I) and (II) are considered. The properties of the model were H = 190 ft., h = 9.5 ft., $H_1 = H_2 = 95$ ft., $A_{11} = A_{12} = 24$ Sq. Ft., $A_{21} = A_{22} = 16$ Sq. Ft., $I_{11} = I_{12} = 1152$ ft.^{4}, $I_{21} = I_{22} = 341$ ft.^{4}, $\ell_1 = 34$ ft., $\ell_2 = 26$ ft., b = 10 ft., $I_p = 0.625$ ft.^{4}, $E_1 = E_2 = 443000$ kips/Sq. ft., $Q_2 = 132$ kips.

The results obtained by the continuous and finite difference methods are consistant. Figs. (3.2), (3.3), (3.4), (3.5) show the distribution of forces and deformations of the model for solutions (I) and (II). We may notice the following at the change of cross-section:

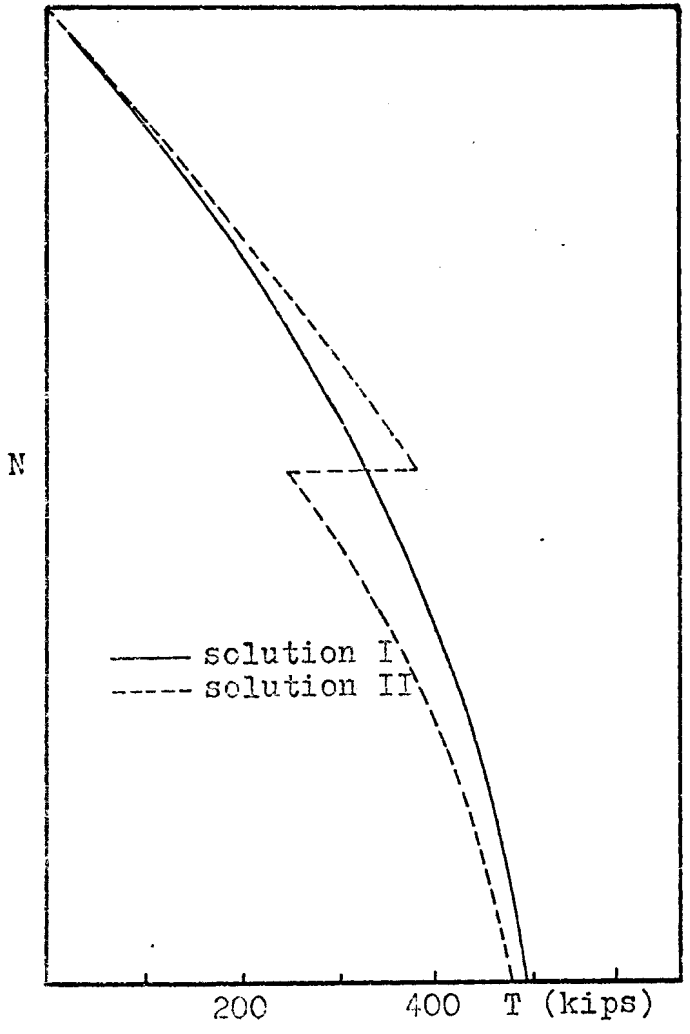

FIG. 3.2 T (DIAGRAM)

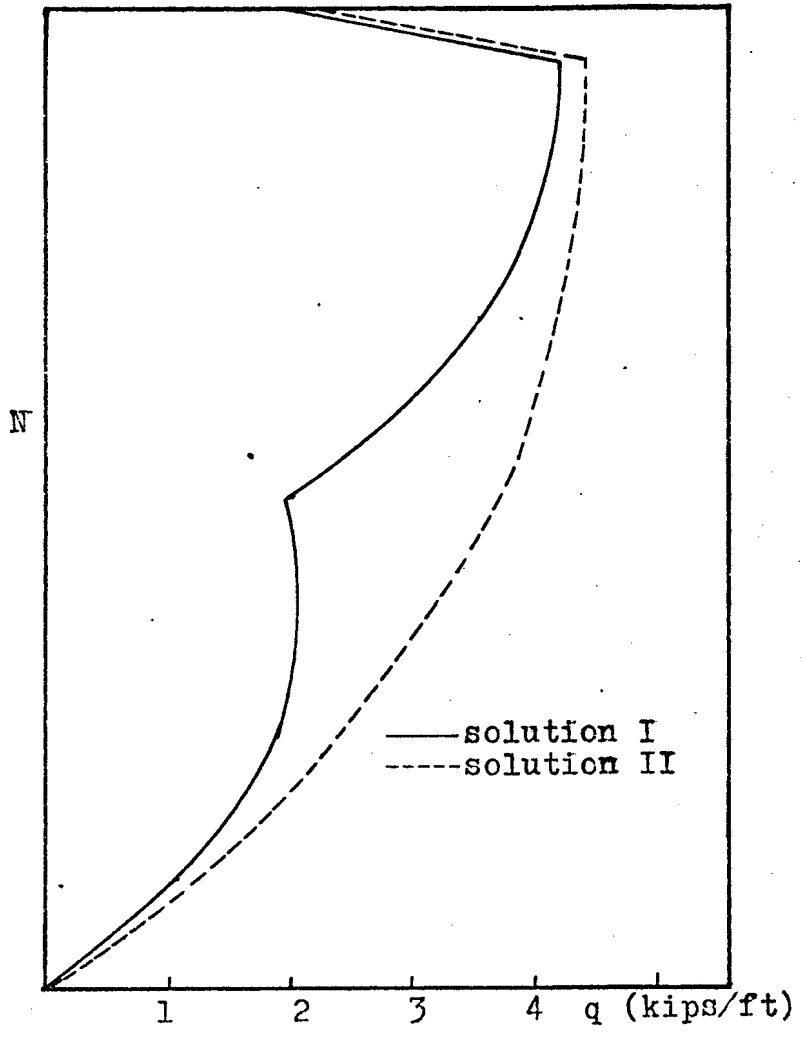

FIG. 3.3 q (DIAGRAM)

1) The axial force is continuous for solution (I) but there is a sudden change for solution (II), Fig. (3.2).

2) The rate of change of the shearing force is unique for solution (II), Fig. (3.3).

3) The strain has aunique value at the point of contraflexure for solution (II), Fig. (3.6).

4) The difference of deflection at the free end is not significant, however solution (II) gives more deflection than solution (I). So, we may say that the internal and external energy with solution (I) is less than that with solution (II). Due to the principle of total potential energy we may say that solution (I) is more realistic. Fig. (3.5).

5) The axial force at the base of the shear wall with solution (I) is less than that with solution (II), Fig. (3.2), while the internal moment with solution (I) is more than that with solution (II), Fig. (3.4).

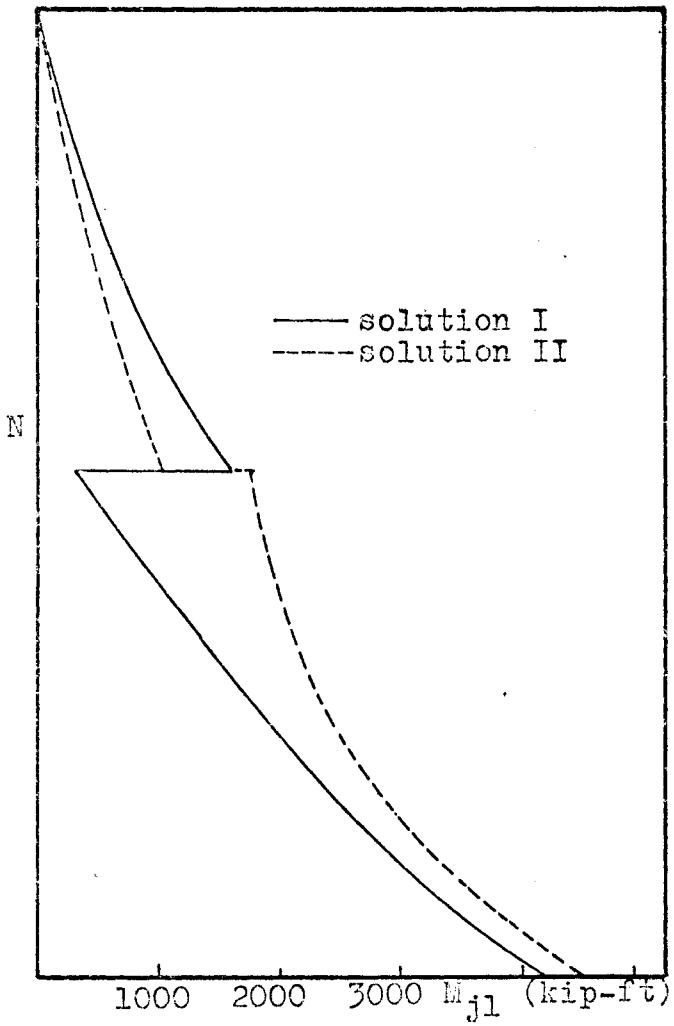

FIG. 3.4 $M_{j1}=M_{j2}$ (DIAGRAM)

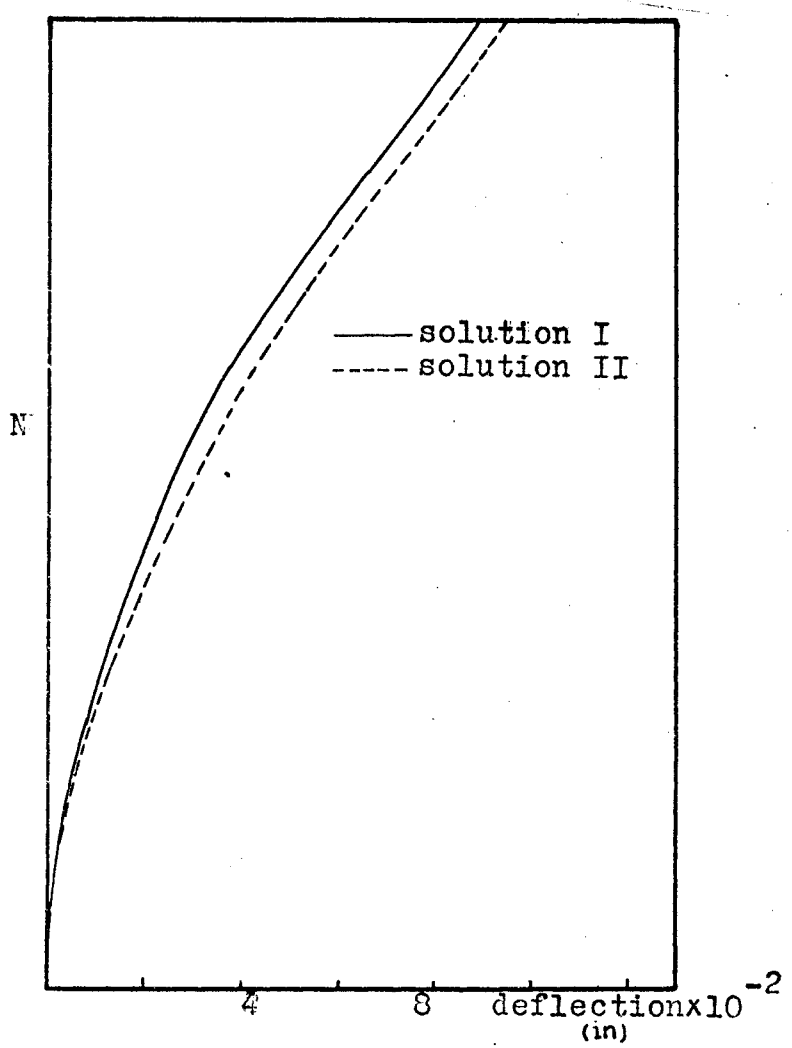

FIG. 3.5 DEFLECTION DIAGRAM

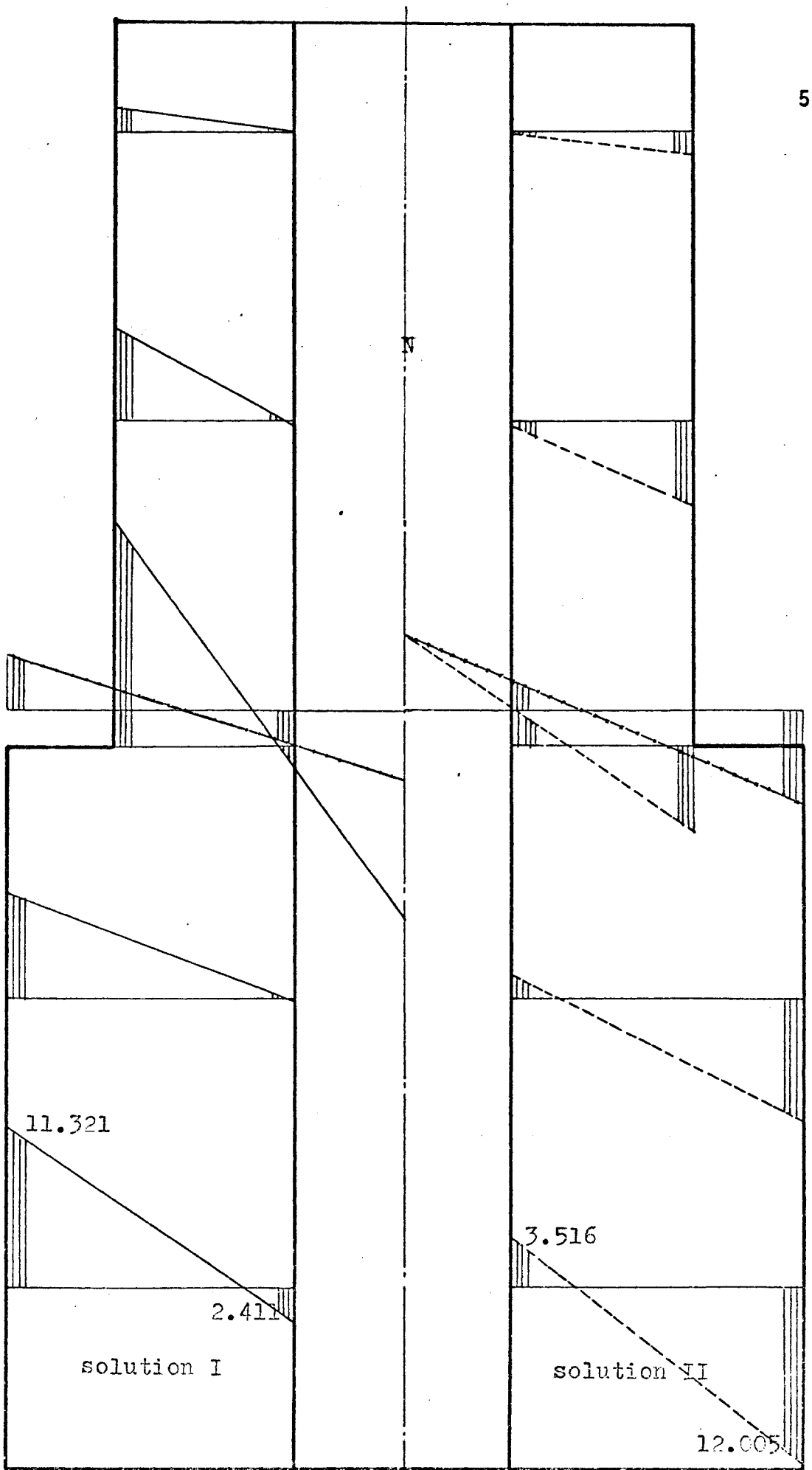

FIG. 3.6 STRAIN DISTRIBUTION AT DIFFERENT LEVELS.

CHAPTER 4

ANALYSIS OF COUPLED SHEAR WALLS BY ENERGY METHOD

4.1 General

The usual assumptions used in analysing coupled shear walls replaces the connecting beams by continuous rigid lamella which can carry only shearing forces. This suggests that a coupled shear wall can be analysed as a sandwich type (15) beam consisting of two faces between which a core is sandwiched.

The principle of the minimum of the total potential is used to analyse a coupled shear wall. The minimal principle furnishes all the necessary and sufficient conditions of equilibrium in the form of differential equations as well as boundary conditions. According to Hoff (15), "the minimal principle yields the easiest, and sometimes the only, solution".

We can analyse coupled shear walls with constant cross-section and then with variable cross-section to decide which of solution (I) or solution (II) presented before is the correct one. Figs. (2.1), (3.1).

4.2 Basic Assumptions

1) The connecting beams are replaced by continuous elastic lamella.

2) The essential components of the strain energy will be taken into account. These are the extensional and the bending strain energy stored in the piers and the shear strain energy stored in the core. The shear strain energy stored in the piers is neglected.

4.3 Prismatic Coupled Shear Walls

4.3.1 The Total Potential

The shear strain in the core is, Fig. (4.1),

$$e = e_1 - e_2 = \frac{u_1 - u_2}{\ell} - \frac{dv}{dx} \qquad (4.1.1)$$

The strain energy in the core is

$$U_c = \frac{G}{2} \int_{Vol} \left[\frac{u_1 - u_2}{\ell} - \frac{dv}{dx} \right]^2 d\,Vol \qquad (4.1.2)$$

Where G is the shear stress required to produce unit shear strain in the core.

It can be shown that

$$q.h = k.\gamma \qquad (4.1.3)$$

Multiplying by $\frac{\ell}{th}$ we get

$$\frac{qh}{th} / \frac{\gamma}{\ell} = \frac{k\ell}{th} \qquad (4.1.4)$$

i.e. $$G = \frac{k\ell}{th} \qquad (4.1.5)$$

where $$k = 1/\left[\frac{b^3}{12EI_p} + \frac{b}{GA^*_b} \right] \qquad (4.1.6)$$

also $$d\,Vol. = t\,dy\,dx \qquad (4.1.7)$$

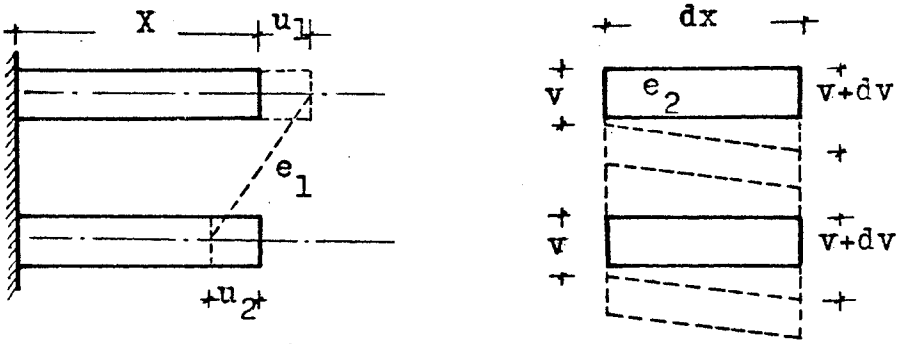

a) Strains caused by displacements

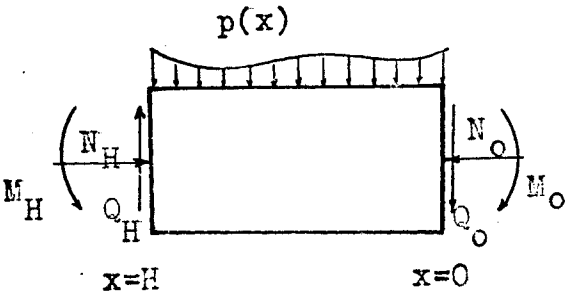

b) General extrnal applied load on prismatic coupled shear wall.

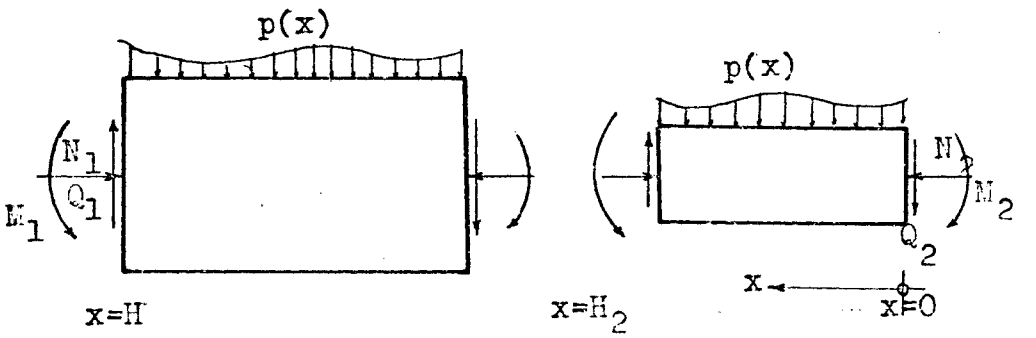

c) General external applied load on stepped coupled shear wall.

d) External forces at free end, case considered.

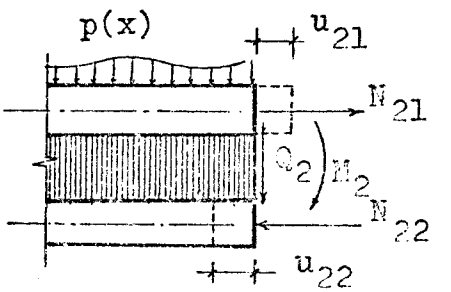

FIG. 4.1 STRAINS IN CORE AND EXTERNAL APPLIED LOADS ON SHEAR WALL.

With substituion of Eqs. (4.1.7), (4.1.5) in Eq. (4.1.2) we get

$$U_c = \frac{1}{2} \frac{k\ell^2}{h} \int_0^H \left[\frac{u_1 - u_2}{\ell} - \frac{dv}{dx} \right]^2 dx \qquad (4.1.8)$$

The total strain energy due to extensional deformation of the piers is

$$U_c = \frac{EA_1}{2} \int_0^H \left(\frac{du_1}{dx} \right)^2 dx + \frac{EA_2}{2} \int_0^H \left(\frac{du_2}{dx} \right) dx \qquad (4.2)$$

The total strain energy of bending stored in the two piers is

$$U_b = \frac{1}{2} (EI_1 + EI_2) \int_0^H \left(\frac{d^2v}{dx^2} \right)^2 dx \qquad (4.3)$$

So, the total strain energy is

$$U = \frac{1}{2} (EI_1 + EI_2) \int_0^H \left(\frac{d^2v}{dx^2} \right)^2 dx + \frac{EA_1}{2} \int_0^H \left(\frac{du_1}{dx} \right)^2 dx + \frac{EA_2}{2} \int_0^H \left(\frac{du_2}{dx} \right)^2 dx + \frac{k\ell^2}{2h} \int_0^H \left[\frac{u_1 - u_2}{\ell} - \frac{dv}{dx} \right]^2 dx \qquad (4.4)$$

Next, consider the change of potential of the applied external load, the total external work done is, Fig. (4.1),

$$V = - \int_0^H p\, v\, dx + M \frac{dv}{du} \Big|_0^H + Q\, v \Big|_0^H + N_1 u_1 \Big|_0^H + N_2 u_2 \Big|_0^H \qquad (4.5)$$

4.3.2 Minimization of Total Potential

Let $\Omega = U + V$ (4.6.1)

So $\delta \Omega = 0$ (4.6.2)

we may consider the various terms in order

$$\delta \left[\frac{1}{2} \int_0^H \left(\frac{d^2v}{dx^2} \right)^2 dx \right] = \int_0^H \left(\frac{d^2v}{dx^2} \delta \frac{d^2v}{dx^2} \right) dx$$

$$= \frac{d^2v}{dx^2} \delta \frac{dv}{dx} \Big|_0^H - \int_0^H \frac{d^3v}{dx^3} \delta \frac{dv}{dx} dx$$

$$= \frac{d^2v}{dx^2}\,\delta\,\frac{dv}{dx}\Big|_0^H - \frac{d^3v}{dx^3}\,\delta\,v\Big|_0^H + \int_0^H \frac{d^4v}{dx^4}\,\delta\,v\,dx$$

$$\delta\left[\frac{1}{2}\int_0^H \left(\frac{du}{dx}\right)^2 dx\right] = \int_0^H \frac{du}{dx}\,\delta\,\frac{du}{dx}\,dx$$

$$= \frac{du}{dx}\,\delta\,u\Big|_0^H - \int_0^H \frac{d^2u}{dx^2}\,\delta\,u\,dx$$

$$\delta\left[\frac{1}{2}\int_0^H \left[\frac{u_1-u_2}{\ell} - \frac{dv}{dx}\right]^2 dx\right] = \delta\int_0^H \frac{1}{2}\left[\left(\frac{u_1-u_2}{\ell}\right)^2 - \frac{2(u_1-u_2)}{\ell}\frac{dv}{dx} + \left(\frac{dv}{dx}\right)^2\right] dx$$

$$= \frac{1}{\ell^2}\int_0^H \frac{\delta(u_1-u_2)^2}{2}\,dx - \frac{1}{\ell}\int_0^H \delta\left[(u_1-u_2)\frac{dv}{dx}\right] dx$$

$$+ \int_0^H \frac{1}{2}\,\delta\left(\frac{dv}{dx}\right)^2 dx \qquad (4.6.1)$$

$$= \frac{1}{\ell^2}\int_0^H \left[(u_1-u_2)\,\delta u_1 + (u_2-u_1)\,\delta u_2\right] dx$$

$$- \frac{1}{\ell}\int_0^H \left(\frac{dv}{dx}\right)(\delta u_1 - \delta u_2)\,dx + \frac{1}{\ell}\int_0^H \left(\frac{du_1}{dx} - \frac{du_2}{dx}\right)\delta\,v\,dx$$

$$- \frac{1}{\ell}(u_1-u_2)\,\delta\,v\Big|_0^H + \frac{dv}{dx}\,\delta v\Big|_0^H - \int_0^H \frac{d^2v}{dx^2}\,\delta\,v\,dx$$

$$= \int_0^H \left[\frac{u_1-u_2}{\ell^2} - \frac{1}{\ell}\frac{dv}{dx}\right](\delta u_1 - \delta u_2)\,dx$$

$$+ \int_0^H \left[\frac{1}{\ell}\left(\frac{du_1}{dx} - \frac{du_2}{dx}\right) - \frac{d^2v}{dx^2}\right]\delta v\,dx + \left[\frac{dv}{dx} - \frac{u_1-u_2}{\ell}\right]\delta v\Big|_0^H$$

$$\delta\left[\int_0^H \frac{du_1}{dx}\,\frac{du_2}{dx}\,dx\right] = \int_0^H \frac{du_1}{dx}\,\delta\,\frac{du_2}{dx}\,dx + \int_0^H \frac{du_2}{dx}\,\delta\,\frac{du_1}{dx}\,dx$$

$$= \frac{du_1}{dx}\,\delta\,u_2\Big|_0^H + \frac{du_2}{dx}\,\delta\,u_1\Big|_0^H - \int_0^H \left[\frac{d^2u_1}{dx^2}\,\delta u_2 + \frac{d^2u_2}{dx^2}\,\delta\,u_1\right] dx$$

$$\delta V = -\int_0^H p\,\delta v\,dx + M\,\delta\frac{dv}{dx}\Big|_0^H + Q\,\delta v\Big|_0^H + N_1\,\delta u_1\Big|_0^H + N_2\,\delta u_2\Big|_0^H$$

Substitution of Eqs. (4.6.3) in Eq. (4.6.2) we get

$$(EI_1 + EI_2)\{ \frac{d^2v}{dx^2}\delta \frac{dv}{dx}\Big|_0^H - \frac{d^3v}{dx^3}\delta v\Big|_0^H + \int_0^H \frac{d^4v}{dx^4}\delta v\, dx \}$$

$$+ EA_1\{ \frac{du_1}{dx}\delta u_1\Big|_0^H - \int_0^H \frac{d^2u_1}{dx^2}\delta u_1\, dx\} + EA_2\{ \frac{du_2}{dx}\delta u_2\Big|_0^H - \int_0^H \frac{d^2u_2}{dx}\delta u_2\, dx\}$$

$$+ \frac{k\ell^2}{h}\{ \int_0^H [\frac{u_1-u_2}{\ell^2} - \frac{1}{\ell}\frac{dv}{dx}](\delta u_1-\delta u_2)\, dx + \int_0^H [\frac{1}{\ell}(\frac{du_1}{dx} - \frac{du_2}{dx}) - \frac{d^2v}{dx^2}]\delta v\, dx$$

$$+ [\frac{dv}{dx} - \frac{u_1-u_2}{\ell}]\delta v\Big|_0^H\} - \int_0^H p\,\delta v\, dx + M\,\delta\frac{dv}{dx}\Big|_0^H + Q\,\delta v\Big|_0^H$$

$$+ N_1\,\delta u_1\Big|_0^H + N_2\,\delta u_2\Big|_0^H = 0 \qquad (4.6.4)$$

$$[(EI_1 + EI_2)\frac{d^2v}{dx^2} + M]_0^H \delta\frac{dv}{dx} + [-(EI_1 + EI_2)\frac{d^3v}{dx^3} - \frac{k\ell^2}{h}(\frac{u_1-u_2}{\ell} - \frac{dv}{dx})$$

$$+ Q]_0^H \delta v + [EA_1\frac{du_1}{dx} - N_1]_0^H \delta u_1 + [EA_2\frac{du_2}{dx} - N_2]_0^H \delta u_2 +$$

$$\int_0^H [(EI_1 + EI_2)\frac{d^4v}{dx^4} + \frac{k\ell^2}{h}[\frac{1}{\ell}(\frac{du_1}{dx} - \frac{du_2}{dx}) - \frac{d^2v}{dx^2}] - p(x)]\,\delta v\, dx$$

$$+ \int_0^H [-EA_1\frac{d^2u_1}{dx^2} + \frac{k\ell^2}{h}\frac{1}{\ell}(\frac{u_1-u_2}{\ell} - \frac{dv}{dx})]\,\delta u_2\, dx +$$

$$\int_0^H [-EA_2\frac{d^2u_2}{dx^2} + \frac{k\ell^2}{h}\frac{1}{\ell}(\frac{u_1-u_2}{\ell} - \frac{dv}{dx})]\,\delta u_2\, dx = 0 \qquad (4.6.5)$$

Due to the fundamental lemma of the calculas of variations we get

$$EA_i\frac{d^2u_i}{dx^2} + \frac{k\ell^2}{h}(\frac{dv}{dx} - \frac{u_1-u_2}{\ell}) = 0 \qquad i = 1,2 \qquad (4.6.6)$$

$$(EI_1 + EI_2)\frac{d^4v}{dx^4} + \frac{k\ell^2}{h}(\frac{d^2v}{dx^2} - \frac{1}{\ell}\frac{d(u_1-u_2)}{dx}) - p(x) = 0 \qquad (4.6.7)$$

$$[(EI_1 + EI_2)\frac{d^2v}{dx^2} + M]_0^H = 0 \qquad (4.6.8)$$

$$[(EI_1 + EI_2)\frac{d^3v}{dx^3} - \frac{k\ell^2}{h}(\frac{dv}{dx} - \frac{u_1-u_2}{\ell}) + Q]_0^H = 0 \qquad (4.6.9)$$

$$\left[EA_i \frac{du_i}{dx} + N_i\right]_0^H = 0 \qquad i = 1, 2 \qquad (4.6.10)$$

Thus, the problem is reduced to solving the two simultaneous differential equations (4.6.6), (4.6.7) with the boundary conditions (4.6.8), (4.6.9), (4.6.10).

4.3.3 Derivation of the Differential Equation

The equilibrium can be written as

$$M_1(x) + M_2(x) = M(x) - T(x).\ell \qquad (4.7.1)$$

i.e. $$(EI_1 + EI_2) \frac{d^2v}{dx^2} = M - T\ell \qquad (4.7.2)$$

Differentiating twice yields

$$(EI_1 + EI_2) \frac{d^4v}{dx^4} = p(x) - \ell \frac{d^2T}{dx^2} \qquad (4.7.3)$$

The axial forces in the piers are

$$T = EA_1 \frac{du_1}{dx} = - EA_2 \frac{du_2}{dx} \qquad (4.7.4)$$

ie. $$\frac{du_1}{dx} = \frac{T}{EA_1} \quad \text{and} \quad \frac{du_2}{dx} = \frac{-T}{EA_2} \qquad (4.7.5)$$

So $$\frac{d(u_1 - u_2)}{dx} = T \left(\frac{1}{EA_1} + \frac{1}{EA_2}\right) \qquad (4.7.6)$$

Substitution of Eqa. (4.7.2), (4.7.3), (4.7.6) in Eq. (4.6.7) yields

$$\frac{d^2T}{dx^2} + \frac{k}{h}\left(\frac{1}{EA_1} + \frac{1}{EA_2} + \frac{\ell^2}{EI_1 + EI_2}\right) T = - \frac{k}{h} \frac{\ell}{EI_1 + EI_2} M \qquad (4.8.1)$$

or $$\frac{d^2T}{dx^2} + \frac{k}{h} \frac{\overline{EI}}{\overline{EA}.\Sigma EI} T = - \frac{k}{h} \frac{\ell}{\Sigma EI} M \qquad (4.8.2)$$

i.e. $$\frac{d^2T}{dx^2} - \alpha' T = - R M \qquad (4.8.3)$$

Eq. (4.8.3) is the well-known governing differential equation for coupled shear walls.

To get the boundary conditions, we proceed as below:

By making a cut at the line of contraflexure, and contraflexure, and considering the relative deformations of the cut system, the compatibility equation may be shown to be,

$$\ell \frac{dv}{dx} - \left[\frac{hb^3}{12EI_p} + \frac{hb}{GA_b^*} \right] q(x) - (u_1 - u_2) = 0 \qquad (4.9.1)$$

ie

$$q(x) = \frac{k\ell}{h} \left(\frac{dv}{dx} - \frac{u_1 - u_2}{\ell} \right) \qquad (4.9.2)$$

at $x = H$ $\quad u_1 = u_2 = 0$ and $\frac{dv}{dx} = 0$

ie $$\left.\frac{dT}{dx}\right|_{x=H} = 0 \qquad (4.10.1)$$

at $x = 0$ $\quad \left. T \right|_{x=0} = N$ from Eq. (4.6.10) $\qquad (4.10.2)$

To get the deflection of the coupled shear wall, substitution of Eq. (4.7.2) in Eq. (4.7.6) yields

$$\frac{d(u_1 - u_2)}{dx} = \frac{1}{\overline{EA}} \frac{1}{\ell} \left[M - \Sigma EI \frac{d^2v}{dx^2} \right] \qquad (4.11.1)$$

Substitution of Eq. (4.11.1) in Eq. (4.5.7) yields

$$\Sigma EI \frac{d^4v}{dx^4} - \frac{k\ell^2}{h} \left[\frac{d^2v}{dx^2} - \frac{1}{\ell^2} \frac{1}{\overline{EA}} (M - \Sigma EI \frac{d^2v}{dx^2}) \right] - p(x) = 0 \qquad (4.11.2)$$

ie $$\Sigma EI \frac{d^4v}{dx^4} - \frac{k\ell^2}{h} \left[1 + \frac{1}{\ell^2} \frac{\Sigma EI}{\overline{EA}} \right] \frac{d^2v}{dx^2} = p(x) - \frac{k}{h} \frac{1}{\overline{EA}} M \qquad (4.11.3)$$

ie $$\frac{d^4v}{dx^4} - \frac{k}{h} \frac{\overline{EI}}{\overline{EA}.\Sigma EI} \frac{d^2v}{dx^2} = \frac{p(x)}{\Sigma EI} - \frac{k}{h} \frac{1}{\overline{EA}.\Sigma EI} M \qquad (4.11.4)$$

or $$\frac{d^4v}{dx^4} - \alpha' \frac{d^2v}{dx^2} = \frac{p(x)}{\Sigma EI} - R' M \qquad (4.11.5)$$

where $$R' = \frac{k}{h} \frac{1}{\overline{EA}.\ \Sigma EI} \qquad (4.11.6)$$

The external moment M is

$$M(x) = + \frac{px^2}{2} + Q_0 x + M_0 + \frac{wx^2}{2} - \frac{wx^3}{6H} \qquad (4.12)$$

The deflection of the coupled shear wall is

$$v = C_1 \cosh\sqrt{\alpha'}x + C_2 \sinh\sqrt{\alpha'}x + C_3 + C_4 x + \left[\frac{p+w}{2}x^2 - \frac{w}{6H}x^3\right]\left[\frac{1}{\alpha'\Sigma EI} + \frac{R'}{\alpha'^2}\right] - \frac{R'}{\alpha'}\left[\frac{p+w}{24}x^4 + \frac{Q}{6}x^3 - \frac{M}{2}x^2 - \frac{w}{120H}x^5\right] \qquad (4.13.1)$$

The boundary conditions are

at $x = H$ $\quad v = 0$

$$\frac{dv}{dx} = 0 \qquad (4.13.2)$$

at $x = 0$ $\quad$ from Eq. (4.6.8) $\Sigma EI \frac{d^2v}{dx^2} = -M_0$

from Eqs. (4.6.9), (4.9.2)

$$\Sigma EI \frac{d^3v}{dx^3} - \ell\, q(x=0) = -Q_0$$

The deflection v can be determined by numerical integration of the curvature.

4.4 Coupled Shear Walls with variable cross-section

4.4.1 The Total Potential

We may assume the following geometrical properties at the sudden change of cross-section,

i.e. at $x = H_2$ $\quad v_1 = v_2 = v$

$$\frac{dv_1}{dx} = \frac{dv_2}{dx} = \frac{dv}{dx}$$

$$u_{11} = u_{21} = u_1, \quad u_{12} = u_{22} = u_2$$

This means that no dissipation of energy occurs at the sudden change of cross-section due to bending moment, shearing force and axial force at this section.

Zone (1): $H_2 \leqslant x \leqslant H$.

The total strain energy is

$$U_{(1)} = \frac{1}{2}(EI_{11} + EI_{12}) \int_{H_2}^{H} \left(\frac{d^2v_1}{dx^2}\right)^2 dx + \frac{EA_{11}}{2} \int_{H_2}^{H} \left(\frac{du_{11}}{dx}\right)^2 dx + \frac{EA_{12}}{2} \int_{H_2}^{H} \left(\frac{du_{12}}{dx}\right)^2 dx + \frac{k_1 \ell_1^2}{2h_1} \int_{H_2}^{H} \left[\frac{u_{11} - u_{12}}{\ell_1} - \frac{dv_1}{dx}\right]^2 dx \qquad (4.14.1)$$

Zone (2) $0 \leqslant x \leqslant H_2$

The total strain energy is

$$U_{(2)} = \frac{1}{2}(EI_{21} + EI_{22}) \int_{0}^{H_2} \left(\frac{d^2v_2}{dx^2}\right)^2 dx + \frac{EA_{21}}{2} \int_{0}^{H_2} \left(\frac{du_{21}}{dx}\right)^2 dx + \frac{EA_{22}}{2} \int_{0}^{H_2} \left(\frac{du_{22}}{dx}\right)^2 dx + \frac{k_2 \ell_2^2}{2h_2} \int_{0}^{H_2} \left[\frac{u_{21} - u_{22}}{\ell} - \frac{dv_2}{dx} - \frac{\ell - \ell_2}{\ell_2}\left(\frac{dv}{dx}\right)_{H_2}\right]^2 dx \qquad (4.14.2)$$

So the total strain energy is

$$U = U_{(1)} + U_{(2)} \qquad (4.14.3)$$

Next, the total external work done, for a general internal applied load, Fig. (4.1)

$$V = -\int_{H_2}^{H} p\, v_1\, dx - \int_0^{H_2} pv_2\, dx + M_1 \frac{dv_1}{dx}\Big|_{H_2}^{H} + Q_1 v_1\Big|_{H_2}^{H} + N_{11} u_{11}\Big|_{H_2}^{H}$$

$$+ N_{12} u_{12}\Big|_{H_2}^{H} + M_2 \frac{dv_2}{dx}\Big|_0^{H_2} + Q_2 v_2\Big|_0^{H_2} + N_{21} u_{21}\Big|_0^{H_2} + N_{22} u_{22}\Big|_0^{H_2} \qquad (4.14.4)$$

4.4.2 Minimization ofTotal Potential

Let $\Omega = U + v$ (4.15.1)

$\delta\, \Omega = 0$ (4.15.2)

consider the term,

$$\delta \{\frac{1}{2} \int_0^{H_2} [\frac{u_{21}-u_{22}}{\ell_2} - \frac{dv_2}{dx} - \frac{\ell_1 - \ell_2}{\ell_2} (\frac{dv}{dx})_{H_2}]^2 dx\} =$$

$$\int_0^{H_2} [\frac{u_{21}-u_{22}}{\ell_2} - \frac{dv_2}{dx} - \frac{\ell_1-\ell_2}{\ell_2} (\frac{dv}{dx}_{H_2})] \delta [\frac{u_{21}-u_{22}}{\ell_2} - \frac{dv_2}{dx} - \frac{\ell_1-\ell_2}{\ell_2}(\frac{dv}{dx}_{H_2})] dx$$

$$= \int_0^{H_2} [\frac{u_{21}-u_{22}}{\ell_2} - \frac{dv_2}{dx} - \frac{\ell_1-\ell_2}{\ell_2} (\frac{dv}{dx}_{H_2})] \delta [\frac{u_{21}-u_{22}}{\ell_2}] dx$$

$$- \int_0^{H_2} [\frac{u_{21}-u_{22}}{\ell_2} - \frac{dv_2}{dx} - \frac{\ell_1-\ell_2}{\ell_2} (\frac{dv}{dx}_{H_2})] \delta (\frac{dv_2}{dx}) dx$$

$$- \int_0^{H_2} [\frac{u_{21}-u_{22}}{\ell_2} - \frac{dv_2}{dx} - \frac{\ell_1-\ell_2}{\ell_2} (\frac{dv}{dx}_{H_2})] \delta [\frac{\ell_1-\ell_2}{\ell_2}(\frac{dv}{dx}_{H_2})] dx$$

$$= \int_0^{H_2} [\frac{u_{21}-u_{22}}{\ell_2} - \frac{dv_2}{dx} - \frac{\ell_1-\ell_2}{\ell_2} (\frac{dv}{dx}_{H_2})] \delta [\frac{u_{21}-u_{22}}{\ell_2}] dx$$

$$- \{[\frac{u_{21}-u_{22}}{\ell_2} - \frac{dv_2}{dx} - \frac{\ell_1-\ell_2}{\ell_2} (\frac{dv}{dx}_{H_2})] \delta v_2\}_0^{H_2}$$

$$+ \int_0^{H_2} [\frac{1}{\ell_2} \frac{d(u_{21}-u_{22})}{dx} - \frac{d^2v_2}{dx^2}] \delta v_2 dx - \int_0^{H_2} [\frac{u_{21}-u_{22}}{\ell_2} - \frac{dv_2}{dx}$$

$$- \frac{\ell_1-\ell_2}{\ell_2} (\frac{dv}{dx}_{H_2})] \delta [\frac{\ell_1-\ell_2}{\ell_2} (\frac{dv}{dx}_{H_2})] dx \qquad (4.15.3)$$

Substitution of Eqs. (4.6.3), (4.15.3) in Eq. (4.15.2) yields

$$[\Sigma EI_1 \frac{d^2v_1}{dx^2} + M_1]_{H_2}^{H} \delta \frac{dv_1}{dx} + [-\Sigma EI_1 \frac{d^3v_1}{dx^3} - \frac{k_{11}\ell^2}{h_1}(\frac{u_{11}-u_{12}}{\ell_1} - \frac{dv_1}{dx}) + Q_1]_{H_2}^{H} \delta v_1$$

$$+ [EA_{11} \frac{du_{11}}{dx} - N_{11}]_{H_2}^{H} \delta u_{11} + [EA_{12} \frac{du_{12}}{dx} - N_{12}]_{H_2}^{H} \delta u_{12} + \int_{H_2}^{H} [\Sigma EI_1 \frac{d^4v_1}{dx^4}$$

$$+ \frac{k_{11}\ell^2}{h_1}(\frac{1}{\ell_1} \frac{d(u_{11}-u_{12})}{dx} - \frac{dv_1^2}{dx^2} - p(x)]\delta v_1 \, dx + \int_{H_2}^{H} [-EA_{11} \frac{d^2u_{11}}{dx^2}$$

$$+ \frac{k_{11}\ell^2}{h_1} \frac{1}{\ell_1} (\frac{u_{11}-u_{12}}{\ell_1} - \frac{dv_1}{dx})] \delta u_{11} dx + \int_{H_2}^{H} [- EA_{12} \frac{d^2u_{12}}{dx^2} + \frac{k_{11}\ell^2}{h_1} \frac{1}{\ell_1}$$

$$(\frac{u_{11}-u_{12}}{\ell_2} - \frac{dv_1}{dx})] \delta u_{12} dx$$

$$+ [\Sigma EI_2 \frac{d^2v_2}{dx^2} + M_2]_{0}^{H_2} \delta \frac{dv_2}{dx} + [- \Sigma EI_1 \frac{d^3v_2}{dx^3} - \frac{k_{22}\ell^2}{h_2}(\frac{u_{21}-u_{22}}{\ell_2} - \frac{dv_2}{dx}$$

$$- \frac{\ell_1 - \ell_2}{\ell_2} (\frac{dv}{dx})_{H_2}) + Q_2]_{0}^{H_2} \delta v_2 + [EA_{21} \frac{du_{21}}{dx} - N_{21}]_{0}^{H_2} \delta u_{21}$$

$$+ [EA_{22} \frac{du_{22}}{dx} - N_{22}]_{0}^{H_2} \delta u_{22} + \int_{0}^{H_2} [\Sigma EI_1 \frac{d^4v_2}{dx^4} + \frac{k_{22}\ell^2}{h_2}(\frac{1}{\ell_2} \frac{d(u_{21}-u_{22})}{dx}$$

$$- \frac{d^2v_2}{dx^2}) - p(x)] \delta v_2 \, dx + \int_{0}^{H_2} [- EA_{21} \frac{d^2u_{21}}{dx^2} + \frac{k_{22}\ell^2}{h_2} \frac{1}{\ell_2}$$

$$(\frac{u_{21}-u_{22}}{\ell_2} - \frac{dv_2}{dx} - \frac{\ell_1 - \ell_2}{\ell_2} (\frac{dv}{dx})_{H_2}] \delta u_{12} dx + \int_{0}^{H_2} [-EA_{22} \frac{d^2u_{22}}{dx^2}$$

$$+ \frac{k_{22}\ell^2}{h_2} \frac{1}{\ell_2} (\frac{u_{21}-u_{22}}{\ell_2} - \frac{dv_2}{dx} - \frac{\ell_1 - \ell_2}{\ell_2} (\frac{dv}{dx})_{H_2}] \delta u_{22} dx -$$

$$\int_{0}^{H_2} [\frac{u_{21}-u_{22}}{\ell_2} - \frac{dv_2}{dx} - \frac{\ell_1 - \ell_2}{\ell_2} (\frac{dv}{dx})_{H_2})]\delta[\frac{\ell_1 - \ell_2}{\ell_2}(\frac{dv}{dx})_{H_2}] dx = 0 \quad (4.15.4)$$

Due to the principles of the calculus of variations we get, for a general external applied loads,

Zone (1):

$$EA_{1i}\frac{d^2u_{1i}}{dx^2}+\frac{k_1\ell_1}{h_1}\left(\frac{dv_1}{dx}-\frac{u_{11}-u_{12}}{\ell_1}\right)=0 \quad i=1,2 \qquad (4.16.1)$$

$$\Sigma EI_1\frac{d^4v_1}{dx^4}-\frac{k_1\ell_1^2}{h_1}\left(\frac{d^2v_1}{dx^2}-\frac{1}{\ell_1}\frac{d(u_{11}-u_{12})}{dx}\right)-p(x)=0 \qquad (4.16.2)$$

$$\left[\Sigma EI_1\frac{d^2v_1}{dx^2}+M_1\right]_{H_2}^{H}\delta\frac{dv_1}{dx}=0 \qquad (4.16.3)$$

$$\left[\Sigma EI_1\frac{d^3v_1}{dx^3}-\frac{k_1\ell_1^2}{h_1}\left(\frac{dv_1}{dx}-\frac{u_{11}-u_{12}}{\ell_1}\right)+Q_1\right]_{H_2}^{H}\delta v_2=0 \qquad (4.16.4)$$

$$\left[EA_{1i}\frac{du_{1i}}{dx}+N_{1i}\right]_{H_2}^{H}\delta u_{1i}=0 \quad i=1,2 \qquad (4.16.5)$$

Zone (2):

$$EA_{2i}\frac{d^2u_{2i}}{dx^2}+\frac{k_2\ell_2}{h_2}\left(\frac{dv_2}{dx}-\frac{u_{21}-u_{22}}{\ell_2}+\frac{\ell_1-\ell_2}{\ell_2}\left(\frac{dv}{dx}\right)_{H_2}\right)=0 \quad i=1,2 \qquad (4.17.1)$$

$$\Sigma EI_2\frac{d^4v_2}{dx^4}-\frac{k_2\ell_2^2}{h_2}\left(\frac{d^2v_2}{dx^2}-\frac{1}{\ell_2}\frac{d(u_{21}-u_{22})}{dx}\right)-p(x)=0 \qquad (4.17.2)$$

$$\left[\Sigma EI_2\frac{d^2v_2}{dx^2}+M_2\right]_{0}^{H_2}\delta\frac{dv_2}{dx} \qquad (4.17.3)$$

$$\left[\Sigma EI_2\frac{d^3v_2}{dx^3}-\frac{k_2\ell_2^2}{h_2}\left(\frac{dv_2}{dx}-\frac{u_{21}-u_{22}}{\ell_2}+\frac{\ell_1-\ell_2}{\ell_2}\left(\frac{dv}{dx}\right)_{H_2}\right)+Q_2\right]_{0}^{H_2}\delta v_2=0 \qquad (4.17.4)$$

$$\left[EA_{2i}\frac{du_{2i}}{dx}+N_{2i}\right]_{0}^{H_2}\delta u_{2i}=0 \quad i=1,2 \qquad (4.17.5)$$

at $x=H_2$

$$\delta\frac{dv_1}{dx}=\delta\frac{dv_2}{dx} \qquad (4.18.1)$$

$$\delta v_1=\delta v_2 \qquad (4.18.2)$$

$$\delta u_{1i}=\delta u_{2i} \quad i=1,2 \qquad (4.18.3)$$

The compatibility condition can be shown to be,

Zone (1):

$$\ell_1\frac{dv_1}{dx}-\left[\frac{h_1b^3}{12EI_{b_1}}+\frac{h_1b}{GA_1^*}\right]q_1-(u_{11}-u_{12})=0 \qquad (4.19.1)$$

Zone (2):

$$\ell_2 \frac{dv_2}{dx} - \left[\frac{h_2 b3}{12EI_{b_2}} + \frac{h_2 b}{GA^*_2}\right] q_2(x) - (u_{21}-u_{22}) + (\ell_1-\ell_2)\left(\frac{dv}{dx}\right)_{x=H_2} = 0 \qquad (4.19.2)$$

4.4.3 Derivation of the Differential Equations

Proceeding the same way as in the analysis of prismatic coupled shear walls, we may get the following differential equations,

Zone (1):

$$\frac{d^2T_1}{dx^2} - \frac{k_1}{h_1}\frac{\overline{EI}_1}{\overline{EA}_1.\Sigma EI_1}T_1 = -\frac{k_1}{h_1}\frac{\ell_1}{\Sigma EI_1}M \qquad (4.20.1)$$

Zone (2):

$$\frac{d^2T_2}{dx^2} - \frac{k_2}{h_2}\frac{\overline{EI}_2}{\overline{EA}_2.\Sigma EI_2}T_2 = -\frac{k_2}{h_2}\frac{\ell_2}{\Sigma EI_2}M \qquad (4.20.2)$$

where

$$\Sigma EI_i = EI_{i1} + EI_{i2} \qquad i = 1,2$$

$$\frac{1}{\overline{EA}_i} = \frac{1}{EA_{i1}} + \frac{1}{EA_{i2}} \qquad i = 1,2 \qquad (4.20.3)$$

$$\overline{EI}_i = \Sigma EI_i + \overline{EA}_i.\ell_i^2 \qquad i = 1,2$$

To get the boundary conditions for couples shear walls with variable cross-section subjected, only, to lateral loads over all its height and loads at the free end, i.e. there are no concentrated loads at the change of cross-section or at the fixed end,

1) at $x = H$ $\quad u_{11} = u_{12} = 0$ and $\dfrac{dv_1}{dx} = 0$

from Eq. (4.19.1) $\left.\dfrac{d T_1}{dx}\right|_{x=H} = 0$ (4.21.1)

2) at $x = 0$

from Eq. (4.17.5) $\left. T_2 \right|_{x=0} = N_2$ (4.21.2)

3) at $x = H_2$ $\quad u_1 = u_2$ and $\dfrac{dv_1}{dx} = \dfrac{dv_2}{dx}$

from Eqs. (4.19.1), (4.19.2)

$$q_1(H_2) = \frac{k_1 h_2}{k_2 h_1} q_2(H_2) \qquad (4.21.3)$$

4) at $x = H_2$

from Eqs. (4.16.5), (4.17.5), (4.18.3) we get

$$E A_{1i} \frac{du_{1i}}{dx} = E A_{2i} \frac{du_{2i}}{dx} \qquad i = 1,2$$

i.e. $$T_1(H_2) = T_2(H_2) \qquad (4.21.4)$$

If the external moment M is expressed as

$$M = + \frac{px^2}{2} + Q_2 x + M_2 + \frac{wx^2}{2} - \frac{wx^3}{6H} \qquad (4.22)$$

We may get the solution of the differential equations (4.20.1), (4.20.2) as,

$$T_2 = C_1 \cosh x\sqrt{\alpha_2'} + C_2 \sinh x\sqrt{\alpha_2'} + \frac{R_2}{\alpha_2'}\left(\frac{px^2}{2} + Q_2 x + M_2 + \frac{wx^2}{2} - \frac{wx^3}{6H}\right) + \frac{R_2}{\alpha_2'^2}\left(p+w - \frac{wx}{H}\right) \qquad (4.23.1)$$

$$T_1 = C_3 \cosh x\sqrt{\alpha_1'} + C_4 \sinh x\sqrt{\alpha_1'} - \frac{R_1}{\alpha_1'}\left(\frac{px^2}{2} + Q_1 x + M_2\right.$$

$$+ \frac{wx^2}{2} - \frac{wx^3}{6H}) + \frac{R_1}{\alpha_1'^2}(p + w - \frac{wx}{H}) \qquad (4.23.2)$$

Substitution of the boundary conditions yields

$$\begin{bmatrix} 1.0 & 0 & 0 & 0 \\ \cosh H_2\sqrt{\alpha_2'} & \sinh H_2\sqrt{\alpha_2'} & -\cosh H_2\sqrt{\alpha_1'} & -\sinh H_2\sqrt{\alpha_1'} \\ \frac{k_1 h_2}{k_2 h_1}\sqrt{\alpha_2'}\sinh H_2\sqrt{\alpha_2'} & \frac{k_1 h_2}{k_2 h_1}\sqrt{\alpha_2'}\cosh H_2\sqrt{\alpha_2'} & -\sqrt{\alpha_1'}\sinh H_2\sqrt{\alpha_1'} & -\sqrt{\alpha_1'}\cosh H_2\sqrt{\alpha_1'} \\ 0 & 0 & \sqrt{\alpha_1'}\sinh H\sqrt{\alpha_1'} & \sqrt{\alpha_1'}\cosh H\sqrt{\alpha_1'} \end{bmatrix} \begin{bmatrix} C_1 \\ C_2 \\ C_3 \\ C_4 \end{bmatrix}$$

$$\begin{bmatrix} \frac{R_2}{\alpha_2'^2}p + \frac{R_2}{\alpha_2'}M_2 + N_2 \\ (\frac{pH_2^2}{2} + Q_2H_2 + M_2 + \frac{wH_2^2}{2} - \frac{wH_2^3}{6H})(\frac{R_2}{\alpha_2'} - \frac{R_1}{\alpha_1'}) + (\frac{R_2}{\alpha_2'^2} - \frac{R_1}{\alpha_1'^2})(p + w - \frac{wH_2}{H}) \\ (pH_2 + Q_2 + wH_2 - \frac{wH_2^2}{2H})(\frac{R_2}{\alpha_2'} - \frac{R_1}{\alpha_1'}) - (\frac{R_2}{\alpha_2'^2} - \frac{R_1}{\alpha_1'^2})\frac{w}{H} \\ (pH + Q_2)\frac{R_1}{\alpha_1'} \end{bmatrix} \qquad (4.23.3)$$

We may notice that the solution obtained by the energy approach is consistent with solution (I) presented earlier if the storey height and the stiffness of the connecting beams are constant over the entire height of the coupled shear walls, i.e. that the term $k_1 h_2 / k_2 h_1$ becomes unity and Eqs. (4.23.3) will be consistent with Eq. (3.14).

The shearing forces can be determined from,

$$q_2 = C_1\sqrt{\alpha_2'}\sinh x\sqrt{\alpha_2'} + C_2\sqrt{\alpha_2'}\cosh x\sqrt{\alpha_2'} + \frac{R_2}{\alpha_2'}(px + Q_2 + wx - \frac{wx^2}{2H}) - \frac{R_2}{\alpha_2'^2}\frac{w}{H} \qquad (4.24.1)$$

$$q_1 = C_3\sqrt{\alpha_1'}\sinh x\sqrt{\alpha_1'} + C_4\sqrt{\alpha_1'}\cosh x\sqrt{\alpha_1'} + \frac{R_1}{\alpha_1'}(px + Q_2 + wx - \frac{wx^2}{2H}) - \frac{R_1}{\alpha_1'^2}\frac{w}{H} \qquad (4.24.2)$$

The internal bending moments of the piers can be determined from

$$M_{ji} = EI_{ji}\left[\frac{M - T_j.\ell_j}{\Sigma EI_j}\right] \qquad \begin{matrix} i = 1,2 \\ j = 1,2 \end{matrix} \qquad (4.25.1)$$

where the curvature of the piers is,

$$\phi_j = \frac{M - T_j.\ell_j}{\Sigma\, EI_j} \qquad j = 1,2 \qquad (4.25.2)$$

The deflection v can be determined by numerical integration of the curvature.

4.5 Conclusions:

1) The same energy approach may be used to analyse coupled shear walls with more than one sudden change of cross-section. Consider, for example, a coupled shear wall model with n cross-sections, i.e. with (n-1) sudden change of cross-section, Fig. (4.2)

The governing differential equations are

$$\frac{d^2T_j}{dx^2} - \frac{k_j}{h_j}\frac{\overline{EI}_j}{\overline{EA}_j.\Sigma EI_j}T_j = -\frac{k_j}{h_j}\frac{\ell_j}{\Sigma EI_j}M \qquad j=1,2,\ldots,n \qquad (4.26)$$

The boundary conditions are,

1) at x = 0

$$T_n(0) = N_n \qquad (4.27.1)$$

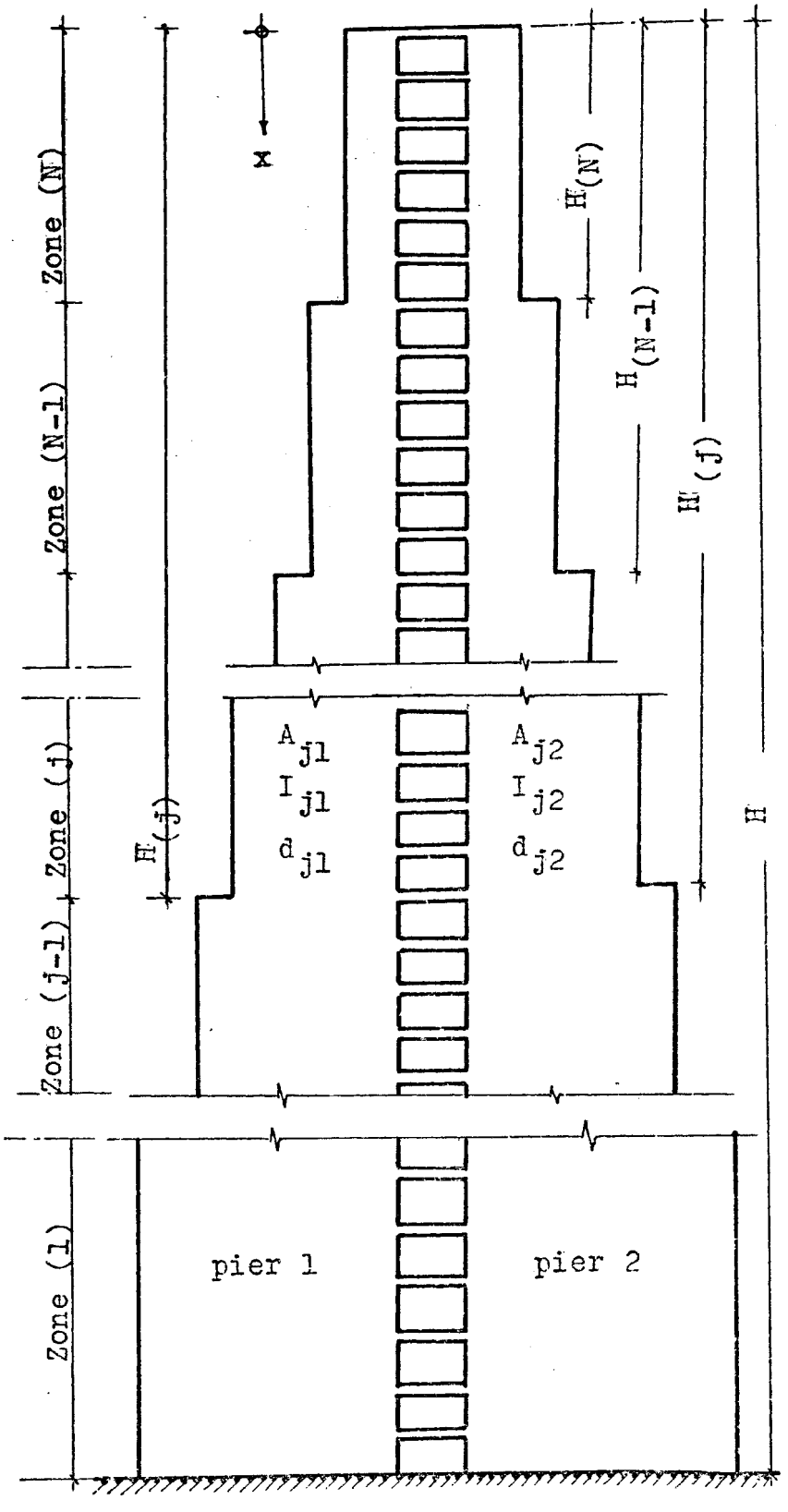

FIG. 4.2 COUPLED SHEAR WALL WITH "N" CROSS SECTIONS.

2) at $x = H$

$$\frac{dT_1}{dx} = 0 \qquad (4.27.2)$$

3) at $x = H_{j+1}$ $\qquad j = 1,2,\ldots,(n-1)$

$$T_j(H_{j+1}) = T_{j+1}(H_{j+1}) \qquad (4.27.3)$$

$$\frac{dT_j}{dx}(H_{j+1}) = \frac{k_j\, h_{j+1}}{k_{j+1} h_j} \frac{dT_{j+1}}{dx} \qquad (4.27.4)$$

This leads to (2n) simultaneous equations with (2n) unknowns. Having obtained C_1 to C_{2n}, the axial forces and shearing forces can be determined.

The curvature of the piers is

$$\phi_j = \frac{M - T_j \ell_j}{\Sigma E I_j} \qquad j = 1,2, \ldots.n \qquad (4.28)$$

The internal bending moments of the piers can be determined from,

$$M_{ji} = EI_{ji} \left[\frac{M - T_j \ell_j}{\Sigma E I_j} \right] \qquad j = 1,2,\ldots,n \qquad (4.29)$$

2) For a coupled shear wall with variable cross-section, Solution (I) presented before, after correction by the factor $k_2 h_1 / k_1 h_2$, is correct.

3) The finite difference solution (I) can be extended to take into account the analysis of coupled shear walls with more than one sudden change of cross-section.

CHAPTER 5

FINITE DIFFERENCE VERSUS FINITE ELEMENT METHODS

5.1 General

The problem of coupled shear walls may be approximated as a plane stress boundary value problem in a multiple connected region. The method has been explained in many publications, and in particular by Zienkiewicz (14). This part of the study, finite difference versus finite element, consists of three parts:

1) A coupled shear wall, with the bottom storey height three times the upper storey heights, was solved by the finite difference method and the results compared with the finite element solution done by Girijavallabhan (11). This shear wall may be solved by the usual continuous method.

2) Coupled shear walls with variable cross-section were solved by the finite element and finite difference methods (I) and (II) discussed earlier. The results are compared to confirm that solution (I) is the correct one. The interaction coefficient, αH, of the stepped shear wall was varied in order to examine the agreement of the finite difference and the continuous methods with the finite element method.

3) Prismatic coupled shear walls with different configurations and interaction coefficient, αH, were analysed to examine the agreement of the finite difference and the continuous methods with the finite element method and the effect of the interaction coefficient, for coupled shear walls of moderate height. For the finite element method the shear wall model was divided into discrete triangular elements. A sufficient number of nodal points and elements were chosen to obtain an accurate result. Figs. (5.6), (5.8), (5.9), (5.10), (5.11) show the different patterns chosen in the analysis.

5.2 Part One, Shear Wall With High Bottom Storey

Fig. (5.1) shows the dimensions of the model shear wall, the connecting beams, and the assumed values of the arbitrary lateral loads. The overall dimensions and loads are the same as those employed in an example problem by Gurfinkel (12) who solved it by the cantilever moment distribution method, and by Girijavallabhan (11), who solved it by the finite element method as a plane stress problem.

Girijavallabhan divided the model shear wall into discrete elements. Triangular elements and rectangular elements were used. The bottom nodal displacements were kept equal to zero.

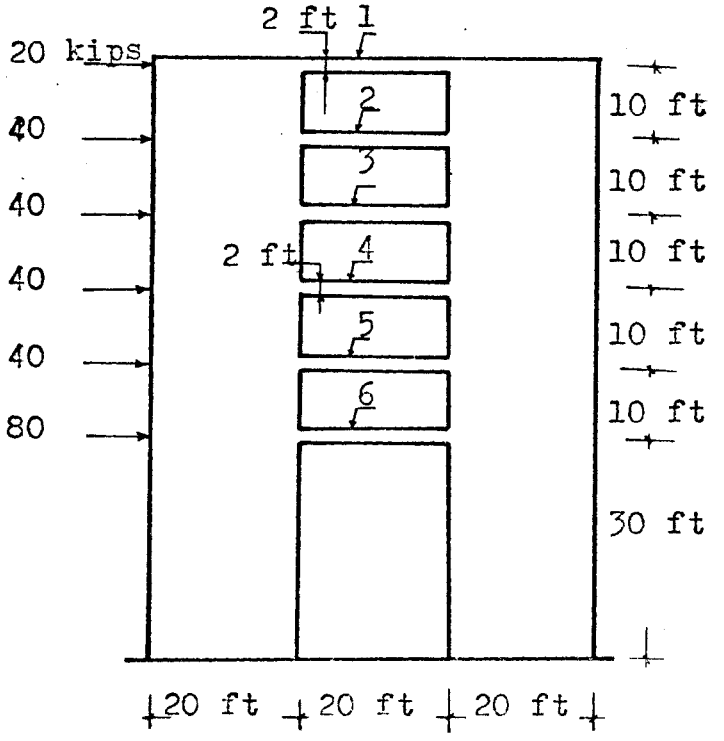

FIG. 5.1 MODEL SHEAR WALL PROBLEM

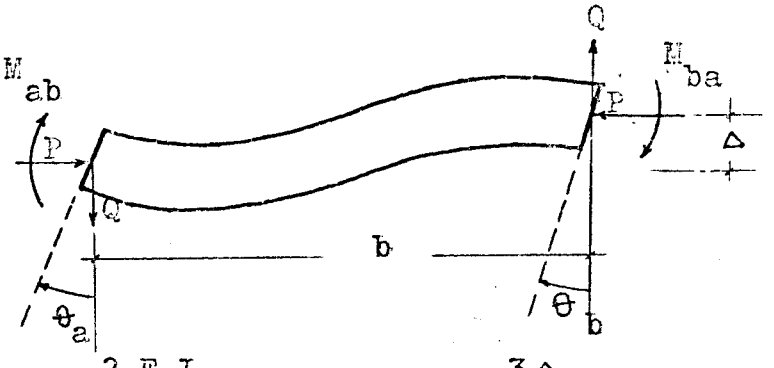

$$M_{ab} = \frac{2EI}{b}\left(2\theta_a + \theta_b + \frac{3\Delta}{b}\right)$$

FIG. 5.2 BEAM FORCES AND DEFORMATIONS

The shear wall was solved by the author using the finite difference method. The values obtained by the finite element method are taken from the paper by Girijavallabham (11).

Fig. (5.3a) shows an agreement between the deflection obtained by the two methods, Fig. (5.4) shows the stresses in y direction at different horizontal levels by the two methods. The difference in stresses at the base is about 8%. Table (5.1) compares the end bending moments in the lintel beams. The finite difference method gives values between those obtained by the finite element and the cantilever moment distribution methods. Generally, the results obtained by the finite difference method is more than that obtained by the finite element method.

Figs. (5.3b), (5.3c), (5.3d) show the distribution of the axial forces, shearing forces and internal moments obtained by the finite difference method together with smooth curves showing a continuous plot, which may be used for design purposes for such structures. No values for T, Q and M were given in Girijavallabham's paper.

TABLE (5.1)

COMPARISON OF RESULTS OBTAINED BY FINITE ELEMENT METHOD BY GIRIJAVALLABHAN, CANTILEVER MOMENT DISTRIBUTION METHOD BY GURFINKEL, AND FINITE DIFFERENCE METHOD

Lintel Beam or Panel No.	FINITE ELEMENT METHOD		CANTILEVER MOMENT DISTRIBUTION METHOD			FINITE DIFFERENCE METHOD			
	M_{ab}, in kip-feet	M_{ba}, in kip-feet	$M_{ab}=M_{ba}$, in kip-feet	T, in kip	M, in kip-feet	Q, in kip	$M_{ab}=M_{ba}$ in kip-feet	T, in kip	M, in kip-feet
1	31.37	31.60	75.97	4.91	97	7.422	74.22	7.6	60
2	38.75	38.27	76.57	9.85	203	7.488	74.88	15.0	125
3	40.29	39.79	76.92	16.41	572	7.532	75.32	23.0	450
4	41.33	41.06	75.77	22.80	1144	7.434	74.34	30.0	1000
5	41.10	40.89	72.02	30.21	1896	7.072	70.72	38.5	1800
6	38.48	38.48	64.10	36.78	5664	6.322	63.22	42.8	5380

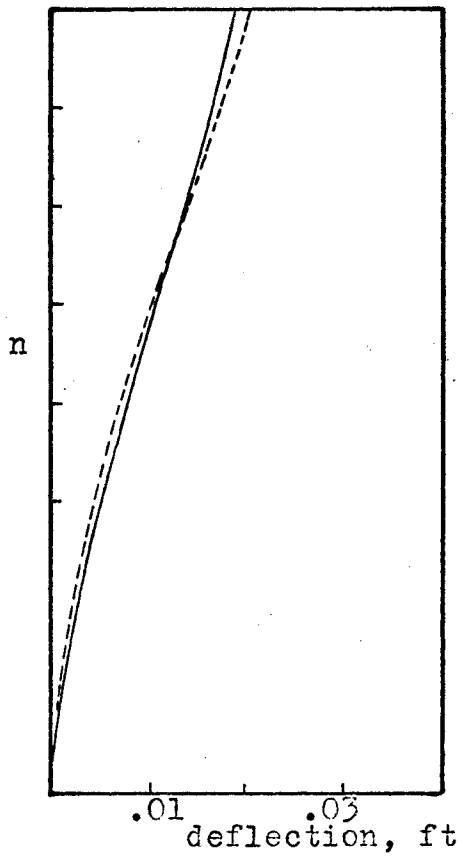

a) deflection diagrams

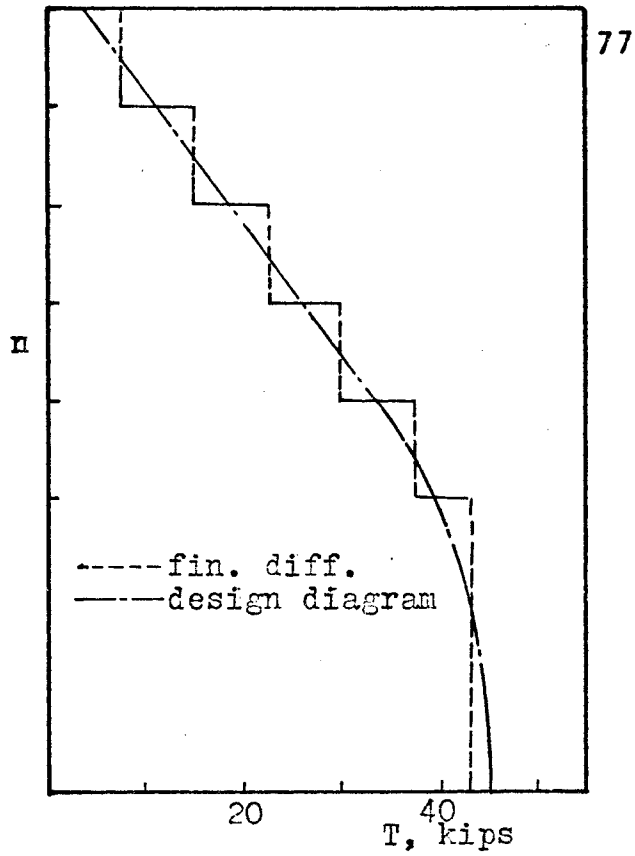

b) T diagrams

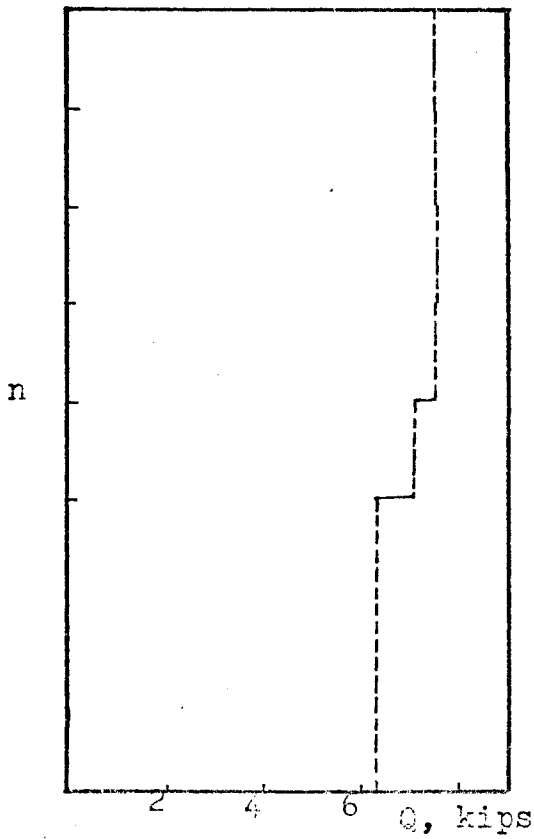

c) Q diagrams

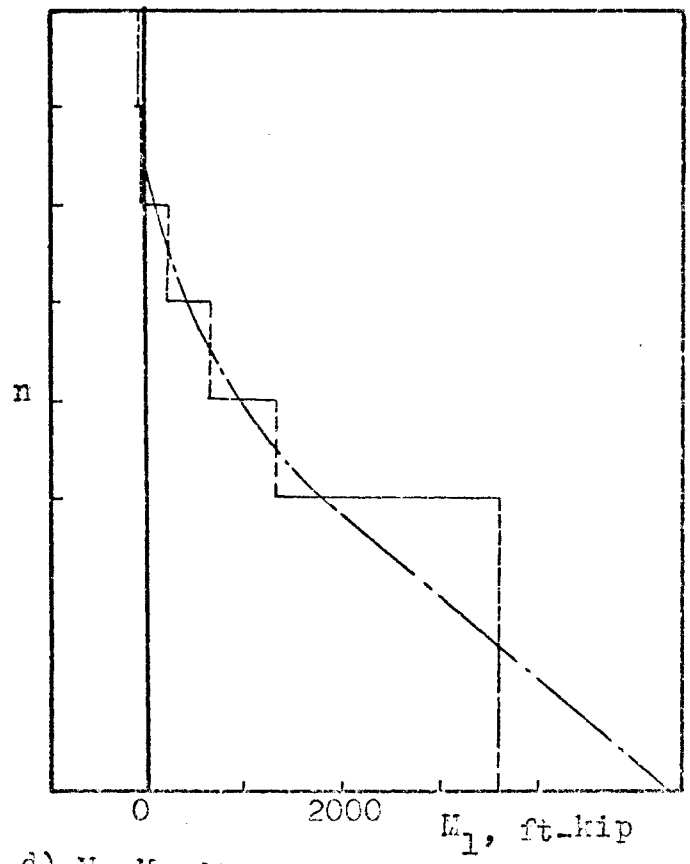

d) $M_1 = M_2$ diagrams

FIG. 5.3 DEFLECTION, T, Q AND M DIAGRAMS.

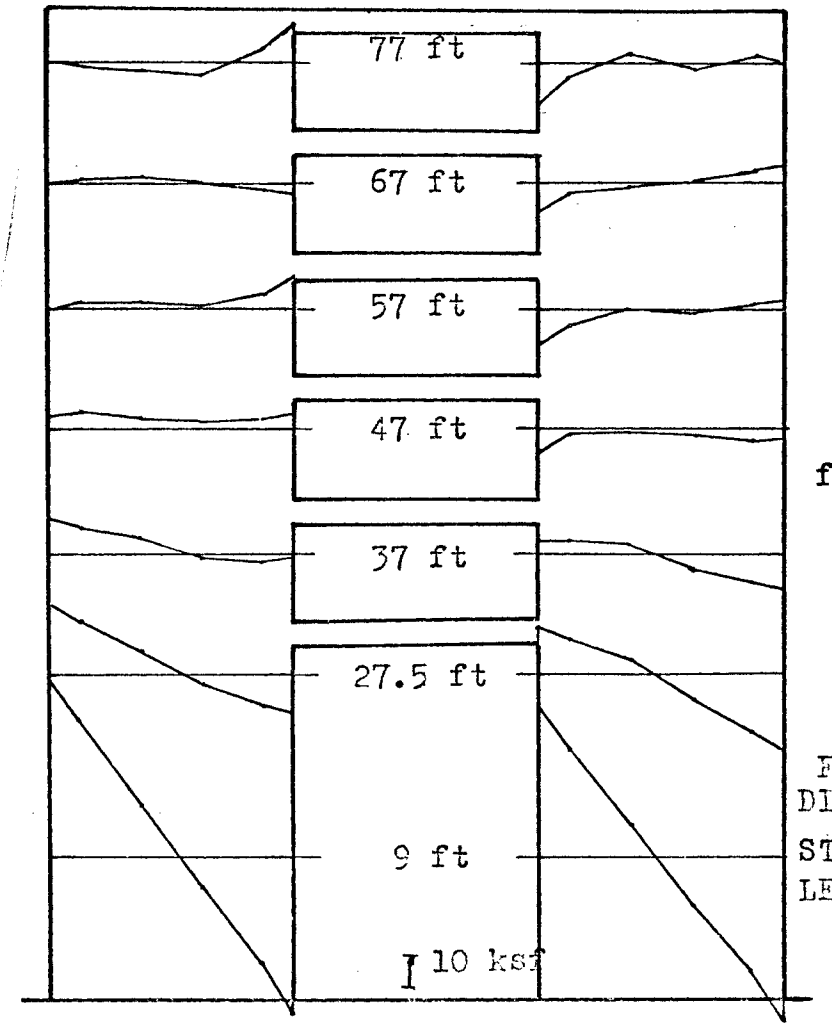

finite element

FIG. 5.4 HORIZONTAL DISTRIBUTION OF σ_y STRESSES AT VARIOUS LEVELS.

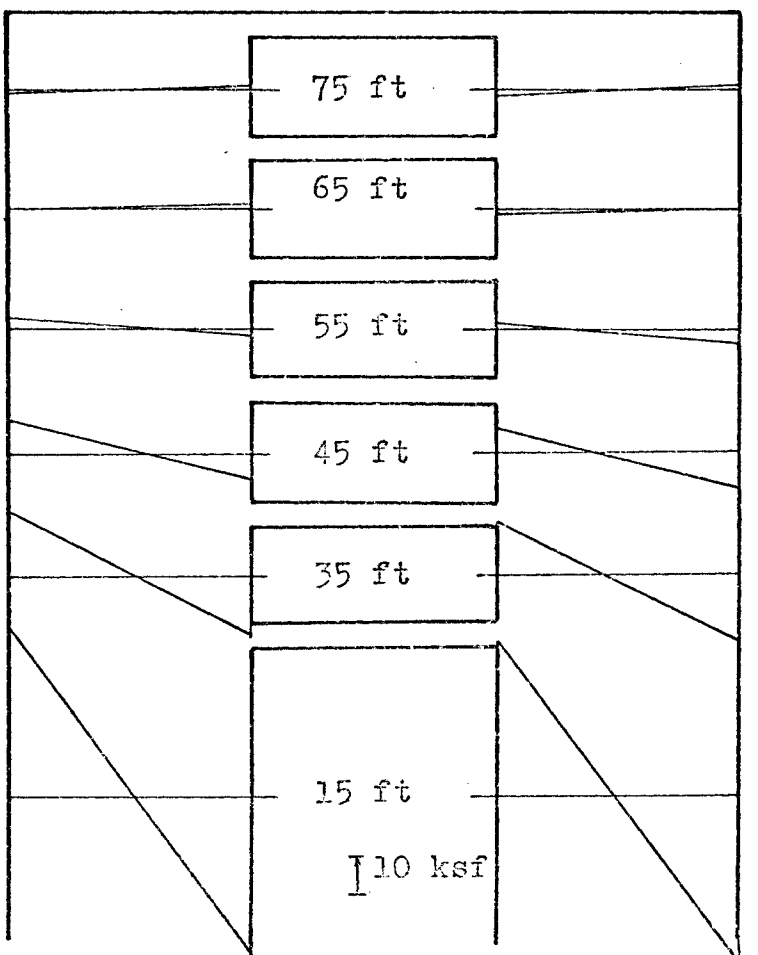

finite difference

5.3 Part Two, Coupled Shear Walls With Variable Cross-Section

5.3.1 Finite Difference Versus Finite Element Methods For a Shear Wall With Discrete Connecting Beams

A 10 storey building with an abrupt change of cross-section was solved by the finite element and the finite difference methods (I) and (II). Fig. (5.5) shows the shear wall model considered.

The end bending moments M_{ab}, M_{ba} in the lintel beams are computed using the slope deflection method, when using the finite element solution, Fig. (5.2). When the span-depth ratio of the connecting beam is small, i.e. for a deep beam, the slope deflection method is not valid, thus the moments M_{ab}, M_{ba} are superscripts by * in Tables, are computed from the shear stresses in the elements. We may mention that the shear stress in the finite elements of the connecting beams in this case was approximately constant.

5.3.2. Finite Element With Continuous Core

The usual assumption used in solving a coupled shear wall is that the connecting beams may be replaced by continuous rigid lamella which can carry shearing forces and has a shear modulus G as obtained before, from Eq. (4.1.5)

$$G = \frac{k\ell}{th} \tag{5.3}$$

The finite element method was used to solve a coupled shear wall with a continuous core. The properties of the core are such that it has only shear resistance. Doing so, i.e. using G as the main material property for the core, the

assembled stiffness matrix of the structure became ill-conditioned. Due to these difficulties arising in calculations some properties were given to the core to enable it to resist normal stresses in the x direction. Hence the results obtained are essentially for an approximate core. The thickness of the core is,

$$t = \frac{A_b^*}{h} \tag{5.4}$$

5.3.3 Discussion of Results

If the governing differential equation of a coupled shear wall is rewritten as,

$$\frac{d^2T}{dx^2} - \alpha^2 T = - R M \tag{5.5.1}$$

where

$$\alpha^2 = \frac{k}{h} \frac{\overline{EI}}{\overline{EA}.\Sigma EI} \tag{5.5.2}$$

We may use the parameter αH to represent the interaction coefficient of the coupled shear walls, similar to the interaction coefficient in composite beams (1) l/c determined as,

$$\frac{l}{c} = \frac{k}{h} \frac{\overline{EI}}{\overline{EA}.\Sigma EI} \cdot \frac{H^2}{\pi^2} \tag{5.5.3}$$

Table (5.2) gives the properties of the coupled shear wall models examined. Figs. (5.6.1), (5.6.4), (5.6.5) show the deformation and stress distribution at the base of the model obtained by finite difference solutions (I) and (II) and by finite element for a model with discrete connecting beams and with approximate core. Table (5.2.1) compares the results for the end moment in the lintel beams obtained

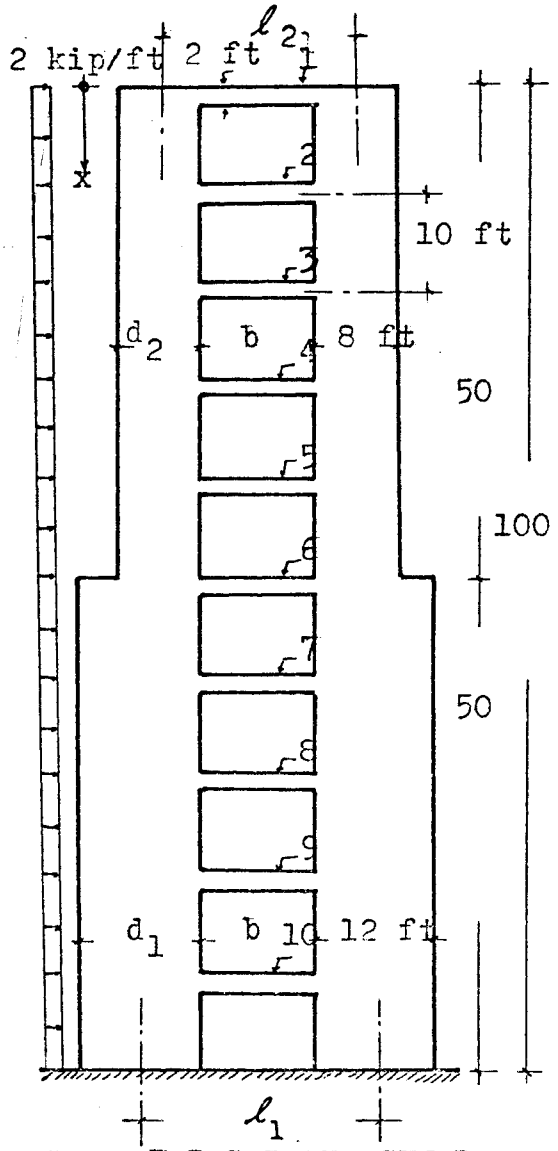

FIG. 5.5 STEPPED SHEAR WALL.

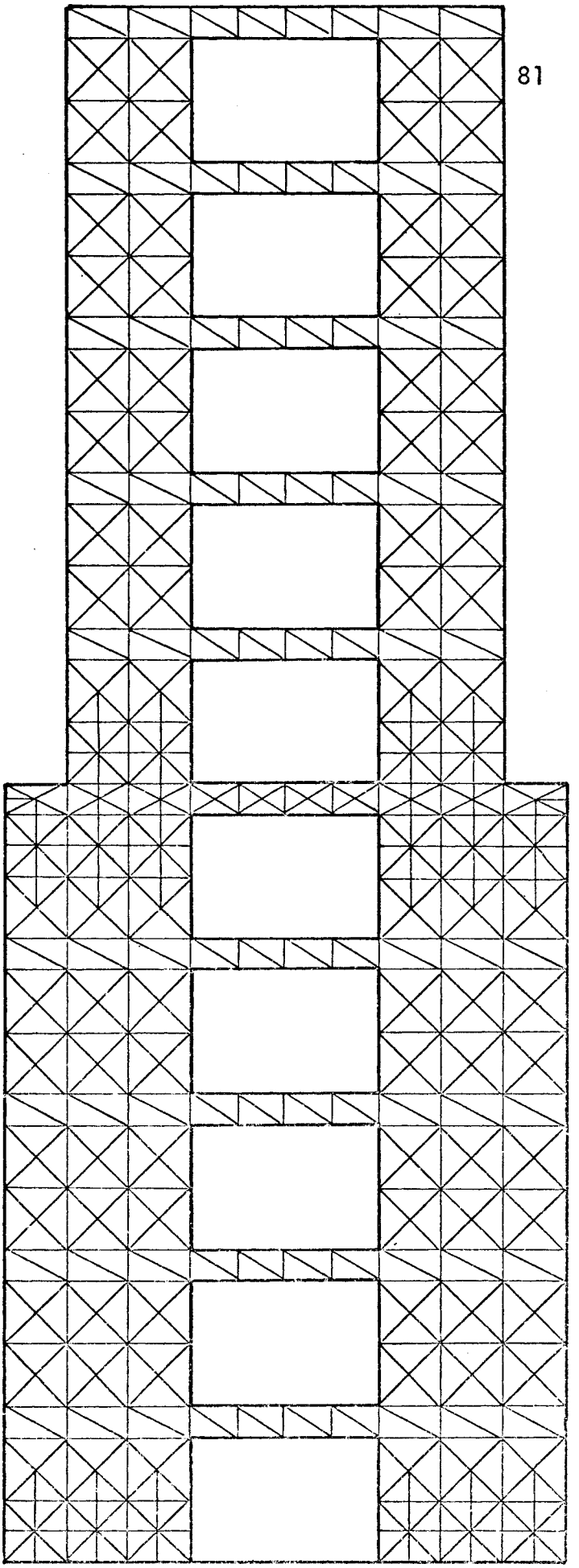

FIG. 5.6 FINITE ELEMENT PATTERN.
NE=692
NP=444

TABLE (5,2)

PROPERTIES OF STEPPED SHEAR WALLS

No.	d_1, in feet	d_2, in feet	ℓ_1, in feet	ℓ_2, in feet	b, in feet	$\frac{d_1}{b}$	$\frac{d_2}{b}$	$\frac{H}{d_1}$	$\frac{H}{d_2}$	k	α H.	
											Zone (1)	Zone (2)
1A	12	8	24	20	12	1.0	.67	8.5	12.5	1900	4.60	3.05
2A	12	8	20	16	8	1.5	1.0	8.5	12.5	7420	7.40	5.10
3A	12	8	16	12	4	3.0	2.0	8.5	12.5	33200	12.00	8.90
4A	12	8	15	11	3	4.0	2.67	8.5	12.5	59930	15.00	11.30

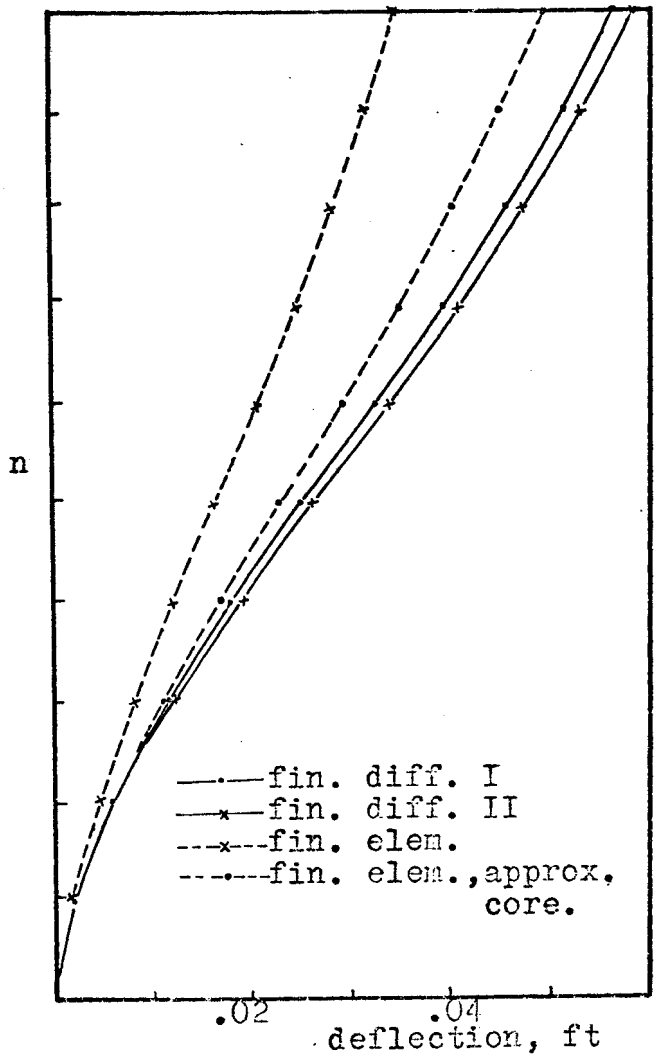

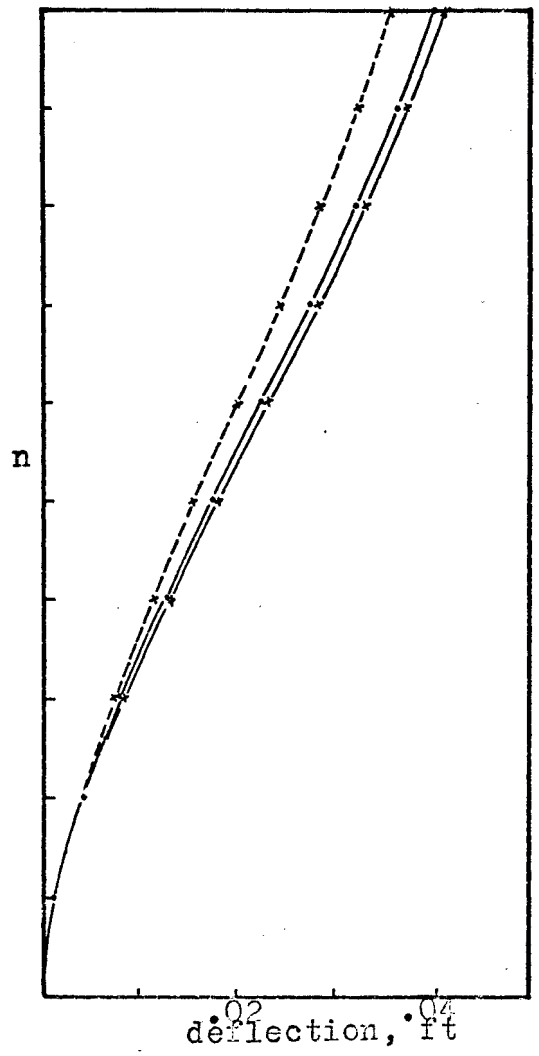

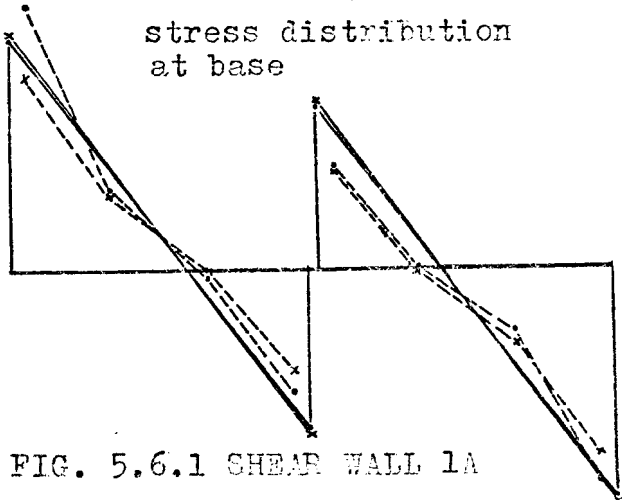

FIG. 5.6.1 SHEAR WALL 1A

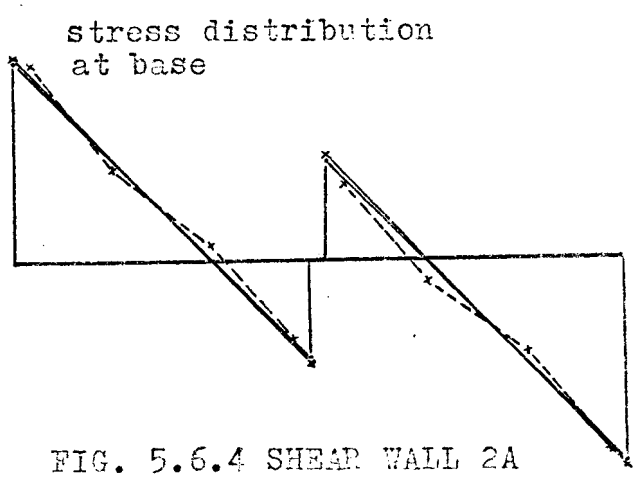

FIG. 5.6.4 SHEAR WALL 2A

OVER ALL DEFLECTION AND STRESS DISTRIBUTION AT BASE.
OF SHEAR WALL.

TABLE (5.2.1)

COMPARISON OF RESULTS OBTAINED BY FINITE ELEMENT METHOD AND FINITE DIFFERENCE METHOD FOR (1A), (4A)

Shear Wall	Lintel Beam	FINITE ELEMENT METHOD					FINITE DIFFERENCE METHOD (I)		FINITE DIFFERENCE METHOD (II)	
		θ_a, in radians, $x10^{-4}$	θ_b, in radians $x10^{-4}$	Δ, in kip-feet	M_{ab}, in kip-feet	M_{ba}, in kip-feet	Q, in kip	$M_{ab}=M_{ba}$ in Kip-feet	Q, in kip	$M_{ab}=M_{ba}$ in Kip-feet
1A	1	1.978	2.017	-1.216	14.4	14.6	13.412	80.5	13.787	82.7
	2	2.202	2.233	-0.962	20.8	21.0	16.087	96.5	16.548	99.2
	3	2.378	2,398	-0.556	28.5	28.6	20.052	120.0	20.705	124.2
	4	2.520	2.540	-0.051	36.7	36.9	24.044	144.0	25.037	150.2
	5	2.541	2.605	0.500	44.0	44.2	26.804	160.7	28.365	170.0
	6	2.818	2.789	1.009	53.8	53.7	26.794	160.7	29.280	176.0
	7	2.257	2.298	1.308	49.7	49.8	27.454	164.7	29.196	175.0
	8	2.051	2.090	1.568	49.7	49.8	26.161	156.7	27.334	164.0
	9	1.675	1.722	1.597	44.7	44.8	22.013	132.0	22.736	136.3
	10	1.103	1.109	1.185	30.9	30.9	13.824	82.9	14.168	85.0
4A	1	-	-	-	10.5	10.5	5.23	7.85	5.26	7.88
	2	-	-	-	27.2	27.2	17.91	26.90	18.01	27.00
	3	-	-	-	47.0	47.0	30.91	46.40	31.29	47.00
	4	-	-	-	66.7	66.7	43.39	65.80	45.40	68.20
	5	-	-	-	80.5	80.5	51.28	77.00	57.31	86.00
	6	-	-	-	52.5	52.5	34.87	52.30	59.04	88.50
	7	-	-	-	83.3	83.3	57.82	86.70	66.03	99.0
	8	-	-	-	104.6	104.6	70.35	105.50	73.14	109.70
	9	-	-	-	111.7	111.7	74.46	111.70	75.40	113.30
	10	-	-	-	93.0	93.0	61.32	92.00	61.61	92.40

by finite difference methods I and II and finite element with discrete connecting beams. Figs. (5.6.2), (5.6.3) give the distribution of σ_y stresses at different horizontal levels by the finite element method with discrete connecting beams and by the finite difference methods I and II. Table (5.2.2) gives a final comparison of the end moments in the connecting beams and the free end deflection obtained by the two methods.

We may come to the following conclusions,

1) The distribution of stresses at the base of the shear wall model follows the theory of simple bending.

2) The agreement between the results obtained by the finite element and the finite difference methods starts with the values of $\alpha H > 9.0$, Tables (5.2.2), (5.2).

3) Examining example 4A, the deflection obtained by the finite difference solutions I and II are consistent, however there is a big difference in the shearing force in the connecting beam at the sudden change of cross-section. Fig. (5.6.7) shows the distribution of M_{ab} obtained by the different methods. The best agreement is between finite difference (I) and the finite element method. Solution (I) is the correct solution for coupled shear walls with variable cross-section.

4) For values of $\alpha H < 9.0$, the finite difference method as well as the continuous connection method gives higher and conservative values for the forces and the deflection of the coupled shear walls compared to the finite element method.

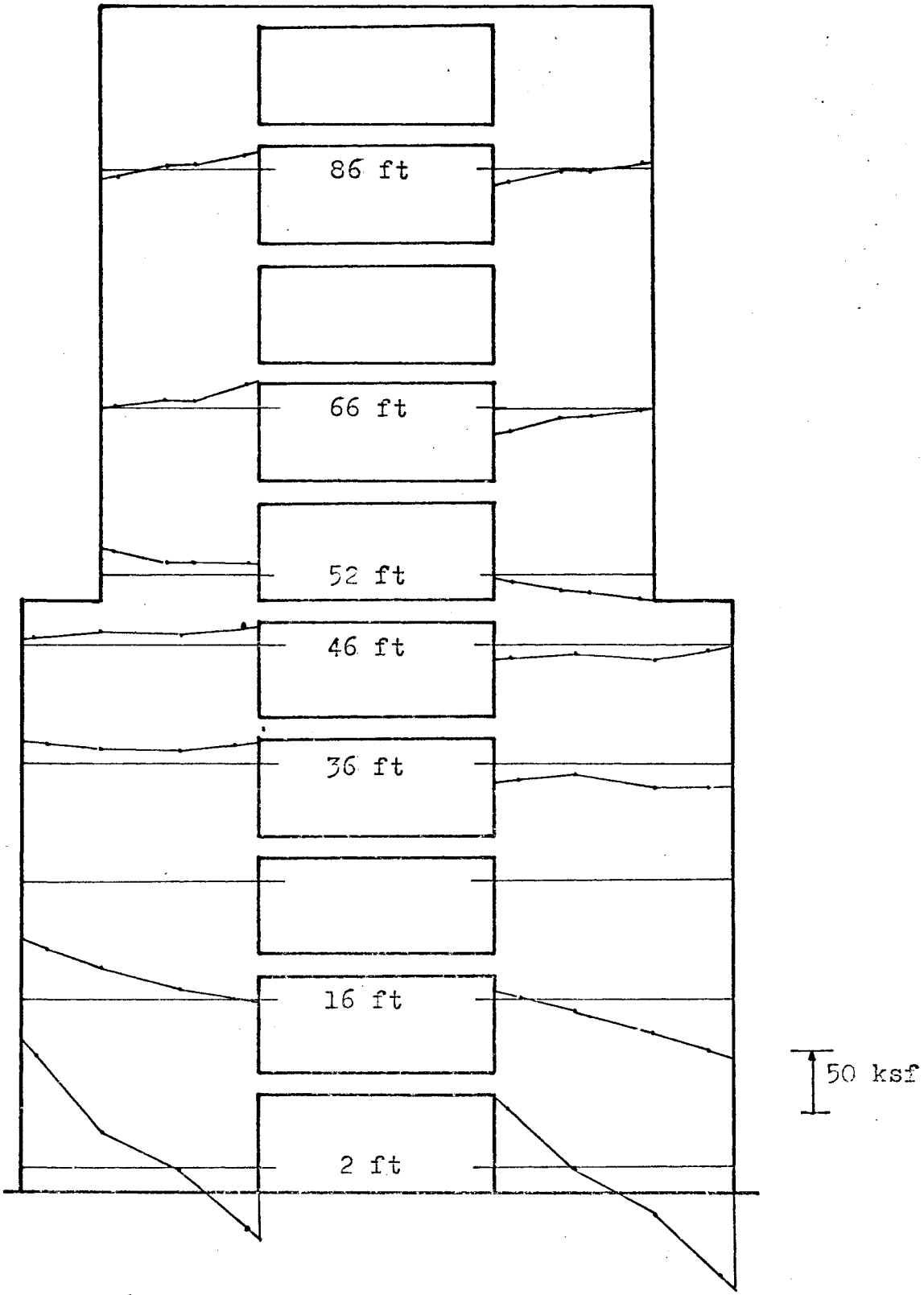

FIG. 5.6.2 HORIZONTAL DISTRIBUTION OF σ_Y STRESSES AT VARIOUS LEVELS. FINITE ELEMENT METHOD.

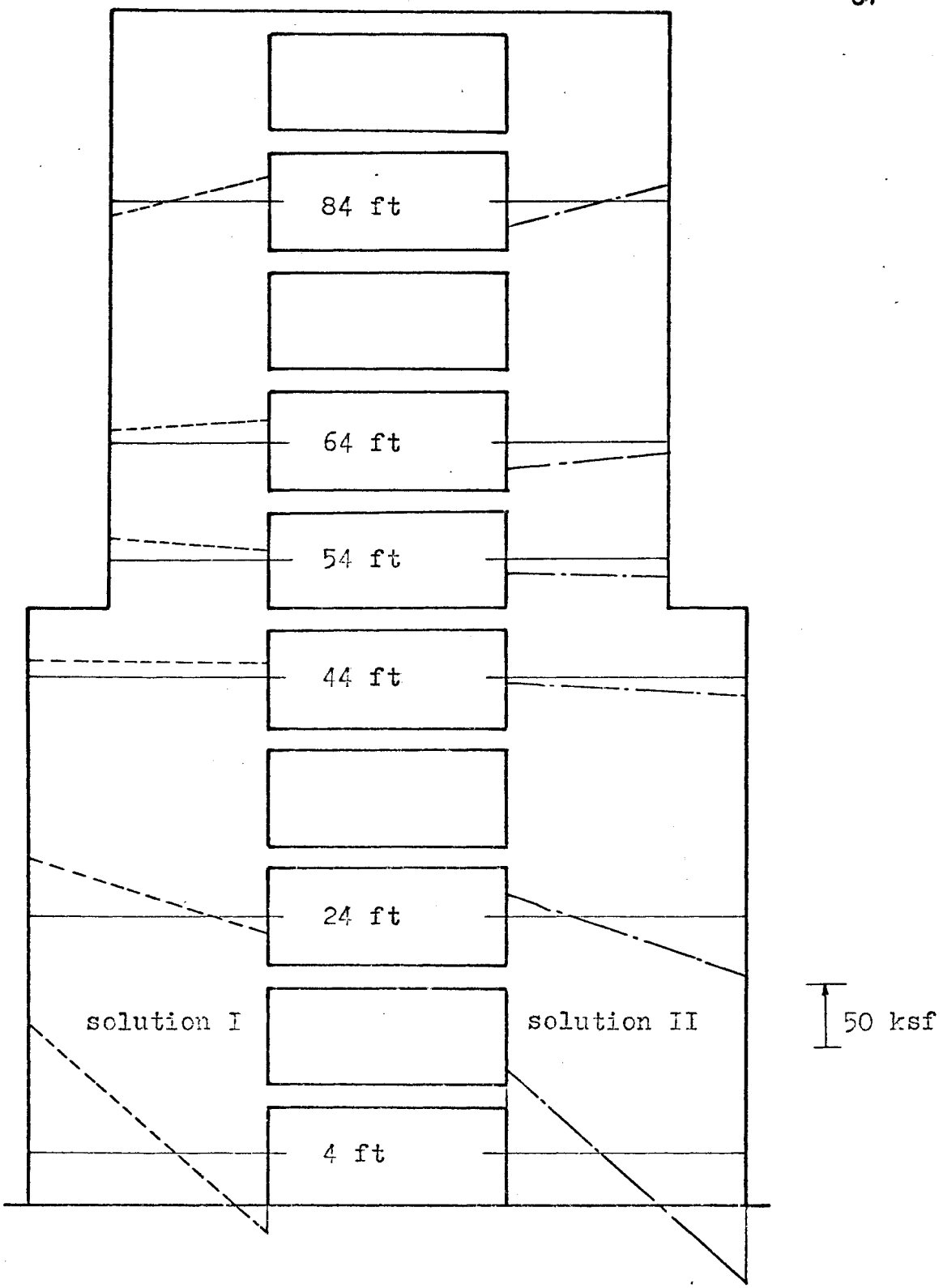

FIG. 5.6.3 HORIZONTAL DISTRIBUTION OF σ_Y STRESSES AT VARIOUS LEVELS.
FINITE DIFFERENCE METHOD.

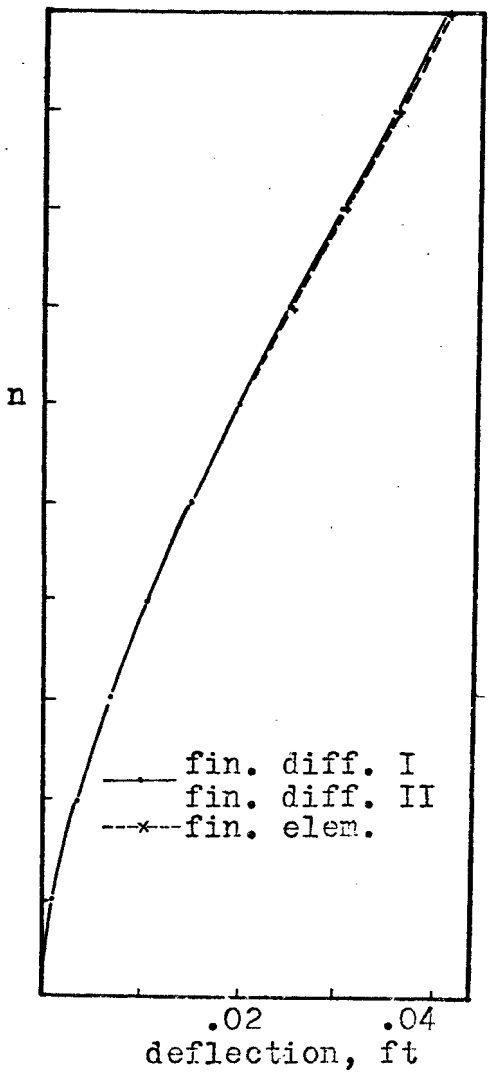

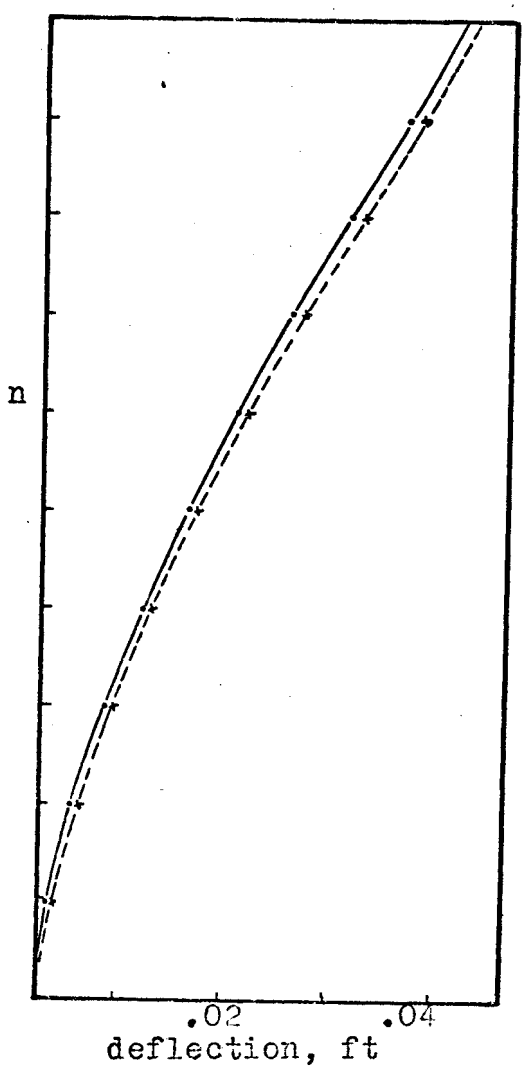

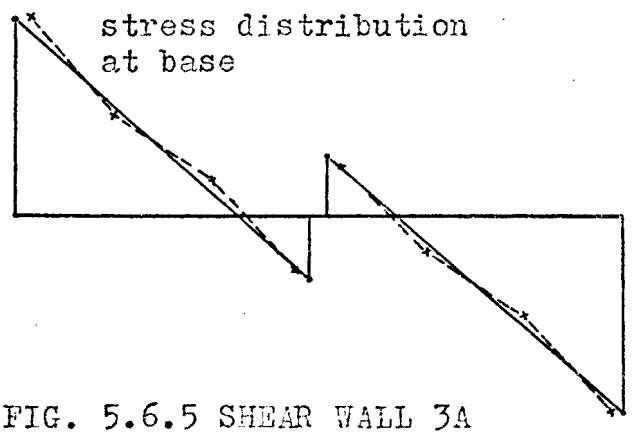

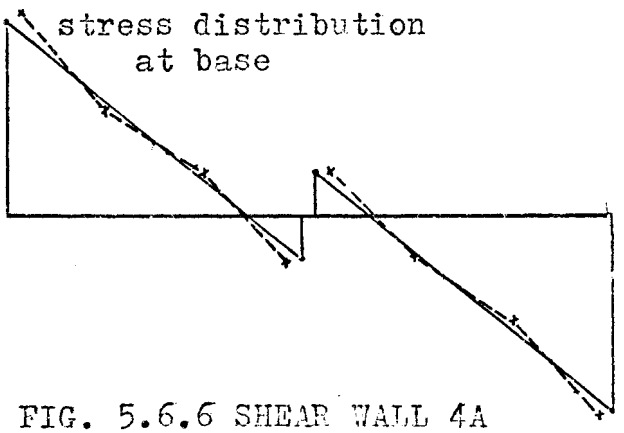

FIG. 5.6.5 SHEAR WALL 3A

FIG. 5.6.6 SHEAR WALL 4A

COVER ALL DEFLECTION AND STRESS DISTRIBUTION AT BASE OF SHEAR WALL.

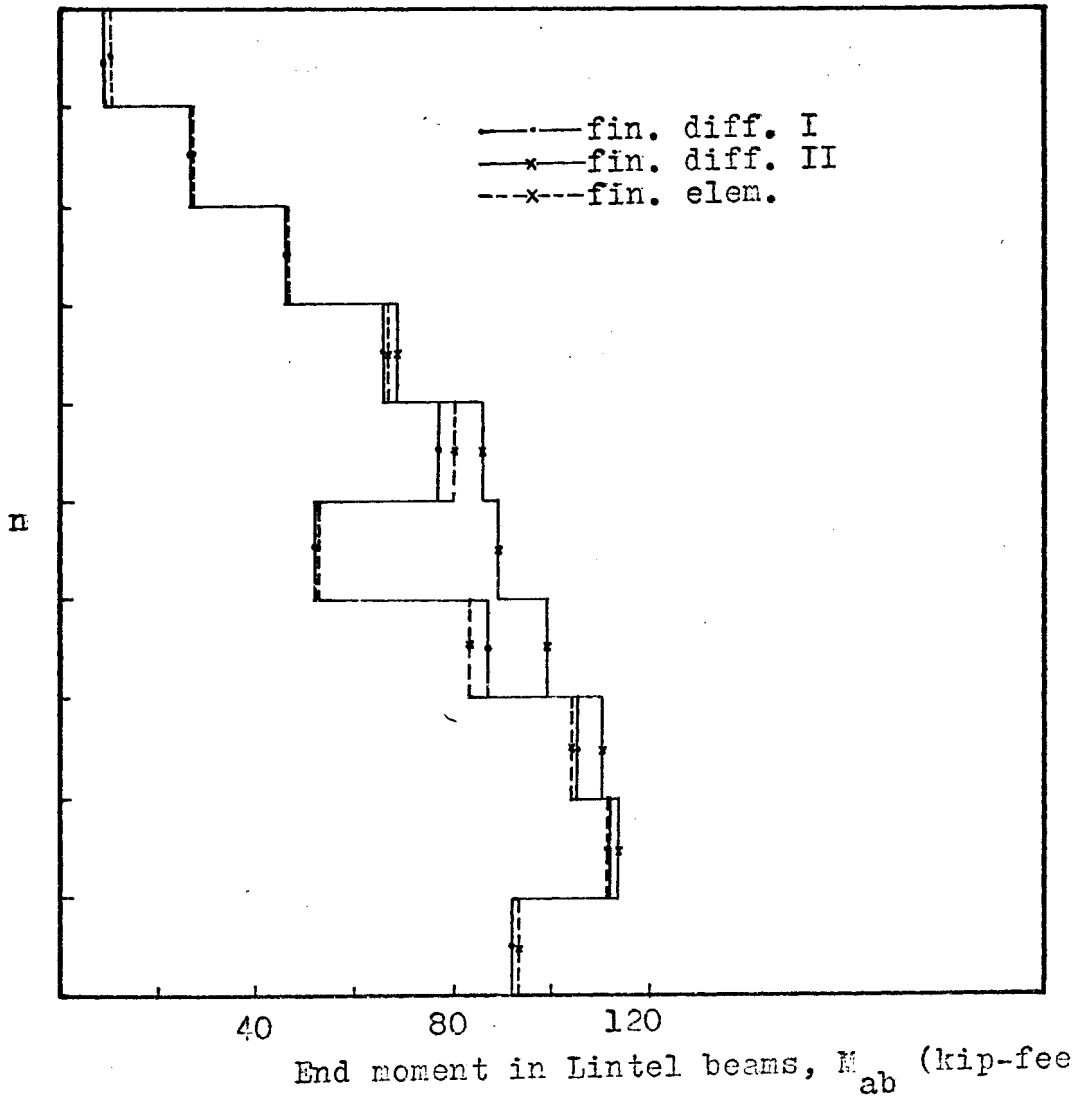

FIG. 5.6.7 M_{ab}, END MOMENT IN LINTEL BEAMS, DIAGRAMS.

TABLE (5.2.2)

COMPARISON OF RESULTS OBTAINED BY FINITE ELEMENT AND FINITE DIFFERENCE METHODS FOR SERIES A

NO.	END MOMEMTN M_{ab}, IN KIP-FEET, IN LINTEL BEAM NO. 6				DEFLECTION AT FREE END IN FEET X 10^{-2}										
	FINITE ELEMENT		FINITE DIFFERENCE		FIN. ELEM. WITH OPENINGS / FIN. DIFF. (I)	FIN. ELEM. WITH OPENINGS / FIN. DIFF. (II)	FIN. DIFF. (I) / FIN. DIFF. (II)	FINITE ELEMENT		FINITE DIFFERENCE		FIN. ELEM. WITH OPENINGS / FIN. DIFF. (I)	FIN. ELEM WITH OPENINGS / FIN. DIFF. (II)	FIN. DIFF. (I) / FIN. DIFF. (II)	
	With Openings 2 Dimen. Prob.	Approx. Core.	Solution (I)	Solution (II)				With Openings 2 Dimen Prob.	Approx. Core.	Solution (I)	Solution (II)				
1A	53.8	114.0	160.7	176.0	.335	.305	.913	3.42	5.01	5.69	5.87	.610	.583	.971	
2A	68.2	-	145.4	169.0	.469	.404	.811	3.54	-	4.00	4.08	.885	.868	.980	
3A	79.3	-	77.0	112.0	1.030	.708	.688	4.11	-	4.046	4.063	1.014	1.010	.995	
4A	52.5*	-	52.3	88.5	1.005	.593	.591	4.396	-	4.232	4.235	1.040	1.040	.999	

5.4 Part Three, Prismatic Coupled Shear Walls

5.4.1 General

The analysis of coupled shear walls by the continuous or finite difference methods is compared to that by the finite element method as a plane stress boundary value problem. The interaction coefficient was varied to study its effect. The depth of the connecting beams to the storey height, d_b/h, was varied between 0.2 and 1.0. The width of the piers to the span of the connecting beam was varied between 0.5 to 4.0. The height of the coupled shear wall to the width of the piers varied from 8.5 to 12.0. The height of the opening of the coupled shear walls to its width varied from zero to 2.67. The storey height was 10.0 ft. and the thickness of the piers and the connecting beams was 1.0 ft. Fig. (5.7) gives the dimensions and properties of the prismatic coupled shear walls considered.

The model of a coupled shear wall with discrete beams was treated by the finite element method in all the examples considered. The model of a coupled shear wall with continuous core was treated by the finite element method in some examples only.

5.4.2 Discussion of Results

Figs. (5.8.1) to (5.8.4), (5.9.1) to (5.9.3), (5.10.1) to (5.10.3), (5.11.1) to (5.11.2) and (5.12.1) to (5.12.3) show the deflections and the stress distributions at the base of the prismatic coupled shear walls obtained by the finite

element and the finite difference methods. Tables (5.3.1) to (5.3.7) show the comparison of the end moments in the lintel beams obtained by the two methods. Tables (5.3.8), (5.4), (5.5), (5.6), (5.7) show the properties and results for the coupled shear walls, series B,C, D,E and F respectively. Each series B to F represents 4 or 5 examples of coupled shear walls with H/d and d_b constant, while d/b takes the values .5, 1., 2., 3. and 4. respectively.

Table (5.8) gives the summary of the properties and results for coupled prismatic shear walls, namely the deflection at the free end, obtained by the finite element and the finite difference methods.

Examining the results we may come to the following conclusions:

1) Fig. (5.14) shows the deflection at the free end of the coupled shear walls obtained by the finite difference method for groups 1 to 5. Each group 1 to 5 represents four or five examples of a coupled shear wall with H/d and d/b constant, while d_b/h varies from 0.2 to 1.0 in increments of 0.2. The coupled shear wall behaves as a homogeneous cantilever, as if there are no openings at all, when the interaction coefficient $\alpha H > 14$.

2) Fig. (5.15) shows the deflection at the free end of the coupled shear walls obtained by the finite element method for groups 1 to 5 mentioned before. The coupled shear walls behave as a single homogeneous cantilever when $\alpha H > 14$.

3) Fig. (5.13) shows the deflection at the free end of the coupled shear wall obtained by the finite element and the finite difference methods versus the interaction coefficient αH. For a ratio H/d = 8.5, the agreement between the results obtained by the two methods starts when $\alpha H > 8.0$. For a ratio H/d = 12.0, the agreement between the results obtained by the two methods starts when $\alpha H > 10.0$, Table (5.8). It is of interest to mention that for the coupled shear walls with variable cross-section, discussed in section 2, for which the value of H/d changes from 8.5 for the lower section to 12 for the upper section, the agreement between the results occurs when $\alpha H > 9.0$, Tables (5.2) and (5.2.5).

4) Figs. (5.16.1), (5.16.2) and (5.16.3) show the deflection at the free end of 20 storey coupled shear walls versus the interaction coefficient αH, for values H/d equal to 8, 10, 12.5 respectively. The ratio d_b/h was varied from 0.1 to 1.0 in increments of 0.1. The ratio d/b takes the values 1, 2 and 4. We may notice that the coupled shear walls behave as a single homogeneous cantilever when $\alpha H > 14$. Also the coupled shear walls may be treated as two separate cantilevers when $\alpha H < 0.5$.

5) For moderate height coupled shear walls, for practical purposes, the finite difference and the continuous methods can be used to analyse coupled shear walls when the ratio H/d is around 10.0, $d/b \geq 2$ and any value of d_b/h between 0.2 to 1.0.

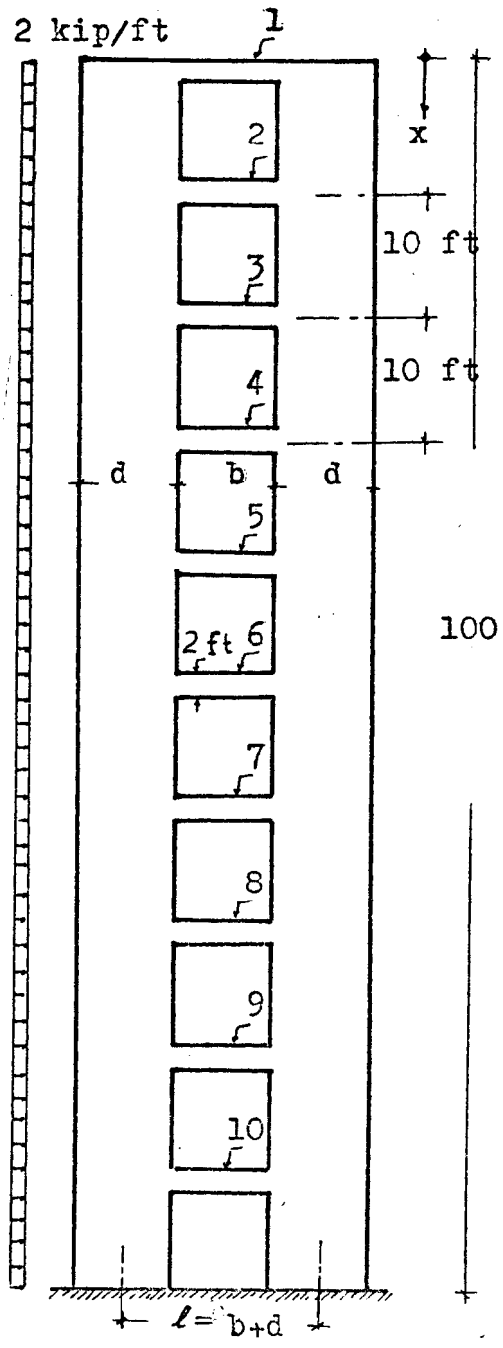

FIG. 5.7 PRISMATIC SHEAR WALL.

FIG. 5.8 FINITE ELEMENT PATTERN.
NE=912
NP=586

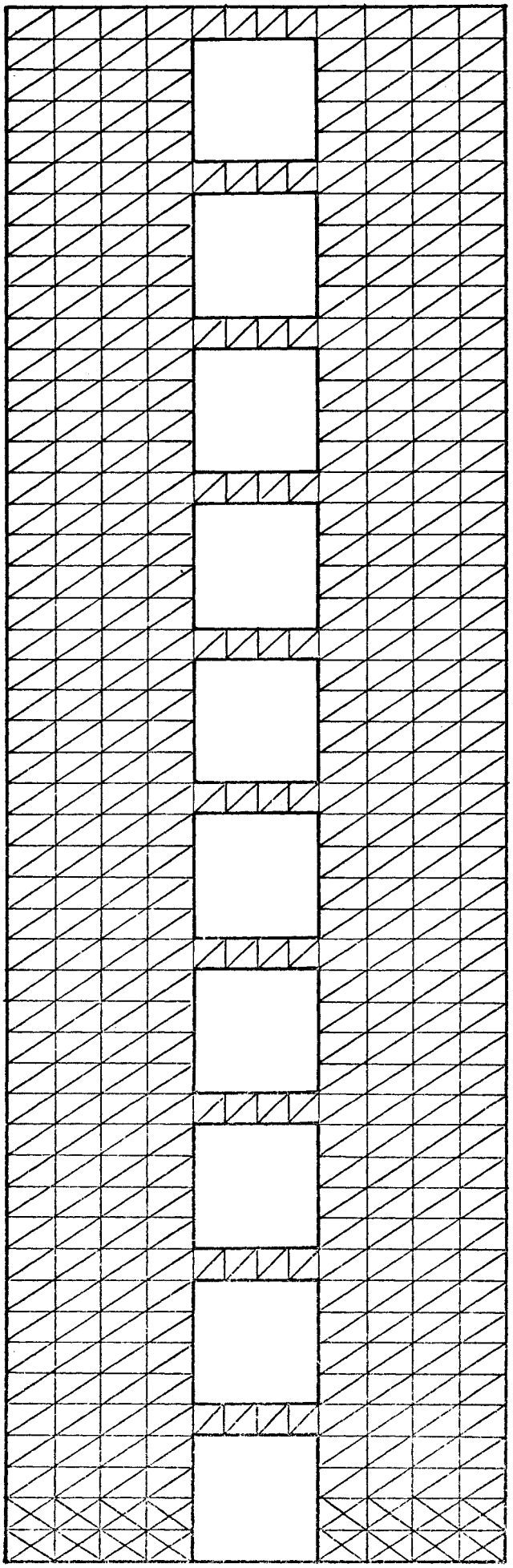

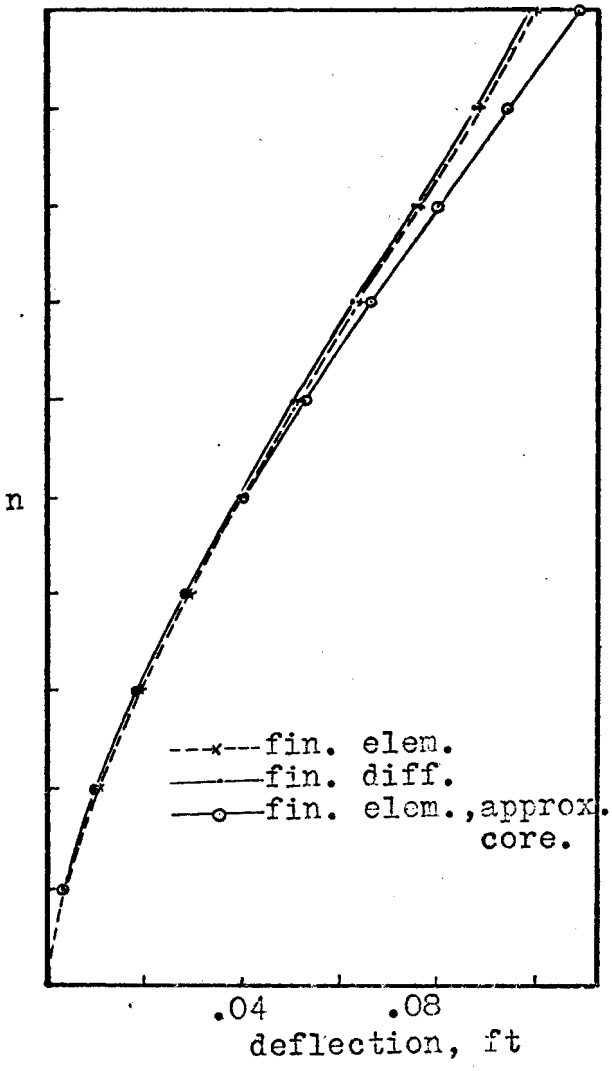

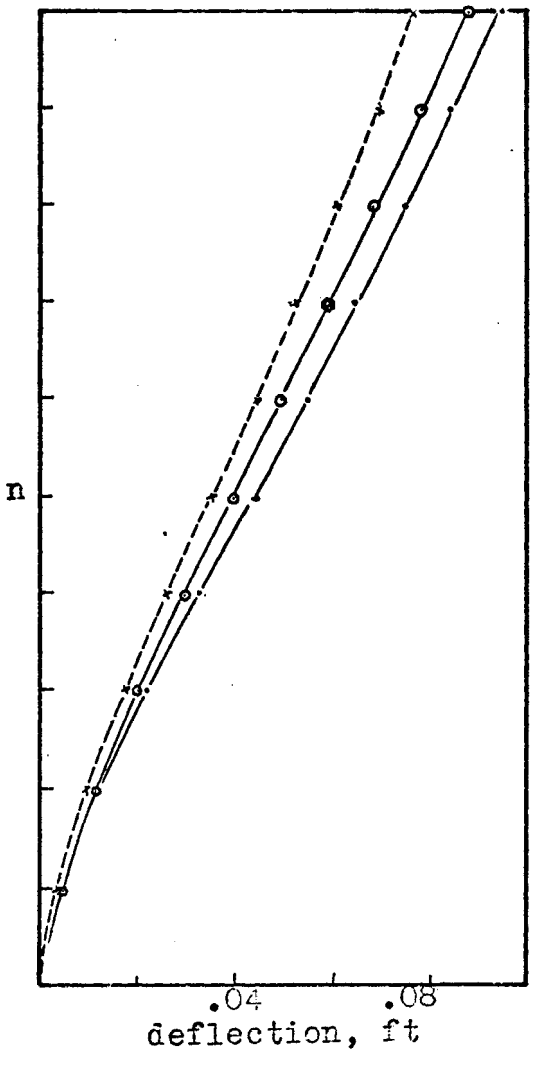

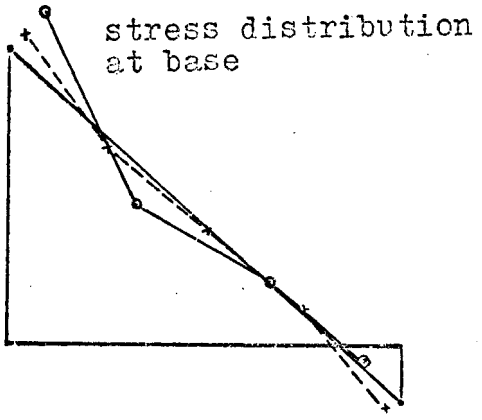

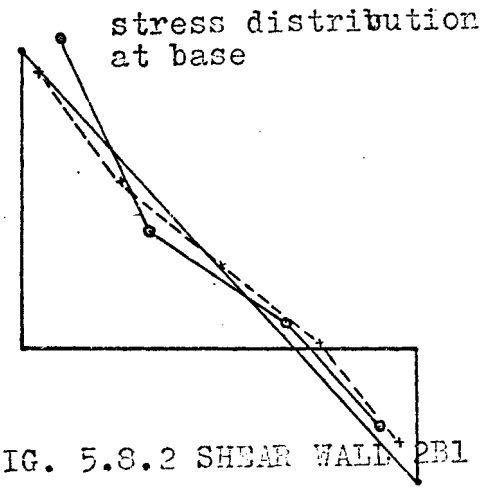

FIG.5.8.1 SHEAR WALL 1B1

FIG. 5.8.2 SHEAR WALL 2B1

OVER ALL DEFLECTION AND STRESS DISTRIBUTION AT BASE OF SHEAR WALL.

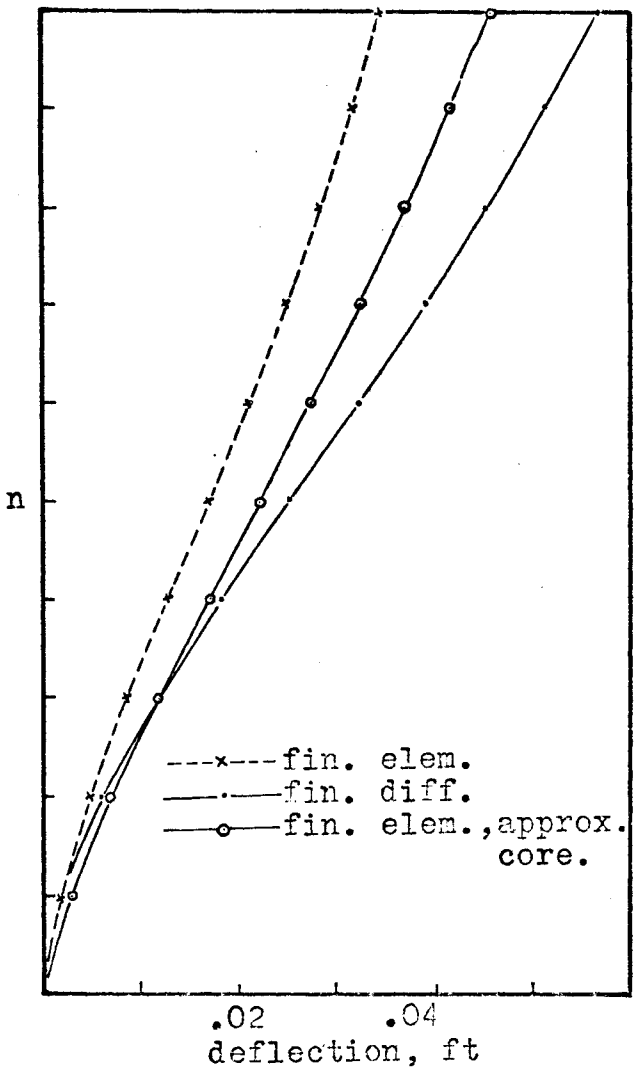

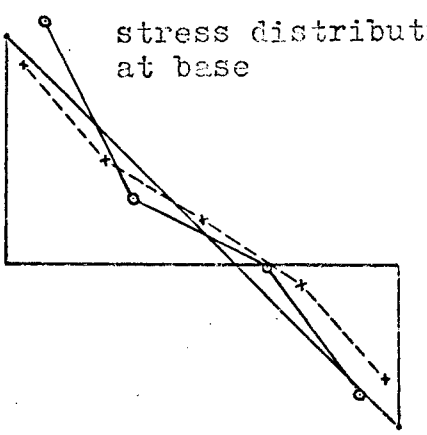

FIG. 5.8.3 SHEAR WALL 2B

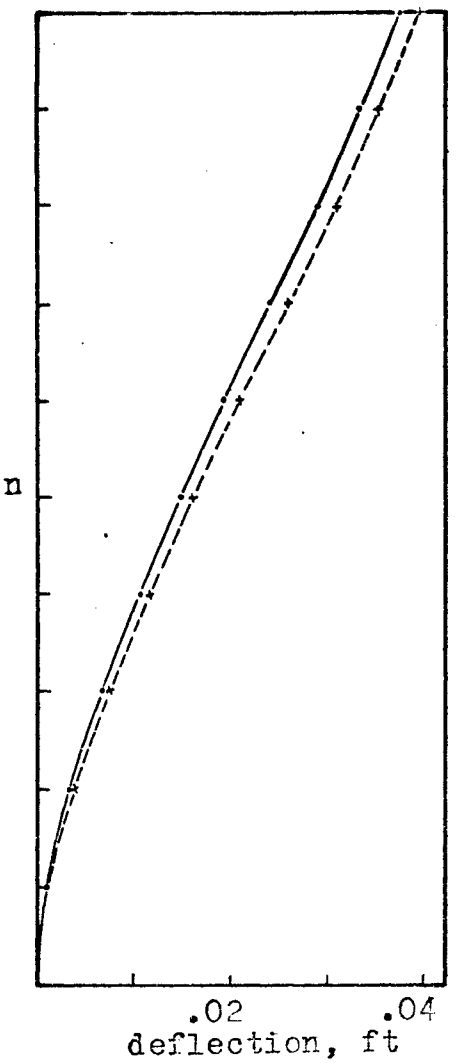

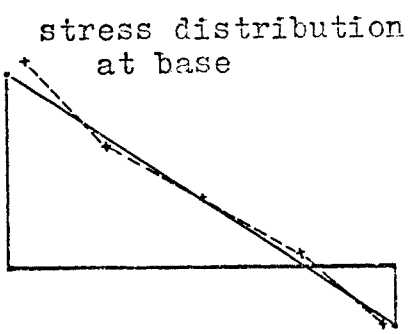

FIG. 5.8.4 SHEAR WALL 4B

OVER ALL DEFLECTION AND STRESS DISTRIBUTION AT BASE OF SHEAR WALL.

TABLE (5.3.1)

COMPARISON OF RESULTS BY FINITE ELEMENT AND FINITE DIFFERENCE METHODS FOR (1B1), (2B1)

	Lintel Beam	FINITE ELEMENT METHOD					FINITE DIFFERENCE METHOD	
		θ_a, in radians $\times 10^{-4}$	θ_b, in radians $\times 10^{-4}$	Δ, in feet, $\times 10^{-3}$	M_{ab}, in kip-feet	M_{ba}, in kip-feet	Q, in kip	$M_{ab} = M_{ba}$, in kip - feet
1B1	1	11.455	11.507	-4.473	12.20	12.40	6.202	12.4
	2	11.525	11.522	-4.315	32.00	32.00	18.546	37.1
	3	11.450	11.433	-4.089	53.00	52.80	30.327	60.6
	4	11.217	11.205	-3.786	76.00	75.60	43.920	87.8
	5	10.787	10.770	-3.392	100.00	98.80	58.031	116.0
	6	10.077	10.060	-2.888	124.00	123.60	72.097	144.2
	7	9.044	9.005	-2.248	148.00	147.60	85.486	171.0
	8	7.606	7.548	-1.456	175.00	174.60	96.622	193.4
	9	5.549	5.848	- .536	187.00	191.00	100.771	201.5
	10	3.050	2.917	.095	141.00	139.00	83.427	166.8
2B1	1	6.893	6.983	-5.040	13.10	13.30	8.699	34.8
	2	7.110	7.112	-4.767	25.60	25.70	20.460	81.8
	3	7.172	7.163	-4.347	38.40	38.30	27.285	109.2
	4	7.154	7.146	-3.800	53.20	53.00	35.884	143.5
	5	7.016	7.010	-3.133	68.70	68.50	45.020	180.0
	6	6.717	6.705	-2.345	83.80	83.00	53.677	214.7
	7	6.213	6.182	-1.439	97.60	97.40	60.640	242.5
	8	5.430	5.408	-0.451	118.00	117.50	63.980	256.0
	9	4.172	4.449	0.481	108.20	110.40	60.234	241.0
	10	2.537	2.434	.797	77.50	76.80	42.960	172.0

TABLE (5.3.2)

COMPARISON OF RESULTS BY FINITE ELEMENT AND FINITE DIFFERENCE METHODS FOR (2B), (4B)

Lintel Beam		FINITE ELEMENT METHOD					FINITE DIFFERENCE METHOD	
		θ_a, in radians $\times 10^{-4}$	θ_b, in radians $\times 10^{-4}$	Δ, in feet $\times 10^{-3}$	M_{ab}, in kip-feet	M_{ba}, in kip-feet	Q, in kip	$M_{ab} = M_{ba}$ in kip-feet
2B	1	2.093	2.187	-1.413	12.00	12.10	8.87	53.2
	2	2.341	2.368	-1.144	20.60	20.80	18.48	111.0
	3	2.409	2.415	-0.769	26.10	26.30	20.23	121.3
	4	2.458	2.457	-0.295	32.70	32.70	22.42	134.5
	5	2.468	2.234	0.234	39.30	39.40	24.56	147.2
	6	2.421	2.430	0.775	45.40	45.60	26.11	156.6
	7	2.300	2.311	1.274	49.70	49.80	26.52	159.0
	8	2.094	2.073	1.652	51.20	51.00	25.09	150.7
	9	1.822	1.558	1.735	47.40	46.60	20.99	126.0
	10	1.074	1.040	1.231	30.90	30.70	13.11	78.6
4B	1	4.150	4.213	-1.558	12.95	13.10	5.93	11.85
	2	4.223	4.224	-1.454	25.6	25.6	15.49	31.0
	3	4.178	4.172	-1.306	40.2	40.2	23.06	46.1
	4	4.074	4.066	-1.120	56.5	56.4	32.22	64.4
	5	3.893	3.863	- .895	72.9	72.8	41.89	82.9
	6	3.616	3.600	- .630	90.2	90.1	51.38	102.8
	7	3.221	3.192	- .323	106.6	106.3	59.88	120.0
	8	2.671	2.663	.020	121.2	121.0	65.78	131.6
	9	1.916	2.085	.331	124.3	126.7	65.45	130.9
	10	1.068	1.053	.370	88.1	88.0	50.30	100.6

TABLE (5.3.3)

COMPARISON OF RESULTS OBTAINED BY FINITE ELEMENT AND FINITE DIFFERENCE METHODS FOR SERIES B1 AND B

10 storey build. h=100 ft. H = 100 ft. t=1.0ft. $E=4.32\times10^5$ k.s.f. $G=1.985\times10^5$ k.s.f. $v=0.15$, $d_b=2$ ft.							END MOMENT M_{ab} IN KIP-FEET IN LINTEL BEAM NO. 8				DEFLECTION AT FREE END IN FET X 10^{-2}			
							FINITE ELEMENT		FINITE DIFFERENCE	Fin. Element with openings / Finite Difference	FINITE ELEMENT		FINITE DIFFERENCE	Fin. Element with openings / Fin. Difference
No.	d. in ft.	b, in ft.	ℓ, in ft	$\frac{d}{b}$	$\frac{H}{b}$	αH	With Openings 2 Dimen Prob.	Approx. Core,			With Openings 2 Dimen. Prob.	Approx. Core,		
1B1	8	4	12	2	12.5	12	174.8	190.0	193.4	.905	10.03	10.56	9.89	1.010
2B1	8	8	16	1	12.5	8.5	117.7	180.0	256.0	.461	7.63	8.65	9.32	.819
3B1	8	16	24	0.5	12.5	3.6	55.6	195.5	241.0	.231	6.17	11.60	14.03	.440
2B	12	12	24	1	8.5	3.05	51.1	106.7	150.7	.339	3.43	4.50	5.69	.602
3B	12	6	18	2	8.5	5.7	90.4	-	150.8	.600	3.645	-	4.00	.911
4B	12	4	16	3	8.5	8.9	121.-	-	131.6	.920	3.920	-	3.75	1.040
5B	12	3	15	4	8.5	15	150.2	-	112.8	1.330	4.144	-	3.68	1.126

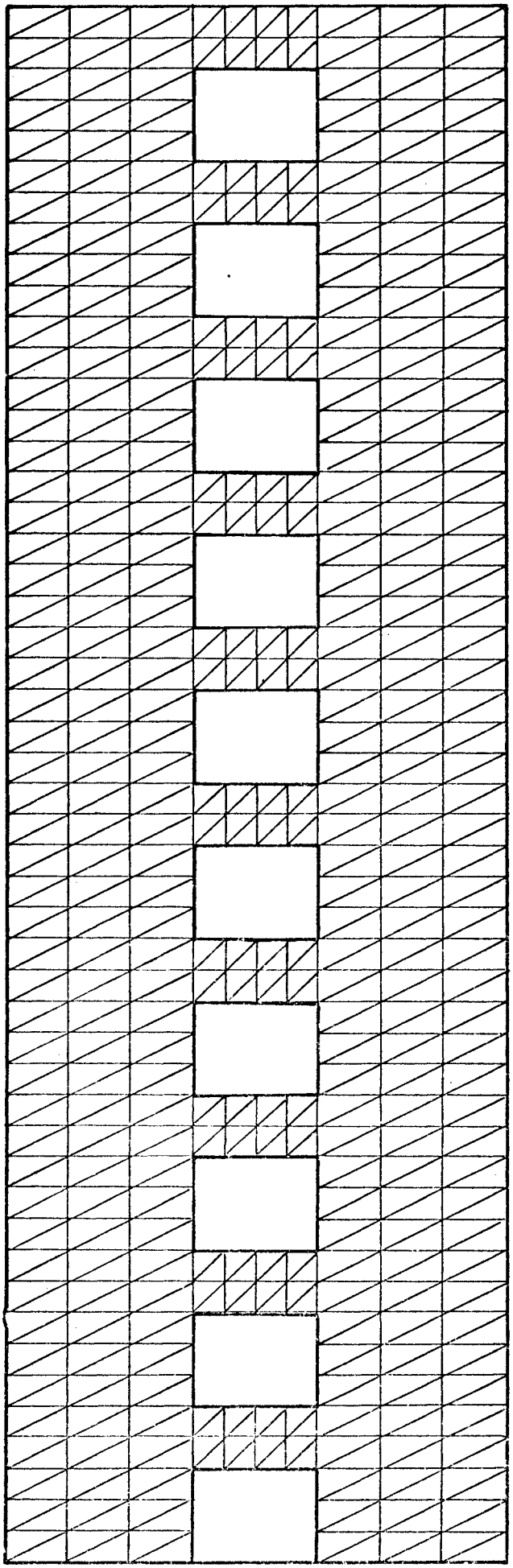

FIG. 5.9 FINITE ELEMENT PATTERN.
NE=760
NP=498

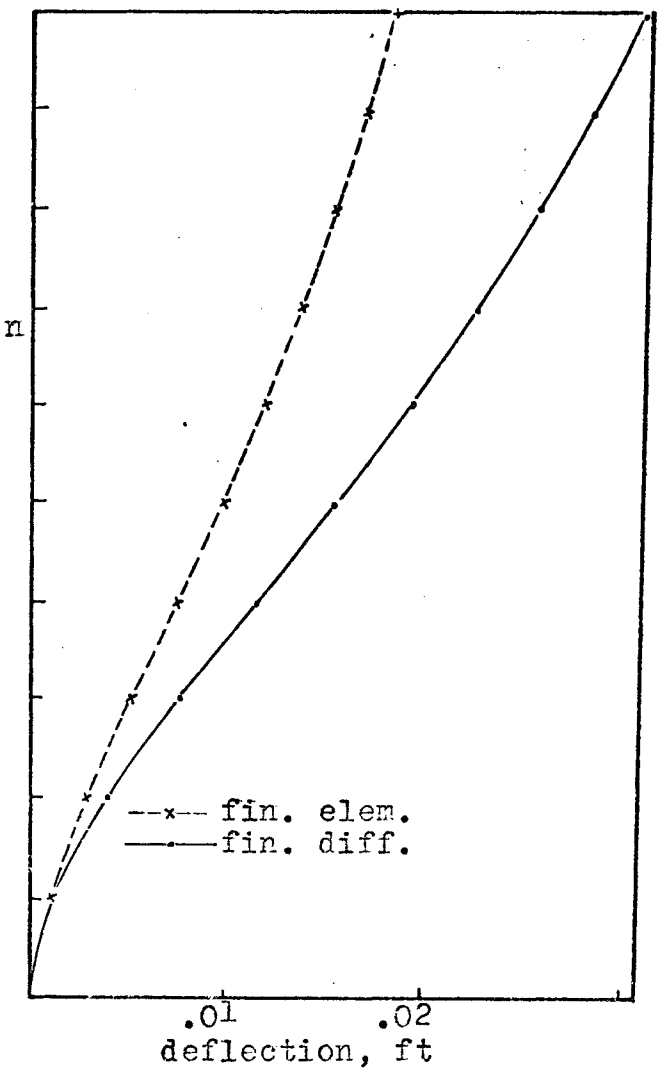

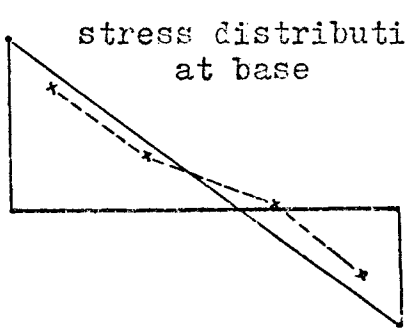

FIG. 5.9.1 SHEAR WALL 1C

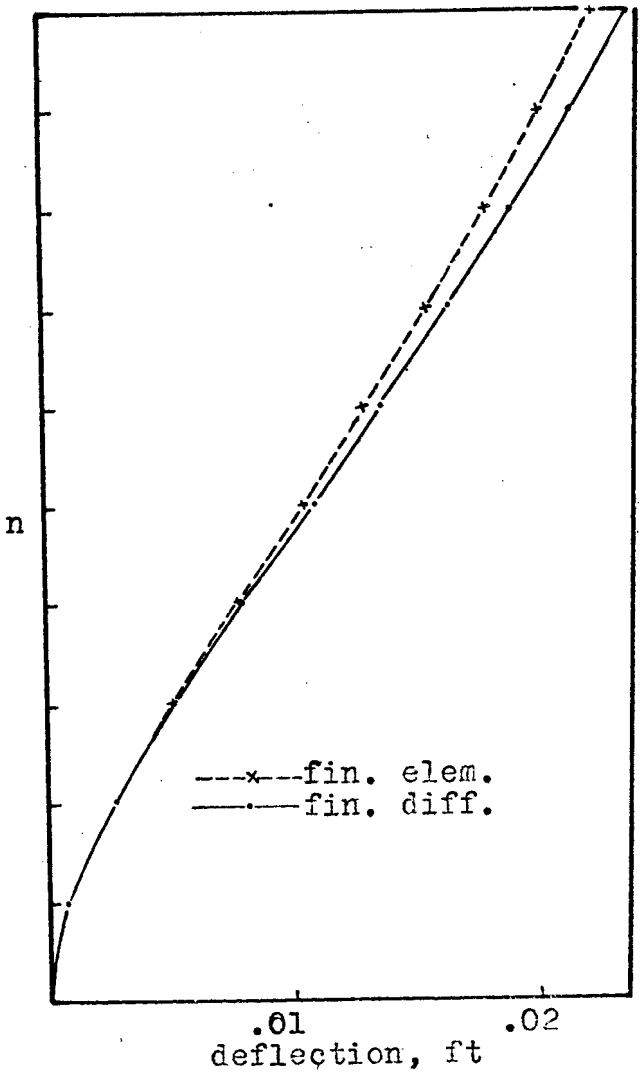

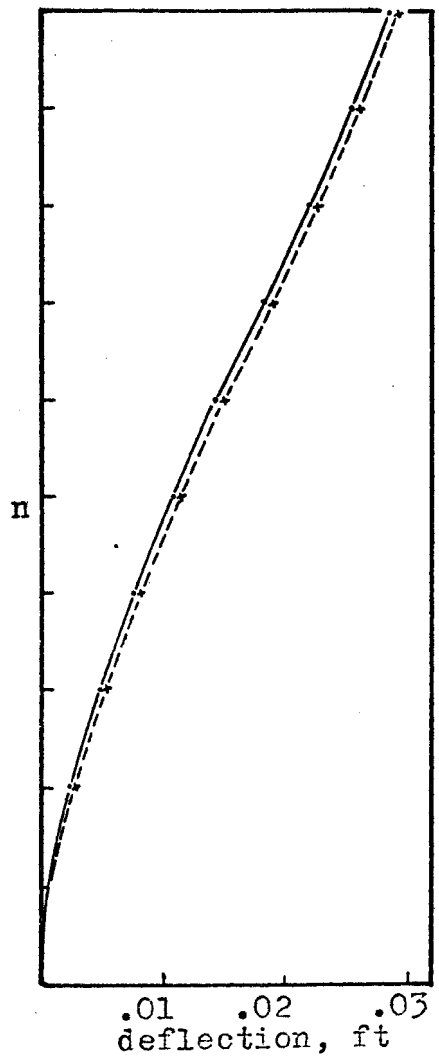

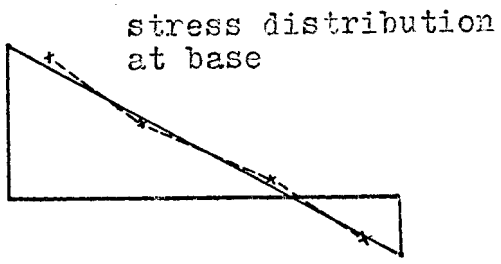

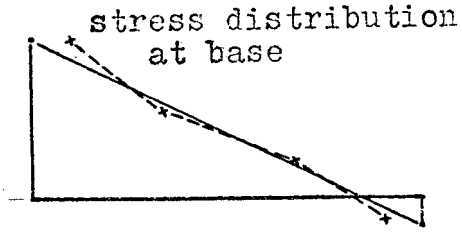

FIG. 5.9.2 SHEAR WALL 2C FIG. 5.9.3 SHEAR WALL 3C

OVER ALL DEFLECTION AND STRESS DISTRIBUTION AT BASE OF SHEAR WALL.

TABLE (5.4)

COMPARISON OF RESULTS OBTAINED BY FINITE ELEMENT AND FINITE DIFFERENCE METHODS FOR SERIES C.

10 Storey coupled Shear Walls, h = 10 feet. H = 100 feet, d_b = 4 feet							END MOMENT M_{ab}, in KIP-FEET IN LINTEL BEAM NO. 8			DEFLECTION AT FREE END IN FEET x 10^{-2}		
NO.	d in ft.	b in feet	ℓ in feet	$\frac{d}{b}$	$\frac{H}{d}$	αH	FINITE ELEMENT	FINITE DIFFERENCE	$\frac{\text{FINITE ELEM}}{\text{FINITE DIFFERENCE}}$	FINITE ELEMENT	FINITE DIFFERENCE	$\frac{\text{FIN. ELEM.}}{\text{FINITE DIFFERENCE}}$
1C	12	24	36	.5	8.5	4.50	205.0	286.0	0.717	1.84	3.13	0.588
2C	12	12	24	1	8.5	7.85	190.0	277.0	0.686	2.25	2.41	0.933
3C	12	6	18	2	8.5	13.20	192.0*	196.2	0.980	2.91	2.86	1.017
4C	12	4	16	3	8.5	17.00	142.3*	145.3	0.980	3.35	3.29	1.018
5C	12	3	15	4	8.5	19.75	112.0*	114.5	0.980	3.63	3.58	1.013

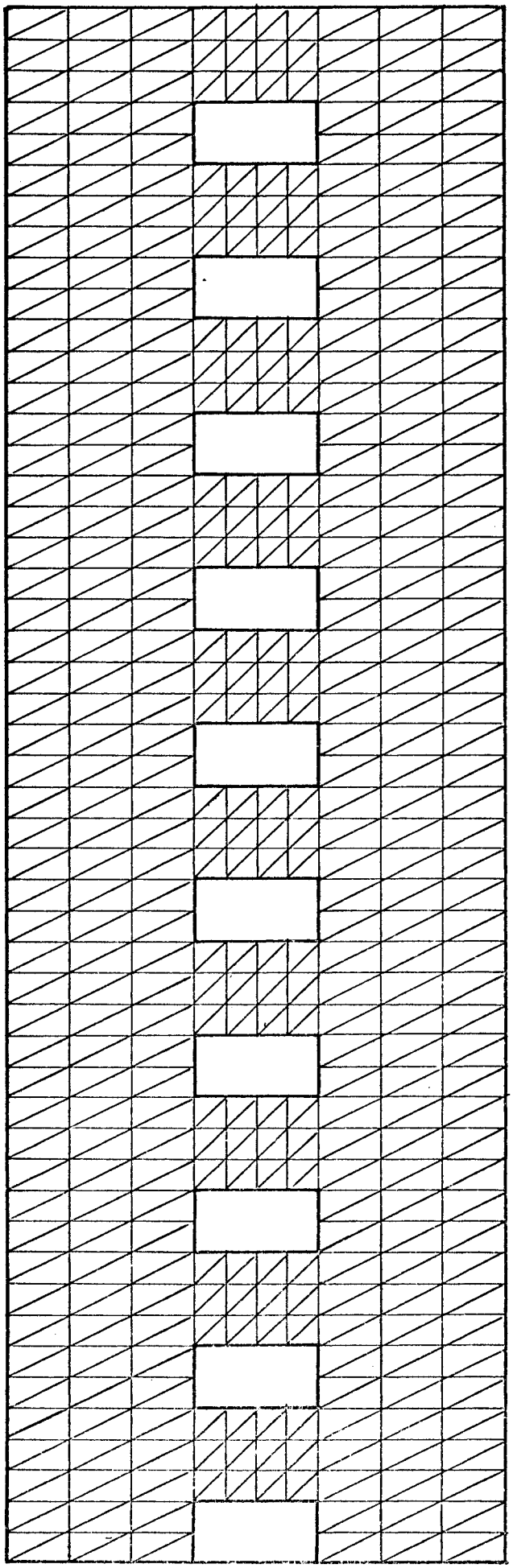

FIG. 5.10 FINITE ELEMENT PATTERN.
NE=840
NP=528

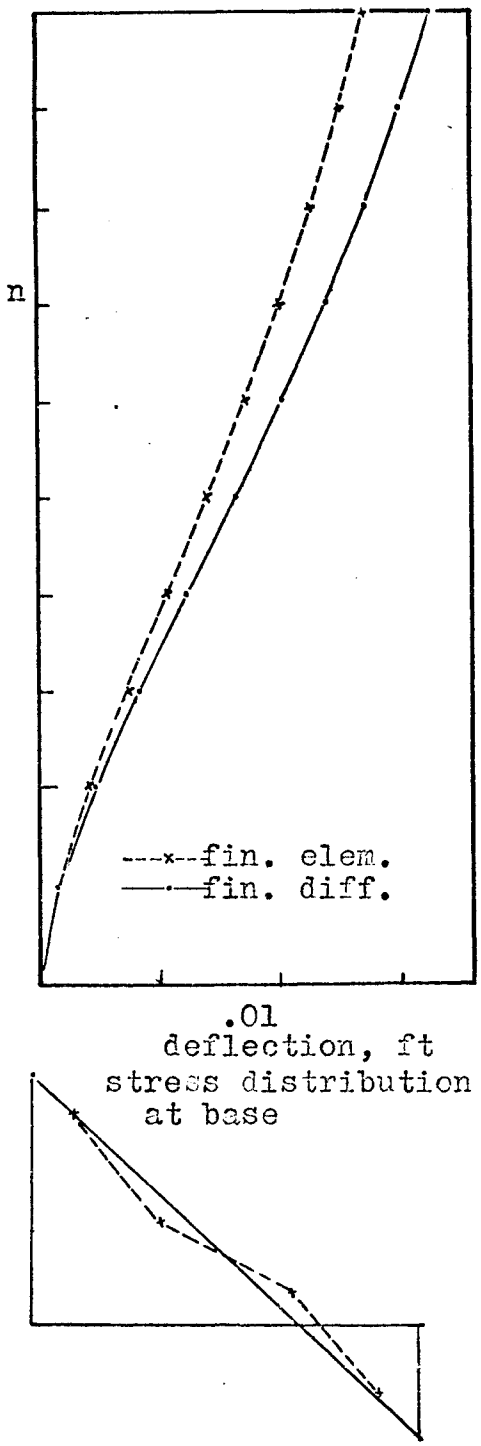

FIG. 5.10.1 SHEAR WALL 1D

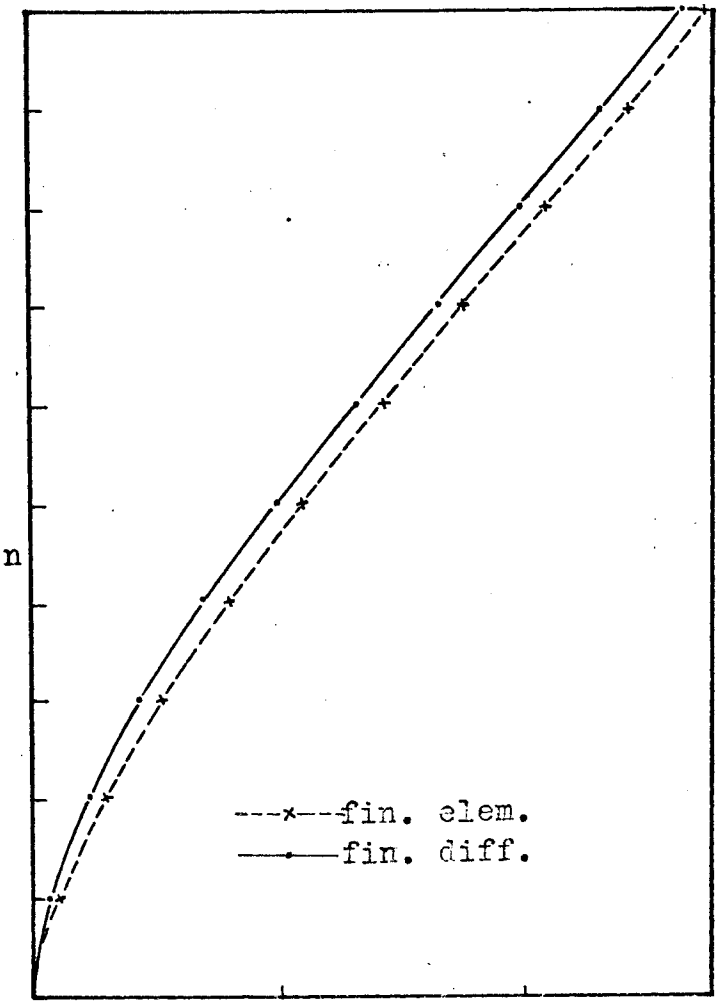

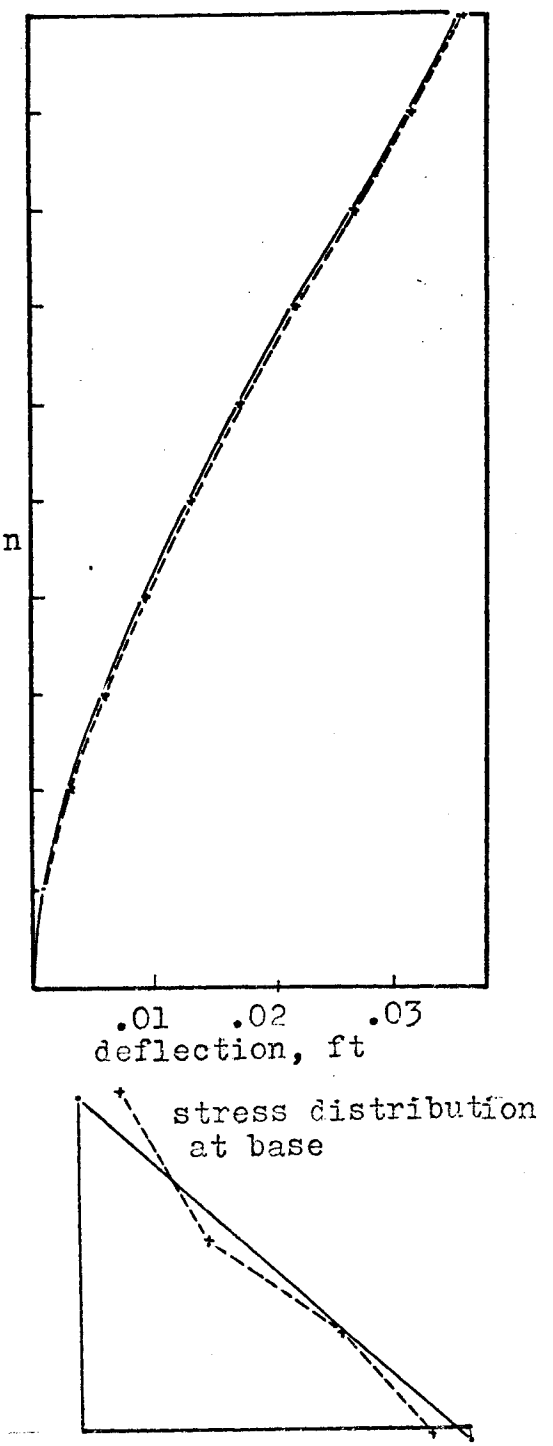

FIG. 5.10.2 SHEAR WALL 3D FIG. 5.10.3 SHEAR WALL 5D

OVER ALL DEFLECTION AND STRESS DISTRIBUTION AT BASE OF SHEAR WALL.

TABLE (5,5)

COMPARISON OF RESULTS OBTAINED BY FINITE ELEMENT AND FINITE DIFFERENCE METHODS FOR SERIES D

10 Storey Coupled Shear Walls h = 10 feet H = 100 feet d_b = 6 feet							END MOMENT M_{ab} IN KIP-FEET IN LINTEL BEAM NO. 8			DEFLECTION AT FREE END IN FEET x 10^{-2}		
NO.	d in feet	b in feet	ℓ in feet	$\frac{d}{b}$	$\frac{H}{d}$	αH	FINITE ELEMENT	FINITE DIFFERENCE	$\frac{\text{FINITE ELEMENT}}{\text{FINITE DIFFERENCE}}$	FINITE ELEMENT	FINITE DIFFERENCE	$\frac{\text{FINITE ELEMENT}}{\text{FINITE DIFFERENCE}}$
1D	12	24	36	.5	8.5	7.90	212.0	387.0	.548	1.35	1.62	.832
2D	12	12	24	1	8.5	12.70	350.0	311.0	1.125	1.92	1.88	1.020
3D	12	6	18	2	8.5	18.70	191.0*	181.3	1.054	2.76	2.68	1.030
4D	12	4	16	3	8.5	22.50	147.3*	146.7	1.004	3.25	3.21	1.012
5D	12	3	15	4	8.5	25.40	115.0*	115.0	.980	3.56	3.53	1.010

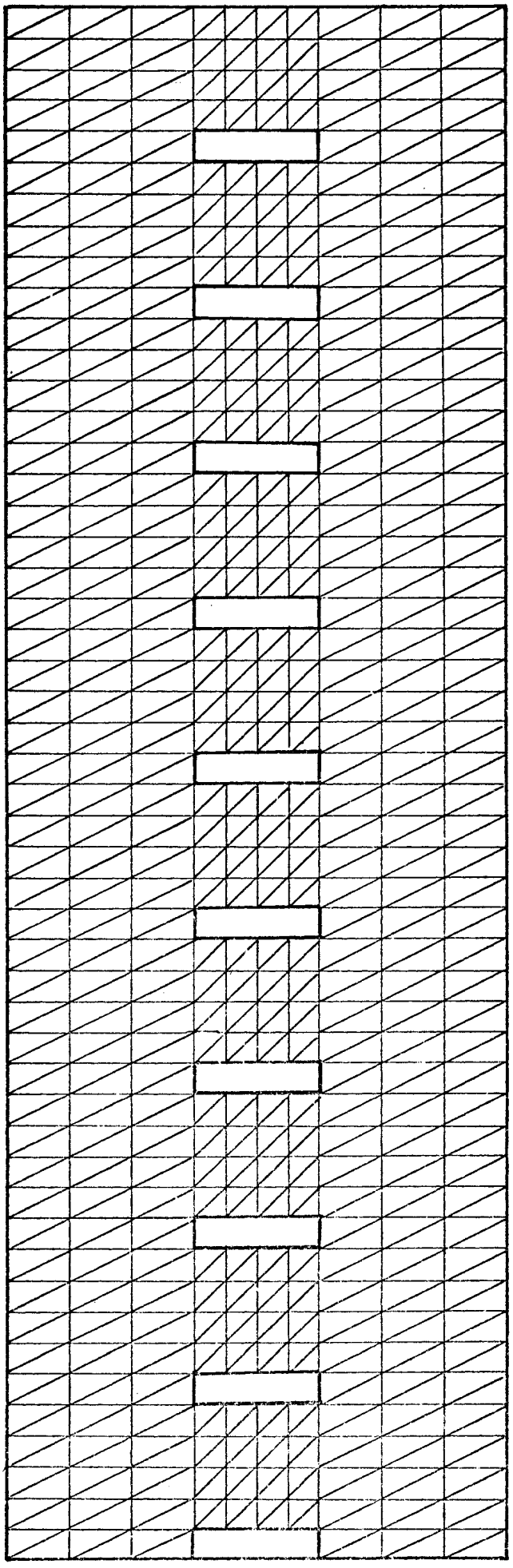

FIG.5.11 FINITE ELEMENT PATTERN.
NE=920
NP=558

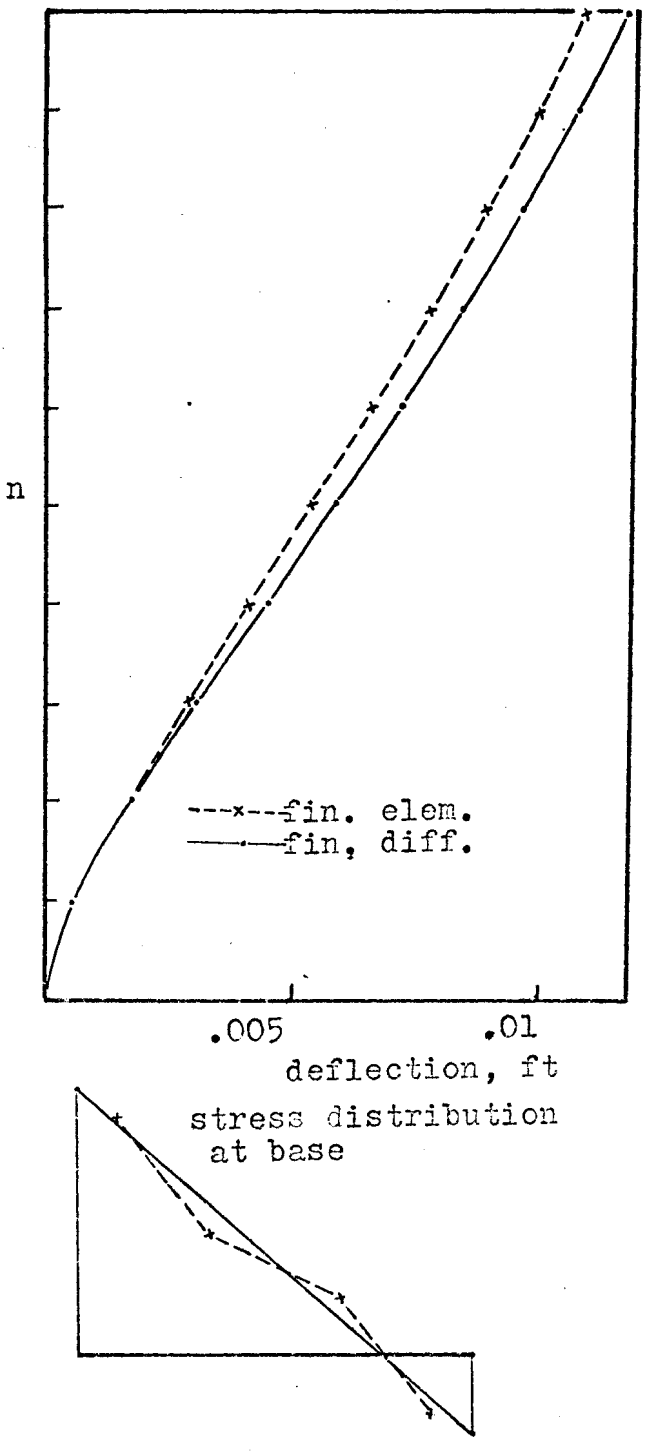

FIG. 5.11.1 SHEAR WALL 1E

TABLE (5.6)

COMPARISON OF RESULTS OBTAINED BY FINITE ELEMENT AND FINITE DIFFERENCE METHODS FOR SERIES E.

10 Storey coupled Shear Walls, h = 10 feet, H = 100 feet, d_b = 8 feet							END MOMENT M_{ab}, IN KIP-FEET IN LINTEL BEAM NO. 8			DEFLECTION AT FREE END IN FEET X 10^{-2}		
NO.	d in feet	b in feet	ℓ in feet	$\frac{d}{b}$	$\frac{H}{d}$	αH	FINITE ELEMENT	FINITE DIFFERENCE	$\frac{\text{FINITE ELEMENT}}{\text{FINITE DIFFERENCE}}$	FINITE ELEMENT	FINITE DIFFERENCE	$\frac{\text{FINITE ELEMENT}}{\text{FINITE DIFFERENCE}}$
1E	12	24	36	.5	8.5	11.50	340.0	426.0	.800	1.09	1.16	.940
2E	12	12	24	1	8.5	17.10	331.0*	318.6	1.037	1.76	1.72	1.023
3E	12	6	18	2	8.5	23.00	208.0*	202.2	1.027	2.68	2.64	1.015
4E	12	4	16	3	8.5	26.80	150.6*	147.1	1.022	3.21	3.18	1.010
5E	12	3	15	4	8.5	29.90	115.5*	115.2	1.005	3.53	3.51	1.005

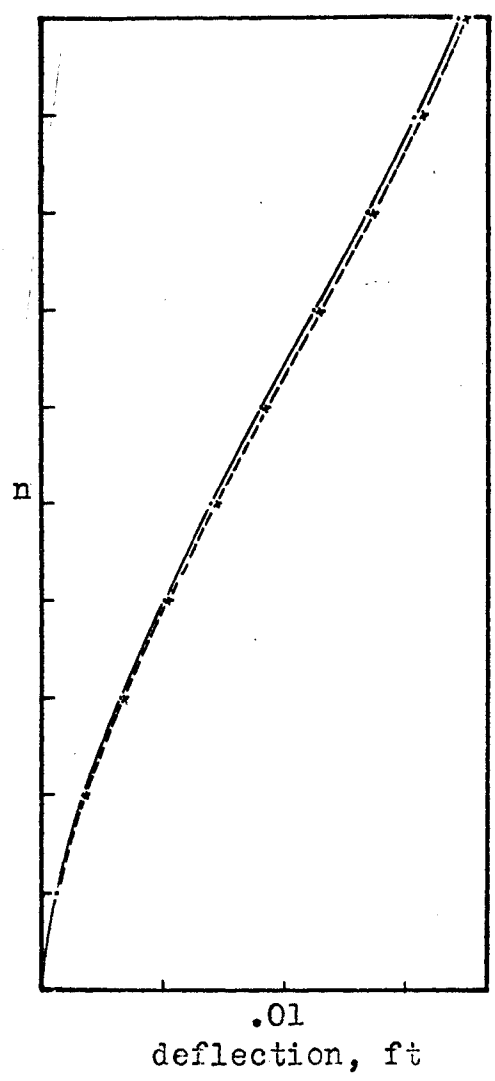

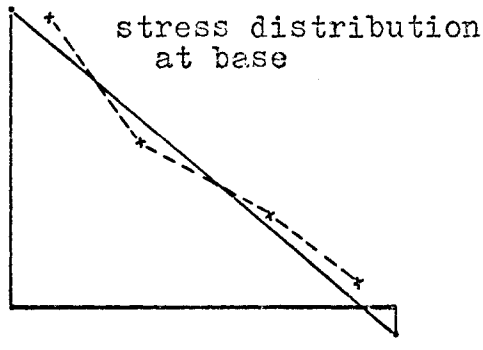

FIG. 5.11.2 SHEAR WALL 2E

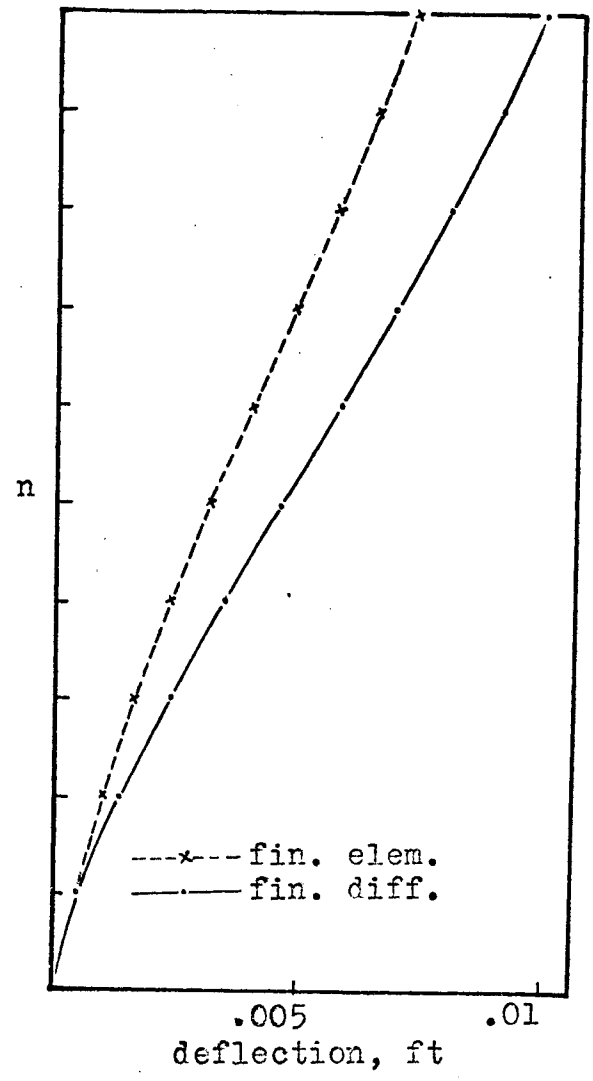

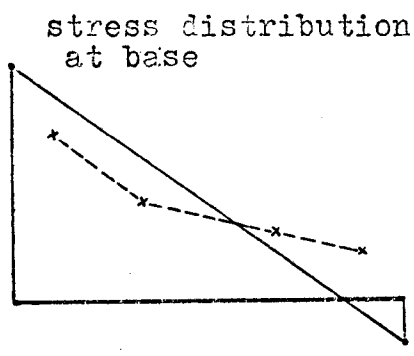

FIG. 5.12.1 SHEAR WALL 1F

OVER ALL DEFLECTION AND STRESS DISTRIBUTION AT BASE OF SHEAR WALL.

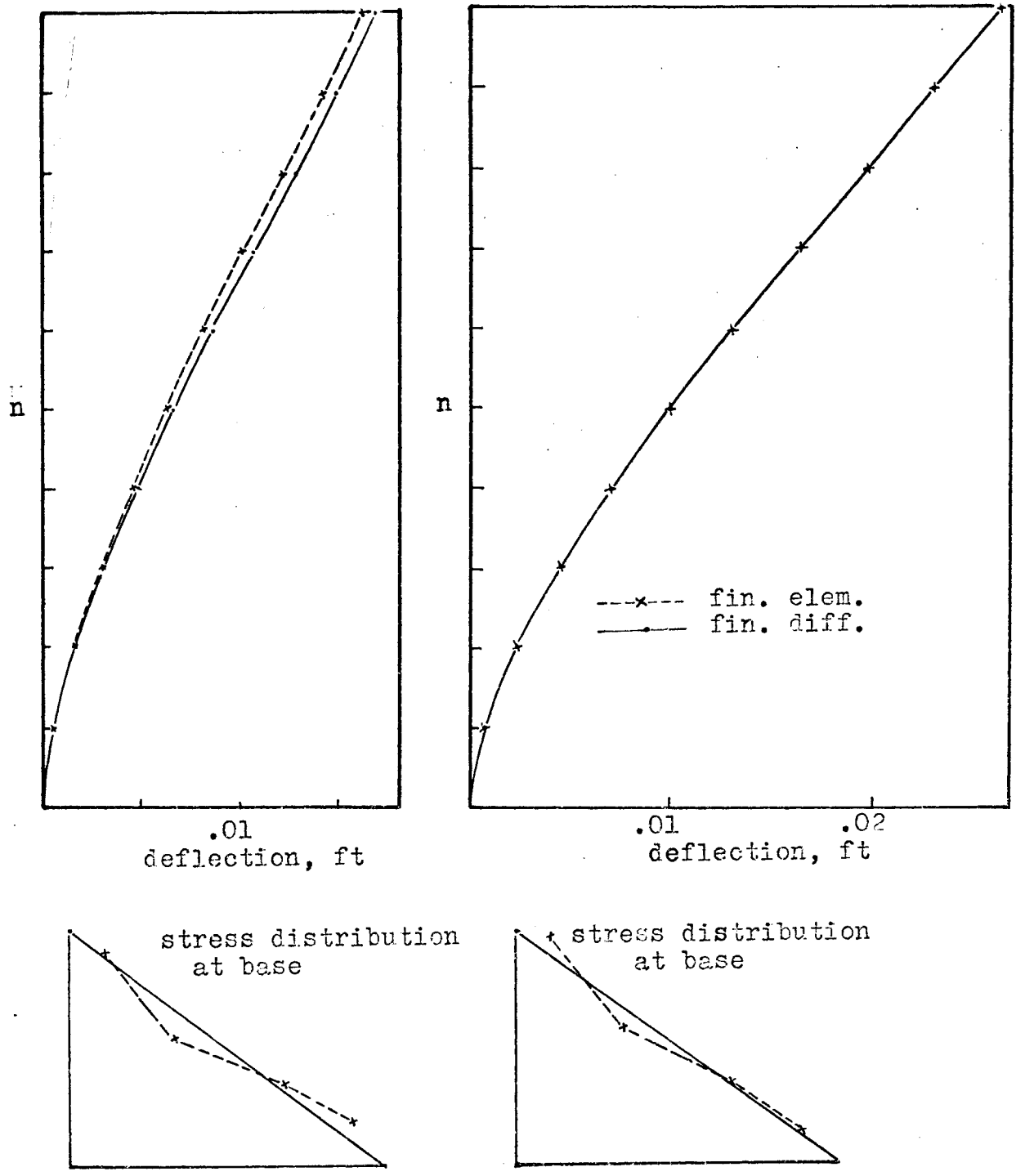

FIG. 5.12.2 SHEAR WALL 2F FIG. 5.12.3 SHEAR WALL 3F
OVER ALL DEFLECTION AND STRESS DISTRIBUTION AT BASE
OF SHEAR WALL.

TABLE (5.7)

COMPARISON OF RESULTS OBTAINED BY FINITE ELEMENT AND FINITE DIFFERENCE METHODS FOR SERIES F.

10 Storey Coupled Shear Walls h = 10 feet H = 100 feet d_b = 10 feet							END MOMENT M_{ab}, IN KIP-FEET IN LINTEL BEAM NO. 8			DEFLECTION AT FREE END IN FEET X 10^{-2}			
NO.	d in feet	b in feet	ℓ in feet	$\frac{d}{b}$	$\frac{H}{d}$	αH	FINITE ELEMENT	FINITE DIFFERENCE	$\frac{\text{FINITE ELEMENT}}{\text{FINITE DIFFERENCE}}$	FINITE ELEMENT	FINITE DIFFERENCE	$\frac{\text{FINITE ELEM.}}{\text{FINITE DIFFERENCE}}$	SIMPLE BENDING THEORY
1F	12	24	36	.5	8.5	15.16	219.0	440.0	0.500	0.73	0.99	.738	.611
2F	12	12	24	1	8.5	20.90	345.0	348.0	0.992	1.60	1.64	.975	1.446
3F	12	6	18	2	8.5	26.60	214.0	217.0	0.986	2.63	2.62	1.010	2.510
4F	12	4	16	3	8.5	30.50	154.0	158.0	0.975	3.17	3.16	1.003	3.090
5F	12	3	15	4	8.5	33.70	95.6	96.0	0.995	3.51	3.51	1.000	3.440

TABLE (5.8)

PROPERTIES & RESULTS OF PRISMATIC SHEAR WALL FOR SERIES B1,B,C,D,E & F

Series	NO.	d in ft.	b in ft.	ℓ in ft.	d_b in ft.	$\frac{d}{b}$	$\frac{h}{b}$	$\frac{d_b}{h}$	$\frac{h-d_b}{b}$	αH	Deflection ratio, Fin. Elem / Fin. Diff	Deflect. Fin.Diff. ft x 10^{-2}	Deflect. Fin Elem ft x10^{-2}	$\frac{1}{c}$	k
B1	1	8	4	12	2	2	12.5	.2	2.00	12	1.010	9.89	10.03	10.03	32000
	2	8	8	16	2	1	12.5	.2	1.00	8.5	.819	9.32	7.63	7.33	5750
	3	8	16	24	2	.5	12.5	.2	.50	3.6	.440	14.03	6.17	1.32	310
B	2	12	12	24	2	1	8.5	.2	.67	3.05	.602	5.69	3.43	.97	1905
	3	12	6	18	2	2	8.5	.2	1.33	5.7	.911	4.00	3.64	3.25	11223
	4	12	4	16	2	3	8.5	.2	2.00	8.9	1.040	3.75	3.91	8.03	33167
	5	12	3	15	2	4	8.5	.2	2.67	15.0	1.126	3.68	4.14	22.80	105730
C	1	12	24	36	4	.5	8.5	.4	.25	4.50	.588	3.13	1.84	2.06	1910
	2	12	12	24	4	1	8.5	.4	.50	7.85	.933	2.41	2.25	6.26	12640
	3	12	6	18	4	2	8.5	.4	1.00	13.20	1.017	2.86	2.91	17.70	59930
	4	12	4	16	4	3	8.5	.4	1.50	17.00	1.018	3.29	3.35	29.30	120400
	5	12	3	15	4	4	8.5	.4	2.00	19.75	1.013	3.58	3.63	39.50	182300
D	1	12	24	36	6	.5	8.5	.6	.16	7.90	.832	1.62	1.35	6.33	5930
	2	12	12	24	6	1	8.5	.6	.33	12.70	1.020	1.88	1.92	16.40	33170
	3	12	6	18	6	2	8.5	.6	.67	18.70	1.030	2.68	2.76	35.50	120400
	4	12	4	16	6	3	8.5	.6	1.00	22.50	1.012	3.21	3.25	51.40	212800
	5	12	3	15	6	4	8.5	.6	1.33	25.40	1.010	3.53	3.56	65.50	302600
E	1	12	24	36	8	.5	8.5	.8	.08	11.50	.940	1.16	1.09	13.40	12640
	2	12	12	24	8	1	8.5	.8	.16	17.10	1.023	1.72	1.76	29.70	59930
	3	12	6	18	8	2	8.5	.8	.33	23.00	1.015	2.64	2.68	53.70	182300
	4	12	4	16	8	3	8.5	.8	.50	26.80	1.010	3.18	3.21	73.00	302600
	5	12	3	15	8	4	8.5	.8	.67	29.90	1.005	3.51	3.53	90.80	419100
F	1	12	24	36	10	.5	8.5	1.0	0.	15.16	.738	.99	.73	23.30	21880
	2	12	12	24	10	1	8.5	1.0	0.	20.90	.975	1.64	1.60	44.40	89650
	3	12	6	18	10	2	8.5	1.0	0.	26.60	1.010	2.62	2.63	71.80	243000
	4	12	4	16	10	3	8.5	1.0	0.	30.50	1.003	3.16	3.17	94.50	390200
	5	12	3	15	10	4	8.5	1.0	0.	33.70	1.000	3.51	3.51	115.00	533500

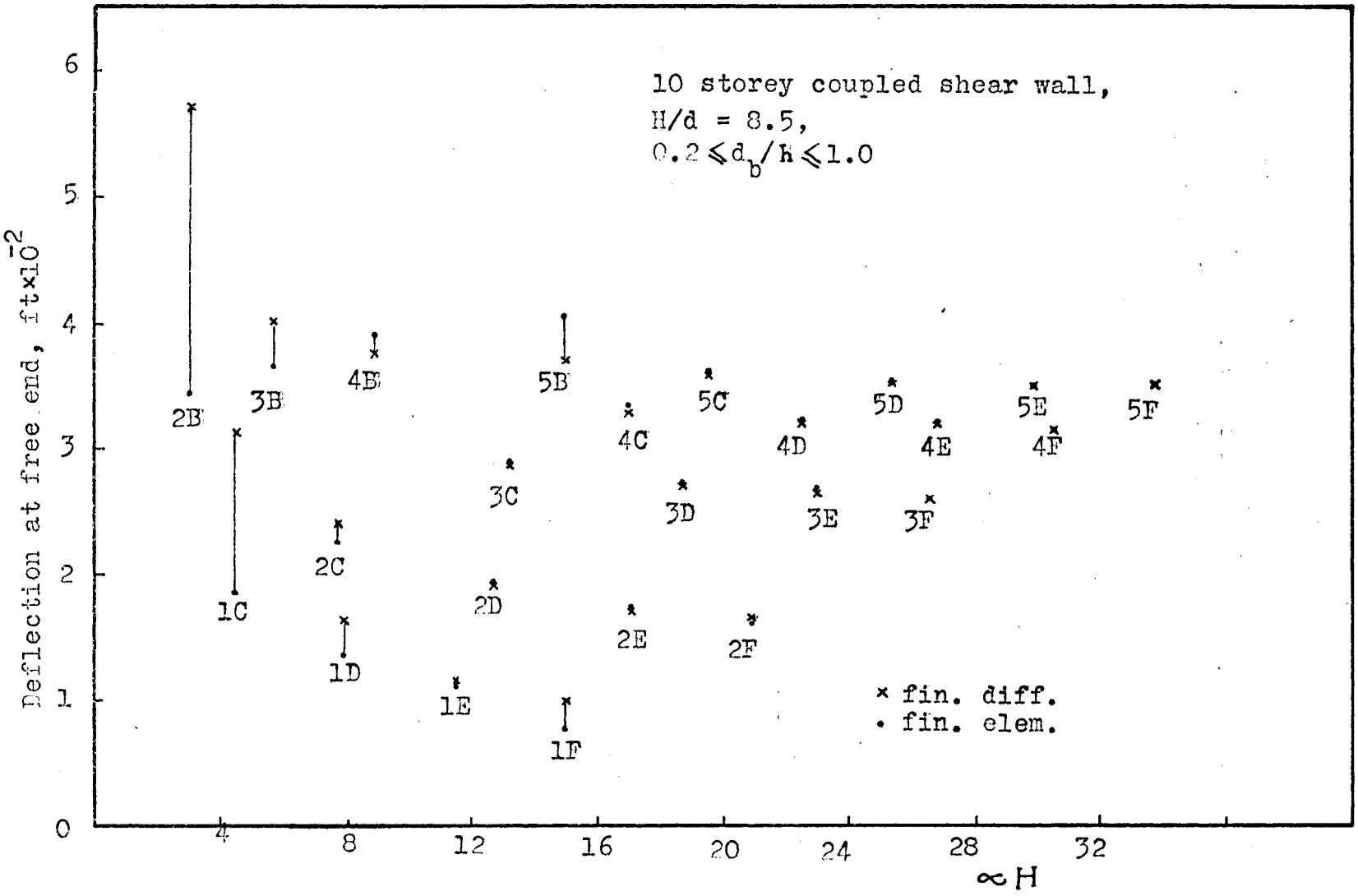

FIG. 5.13 FINITE ELEMENT METHOD VERSUS FINITE DIFFERENCE METHOD
(DEFLECTION*INTERACTION COEFFICIENT DIAGRAM)

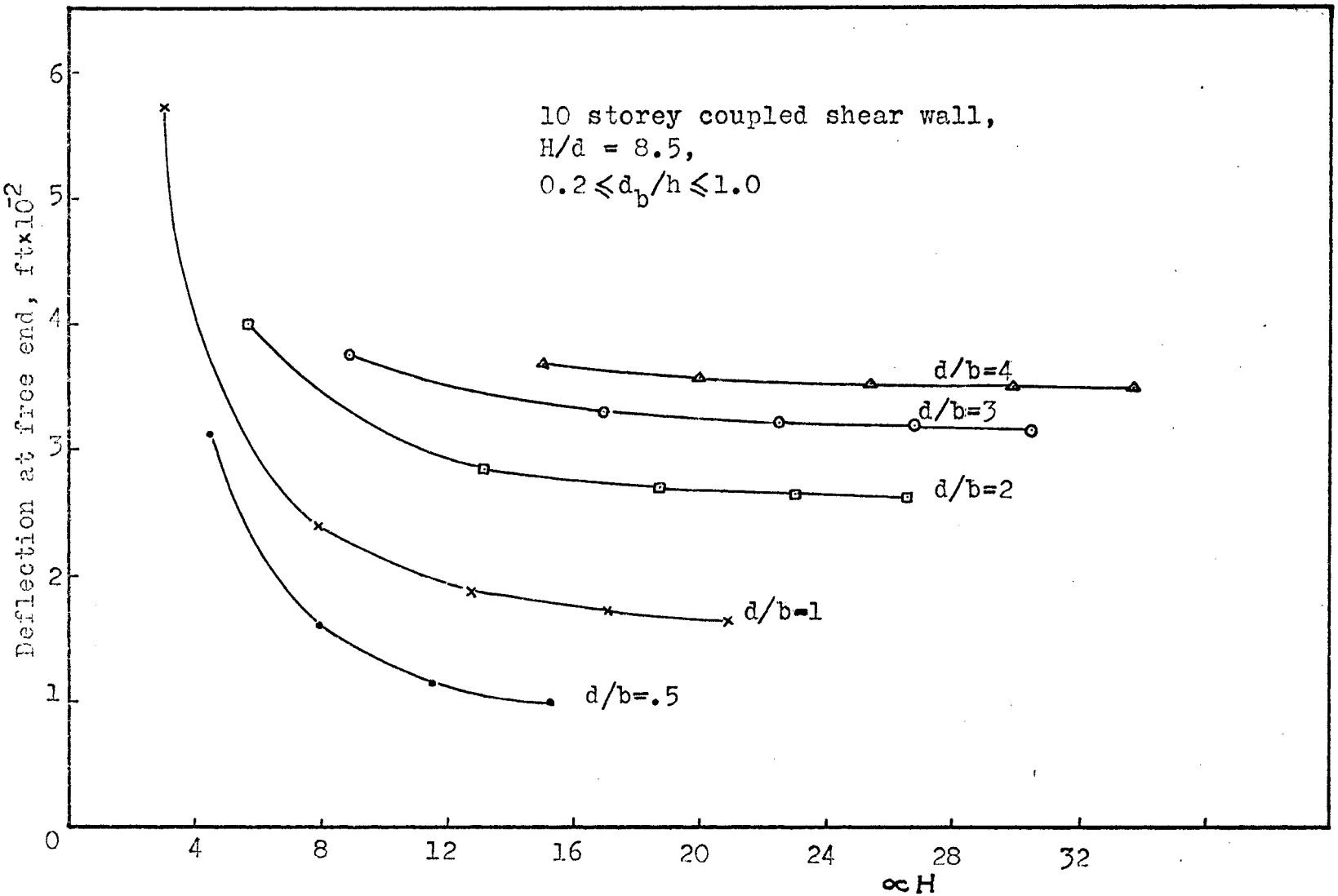

FIG. 5.14 FINITE DIFFERENCE METHOD
(DEFLECTION*INTERACTION COEFFICIENT DIAGRAMS)

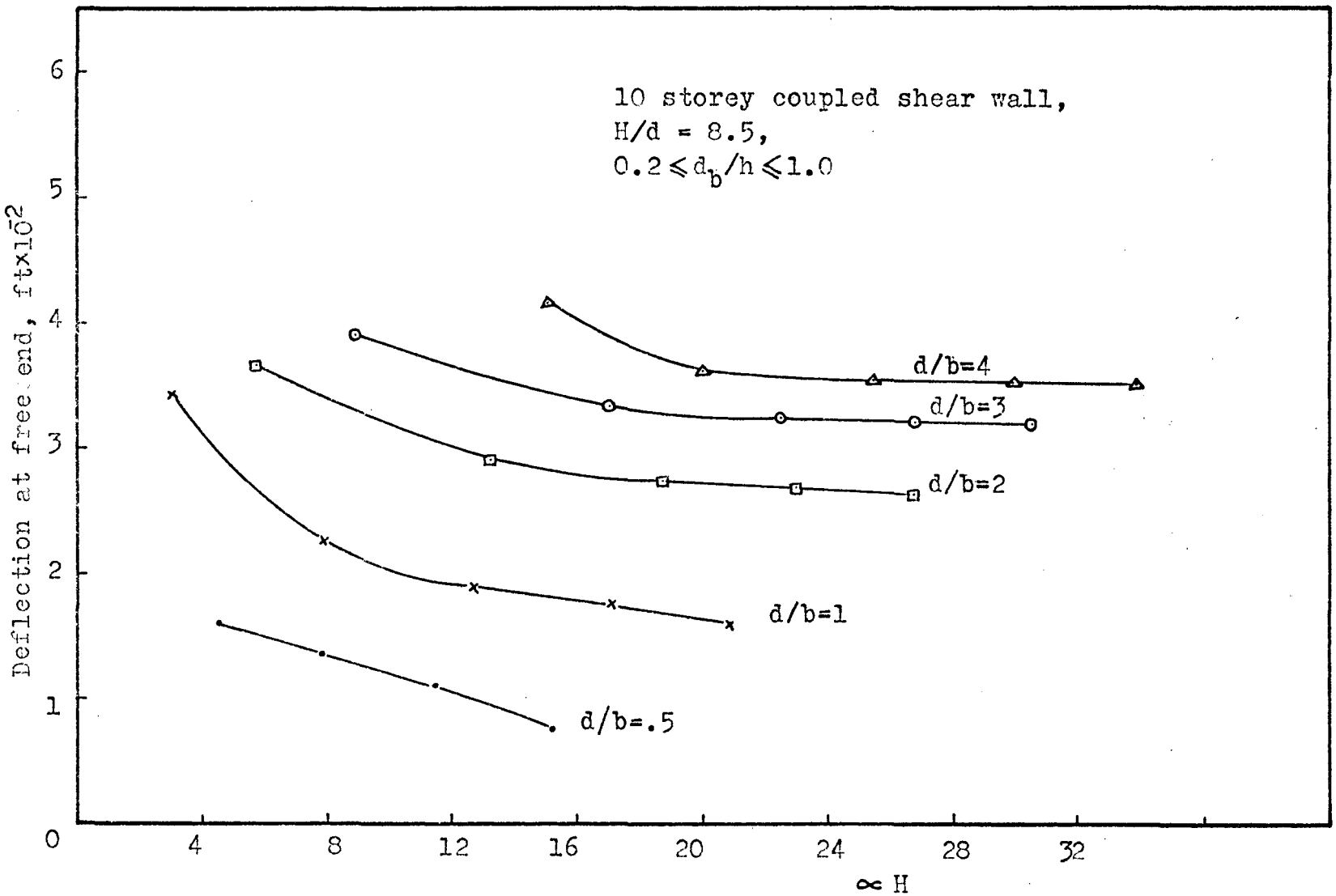

FIG. 5.15 FINITE ELEMENT METHOD
(DEFLECTION*INTERACTION COEFFICIENT DIAGRAMS)

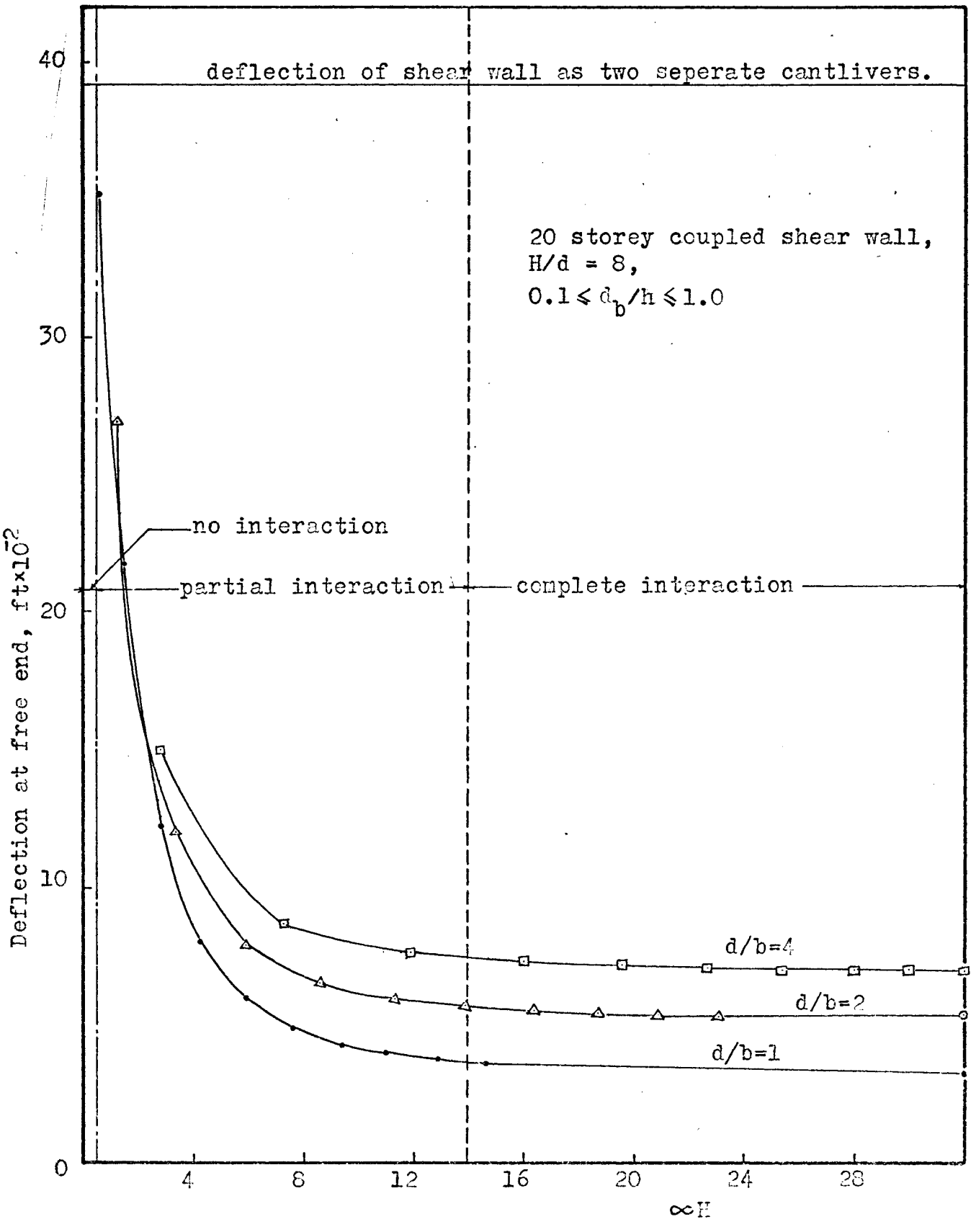

FIG. 5.16.1 FINITE DIFFERENCE METHOD
(DEFLECTION-INTERACTION COEFFICIENT DIAGRAMS)

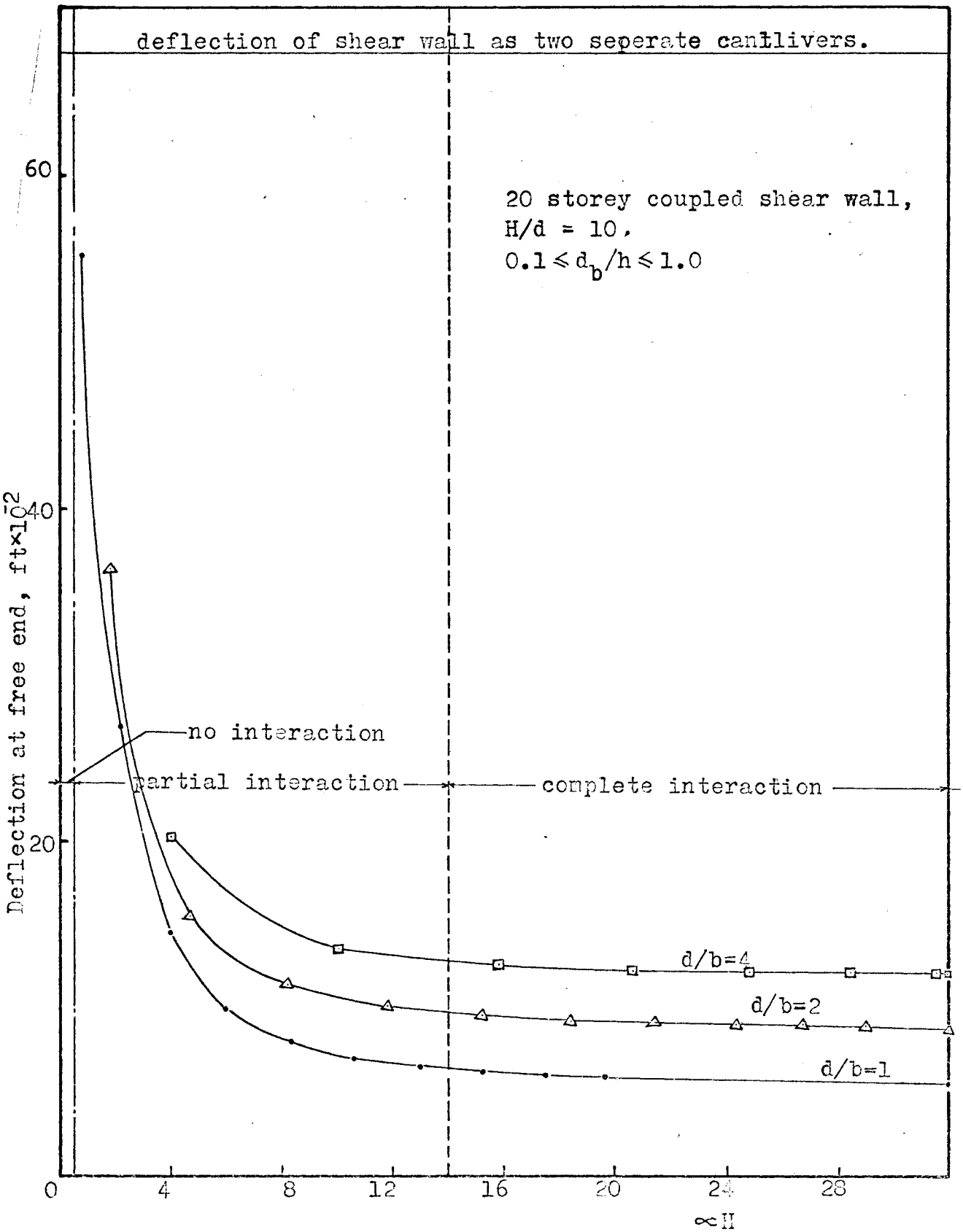

FIG. 5.16.2 FINITE DIFFERENCE METHOD
(DEFLECTION*INTERACTION COEFFICIENT DIAGRAMS)

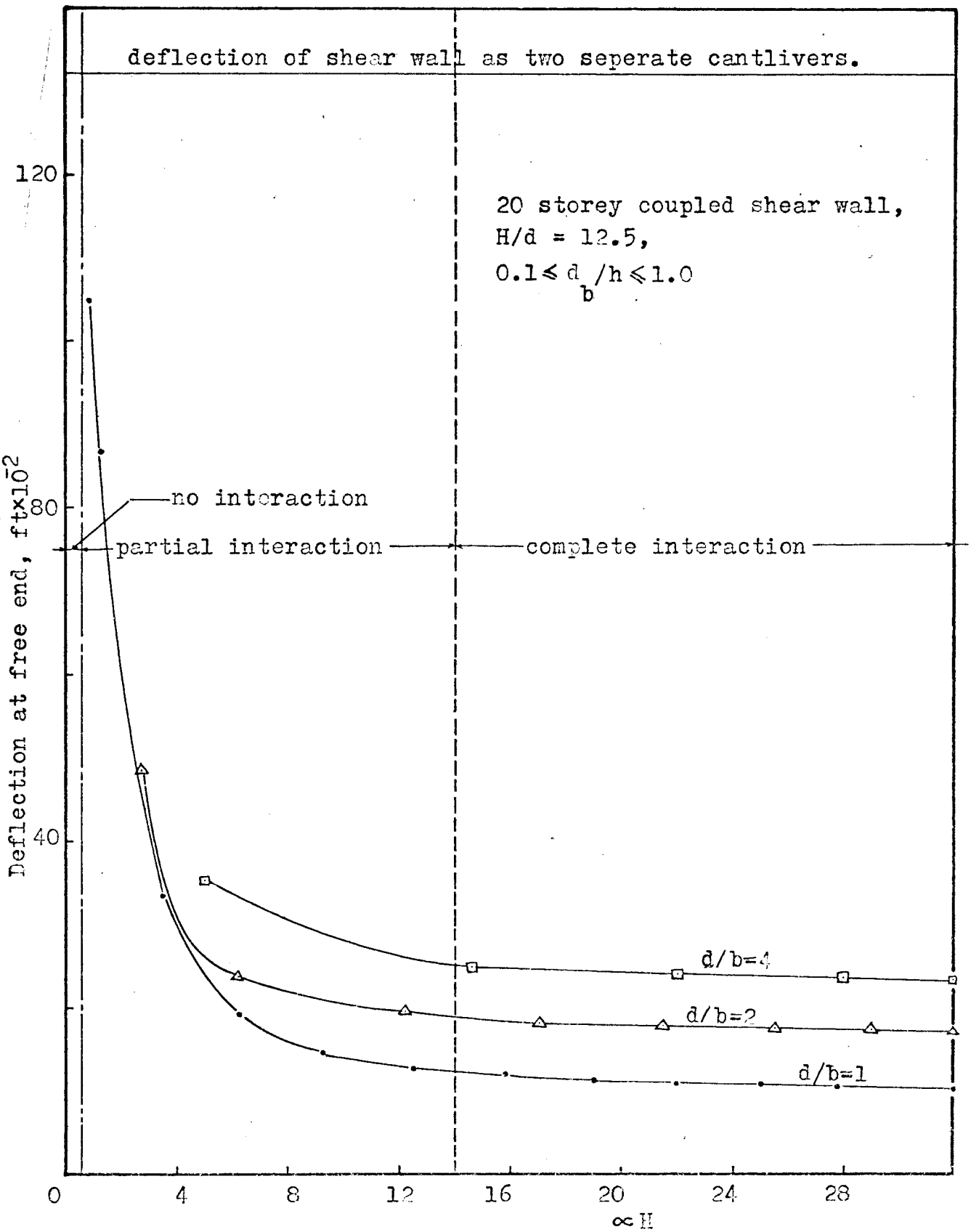

FIG. 5.16.3 FINITE DIFFERENCE METHOD
(DEFLECTION*INTERACTION COEFFICIENT DIAGRAMS)

6) For $H/d = 8.5$ and $\alpha H < 8$, $H/d = 12$ and $\alpha H < 10$, the finite difference method as well as the continuous connection method gives higher values for the forces and the deflection of the coupled shear walls compared to the finite element method. That is to say the finite difference and continuous methods give conservative forces and deflections for such structures.

For $H/d = 8.5$ and $\alpha H > 8$, $H/d = 12$ and $\alpha H > 10$ the agreement between the finite difference and continuous methods compared to the finite element method is good.

CHAPTER 6

ANALYSIS OF MULTI-LAYERED BEAMS

6.1 General

Fig. (6.1) shows a multi-layered beam of "m" layers connected together by shear connectors and having "2n" panels in the case of a simply supported beam symmetrical case, and "n" panels in the case of a cantilever. The finite difference method for composite beams was used to analyse this problem. This problem is analogous to that of a multi-piered coupled shear wall.

6.2 Basic Assumptions

1) The layers of the sandwich beam deflect equally at all points along their lengths; and have equal curvatures at any section.

2) The strain distribution in each layer is linear; however, the strain distribution, in general, is not continuous, Fig. (6.2).

3) The shear connection between the slab and the beam is provided by shear connectors placed at discrete points along the span of the beam.

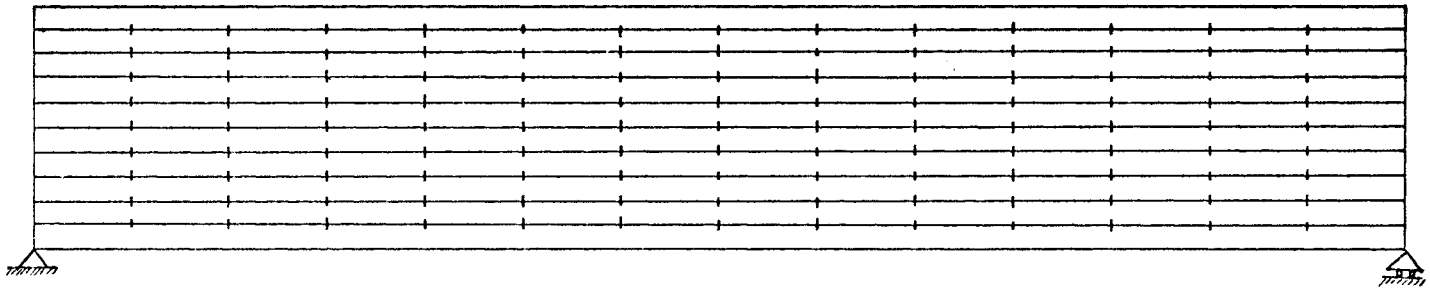

a) Real Structure
Simply supported multi-layered beam
number of panels = 2n
number of layers = m

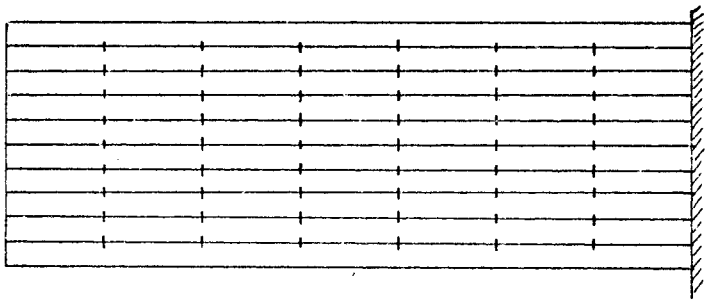

b) Equivalent system.

c) Real Structure
Cantliver multi-layered beam
number of panels = n
number of layers = m

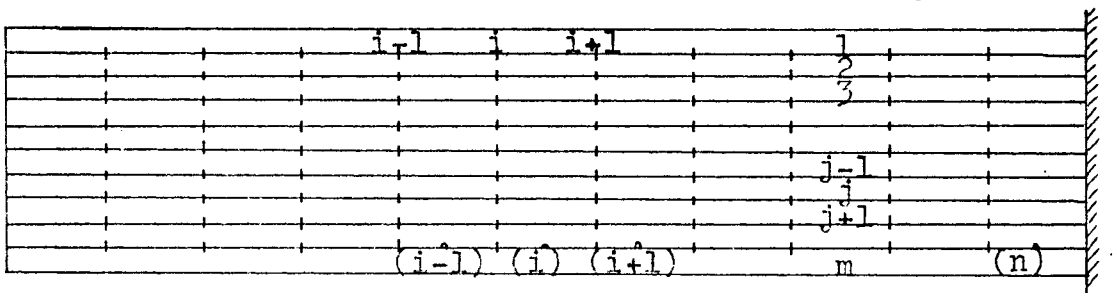

FIG. 6.1 MODEL OF MULTI*LAYERED BEAMS

6.3 Formulation of the Problem, Finite Difference Solution

The equilibrium and compatibility conditions are Fig. (6.2).

$$\gamma^{j(j-1)}_{i+1} - \gamma^{j(j-1)}_{i} = \int_{h(i)} (\epsilon_{j(j-1)} - \epsilon_{(j-1)j})\, dx$$

$$j = 2,3,4 \ldots\ldots, m$$

$$i = 1,2,3,\ldots\ldots, n \qquad (6.1)$$

$$M_i = M_{1i} + M_{2i} + M_{3i} + \ldots\ldots + M_{(j-1)i} + M_{ji} + M_{(j+1)i} + \ldots\ldots$$
$$+ M_{ni} + [T_{(1)(i)}\ell_{12} + T_{2(i)}\ell_{23} + \ldots\ldots + T_{(j-1)(i)}\ell_{(j-1)j}$$
$$+ T_{(j)(i)}\ell_{j(j+1)} + \ldots\ldots + T_{(m-1)(i)}\ell_{(m-1)m}]$$

$$j = 2,3,4, \ldots\ldots, m$$

$$i = 1,2,3, \ldots\ldots, n \qquad (6.2)$$

The strains can be found as, Fig. (6.2)

$$\epsilon_{j(j-1)} = \frac{T_{(j-1)(i)}}{EA_j} - \frac{T_{(j)(i)}}{EA_j} - \frac{M_{(j)i}\, c_{(j-1)j}}{EI_j}$$

$$\epsilon_{(j-1)j} = \frac{T_{(j-2)(i)}}{EA_{j-1}} - \frac{T_{(j-1)(i)}}{EA_{j-1}} + \frac{M_{(j-1)i} c_{(j-1)j}}{EI_{j-1}}$$

$$j = 2,3,4,\ldots\ldots, m$$

$$i = 1,2,3, \ldots\ldots, n \qquad (6.3)$$

The layers have equal curvature yields,

$$\frac{M_{1i}}{EI_1} = \frac{M_{1i}}{EI_2} = \ldots\ldots = \frac{M_{(j-1)i}}{EI_{j-1}} = \frac{M_{(j)i}}{E\, I_j} = \frac{M_{(j+1)i}}{EI_{j+1}} = \ldots\ldots$$

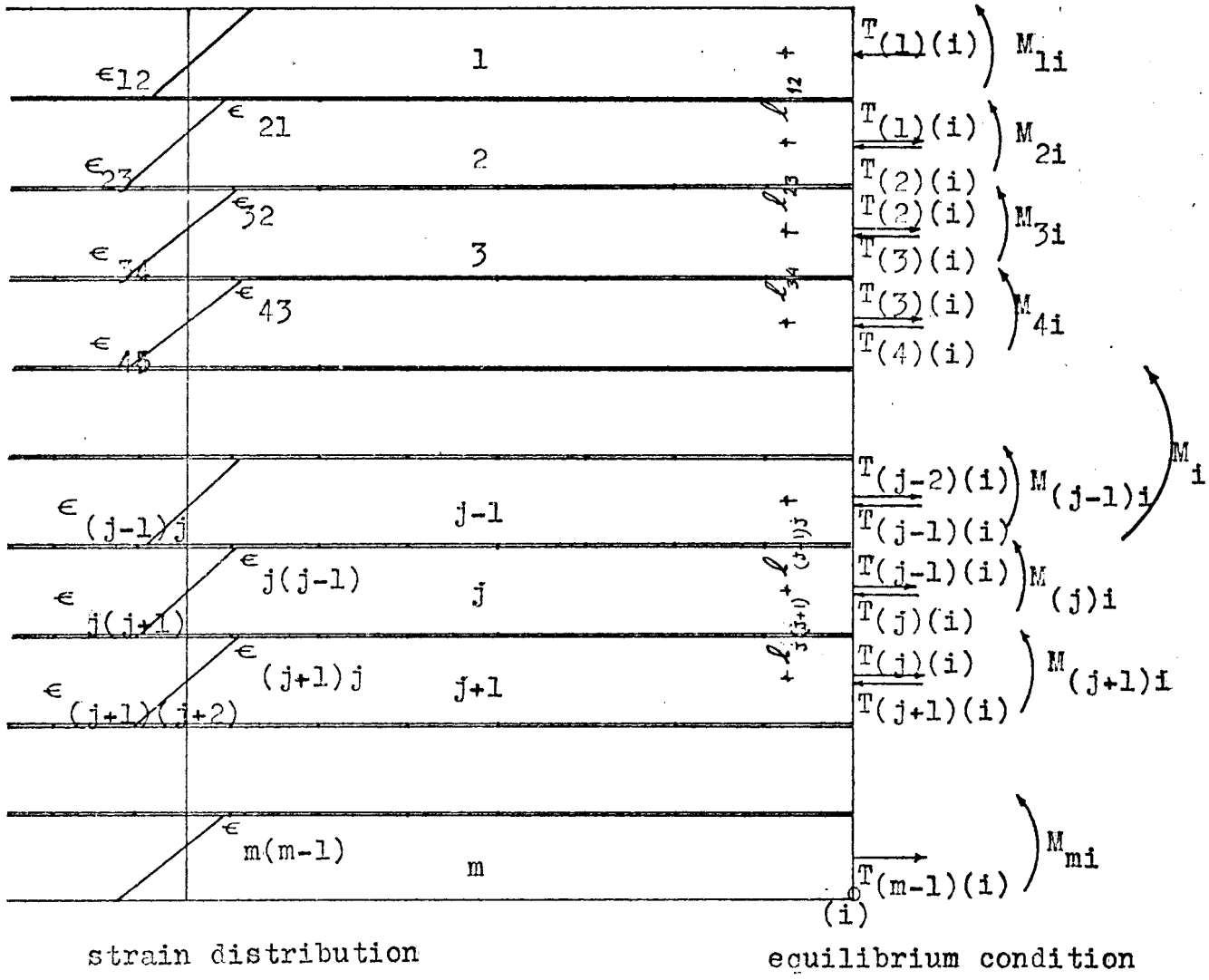

FIG. 6.2 STRAIN DISTRIBUTION AND EQUILIBRIUM CONDITION

$$= \frac{M_{mi}}{EI_m} = \frac{M_i - [T_{(1)(i)}\ell_{12} + T_{2(i)}\ell_{23} + \ldots + T_{(m-1)(i)}\ell_{(m-1)m}]}{\Sigma EI} \qquad (6.4.1)$$

where

$$\Sigma EI = EI_1 + EI_2 + \ldots + EI_{j-1} + EI_j + EI_{j+1} + \ldots + EI_m$$

$$j = 2,3, \ldots, m$$
$$i = 1,2, \ldots, n \qquad (6.4.2)$$

If the amount of slip permitted by the connector (γ) is directly proportional to the load transmitted, we get,

$$Q_i^{j(j-1)} = k_i^{j(j-1)} \gamma_i^{j(j-1)}$$

$$j = 2,3,4, \ldots, m$$
$$i = 1,2,3, \ldots, n \qquad (6.5)$$

The equilibrium of forces in the horizontal direction yields, Fig. (6.2),

$$Q_i^{j(j-1)} = T_{(j-1)(i)} - T_{(j-1)(i-1)}$$

$$j = 2,3, \ldots, m$$
$$i = 1,2, \ldots, n \qquad (6.6)$$

Substitution of Eqs. (6.6), (6.5), (6.3) in Eq. (6.1) yields,

$$\frac{T_{(j-1)(i+1)} - T_{(j-1)(i)}}{k_{i+1}^{j(j-1)}} - \frac{T_{(j-1)(i)} - T_{(j-1)(i-1)}}{k_i^{j(j-1)}} = \int \left[\frac{T_{(j-1)(i)}}{EA_j} - \frac{T_{(j)(i)}}{EA_j} - \frac{M_{(j)i}\, c_{(j-1)j}}{EI_j} - \frac{T_{(j-2)(i)}}{EA_{j-1}} + \frac{T_{(j-1)(i)}}{EA_{j-1}} - \frac{M_{(j-1)i}\, c_{(j-1)j}}{EI_{j-1}} \right] dx \qquad (6.7.1)$$

Substitution of Eq. (6.4.1) in Eq. (6.7.1) yields,

$$\frac{T_{(j-1)(i-1)}}{k_i\, j(j-1)} - \left[\frac{1}{k_i\, j(j-1)} + \frac{1}{k_{i+1}\, j(j-1)}\right] T_{(j-1)(i)} + \frac{T_{(j-1)(i+1)}}{k_{i+1}\, j(j-1)} =$$

$$\int \left\{ \left[\frac{1}{EA_{j-1}} + \frac{1}{EA_j}\right] T_{(j-1)(i)} - \frac{T_{(j)(i)}}{EA_j} - \frac{T_{(j-2)(i)}}{EA_{j-1}} \right.$$

$$\left. - \ell_{j(j-1)} \left[\frac{M_i - [T_{(1)(i)} \ell_{12} + T_{(2)(i)} \ell_{23} + \ldots + T_{(m-1)(i)} \ell_{(m-1)m}]}{\Sigma EI} \right] \right\} dx$$

i.e. (6.7.2)

$$\frac{T_{(j-1)(i-1)}}{k_i\, j(j-1)} - \left[\frac{1}{k_i\, j(j-1)} + \frac{1}{k_{i+1}\, j(j-1)}\right] T_{(j-1)(i)} + \frac{T_{(j-1)(i+1)}}{k_{i+1}\, j(j-1)} =$$

$$\int \left\{ \left[\left[\frac{1}{EA_{j-1}} + \frac{1}{EA_j} + \frac{\ell^2_{j(j-1)}}{\Sigma EI}\right] T_{(j-1)(i)} + \frac{\ell_{j(j-1)}}{\Sigma EI} \left[T_{(1)(i)} \ell_{12} + \right.\right.\right.$$

$$T_{(2)(i)}\, \ell_{23} + \ldots + T_{(j-3)(i)} \ell_{(j-3)(j-2)} + T_{(j+1)(i)} \ell_{(j+1)j} + \ldots +$$

$$\left.\left.\left. T_{(m-1)(i)}\, \ell_{(m-1)m} \right] - \left[\frac{1}{EA_j} - \frac{\ell_{j(j-1)} \cdot \ell_{j(j+1)}}{\Sigma EI}\right] T_{(j)(i)} \right.\right.$$

$$\left. \left. - \left[\frac{1}{EA_{j-1}} - \frac{\ell_{j(j-1)} \ell_{(j-2)(j-1)}}{\Sigma EI}\right] T_{(j-2)(i)} \right\} dx - \int \frac{\ell_{j(j-1)}}{\Sigma EI} M_i\, dx \right.$$

(6.7.3)

i.e.

$$\frac{T_{(j-1)(i-1)}}{k_i\, j(j-1)} + \left[\frac{1}{EA_{j-1}} - \frac{\ell_{j(j-1)} \ell_{(j-1)(j-2)}}{\Sigma EI}\right] h_{(i)} T_{(j-2)(i)}$$

$$- \left[\frac{1}{k_i\, j(j-1)} + \frac{1}{k_{i+1}\, j(j-1)} + \left[\frac{1}{EA_{j-1}} + \frac{1}{EA_j} + \frac{\ell^2_{j(j-1)}}{\Sigma EI}\right] h_{(i)}\right] T_{(j-1)(i)}$$

$$+ \left[\frac{1}{EA_j} - \frac{\ell_{j(j-1)} \ell_{j(j+1)}}{\Sigma EI}\right] h_{(i)}\, T_{(j)(i)} - \frac{\ell_{j(j-1)}}{\Sigma EI} \left[T_{(1)(i)} \ell_{12} + \right.$$

$$T_{(2)(i)}\ell_{23} + \ldots\ldots + T_{(j-3)(i)}\,\ell_{(i-3)(j-2)} + T_{(j+1)}\ell_{(j+1)j} + \ldots\ldots + T_{(m-1)(i)}\,\ell_{(m-1)m}\Big]\, h_{(i)}$$

$$+ \frac{T_{(j-1)(i+1)}}{k_{i+1}} = -\int \frac{\ell_{j(j-1)}}{\Sigma EI} M_i\, dx \quad \ldots\ldots \quad (6.7.4)$$

i.e.

$$\frac{T_{(j-1)(i-1)}}{k_i} - \frac{h_{(i)}\ell_{j(j-1)}}{\Sigma EI}\Big[T_{(1)(i)}\ell_{12} + T_{(2)(i)}\ell_{23} + \ldots\ldots + T_{(j-3)(i)}\ell_{(j-3)(j-2)}\Big]$$

$$+ \left[\frac{1}{EA_{j-1}} - \frac{\ell_{j(j-1)}\ell_{(j-1)(j-2)}}{\Sigma EI}\right] h_{(i)}\, T_{(j-2)(i)}$$

$$- \left[\frac{1}{k_i} + \frac{1}{k_{i+1}} + \left(\frac{1}{EA_{j-1}} + \frac{1}{EA_j} + \frac{\ell^2_{j(j-1)}}{\Sigma EI}\right) h_{(i)}\right]$$

$$T_{(j-1)(i)} + \left[\frac{1}{EA_j} - \frac{\ell_{j(j-1)}\ell_{j(j+1)}}{\Sigma EI}\right] h_{(i)}\, T_{(j)(i)}$$

$$- \frac{h_{(i)}\ell_{j(j-1)}}{\Sigma EI}\Big[T_{(j+1)(i)}\ell_{(j+1)(j+2)} + \ldots + T_{(m-1)(i)}\ell_{(m-1)(m)}\Big]$$

$$+ \frac{T_{(j-1)(i+1)}}{k_{i+1}} = -\int \frac{\ell_{j(j-1)}}{\Sigma EI} M_i\, dx$$

$$j = 2,3,4, \ldots, m$$
$$i = 1,2,3, \ldots, n$$

(6.8)

The boundary conditions are, for the cantilever, fig. (6.1C),

$$T_{(j-1)(0)} = 0 \qquad j = 2,3, \ldots, m \quad ..(6.9.1)$$

&

$$Q^{j(j-1)}_{n+1} = 0$$

i.e. $K_{n+1}^{j(j-1)} = \infty \qquad j = 2,3, \ldots,m$ (6.9.2)

Equation (6.3) represents a typical equation for panel (i), (i = 1,2,3,...,n), between two layers (j) and (j-1), (j= 2,3,4, ...,m). For a multi-layered beam with "n" panels and "m" layers there are [n.(m-1)] such equations resulting in a set of [n.(m-1)] simultaneous equations.

This can be written in matrix notation as

$[B]\{T\} = \{A\}$ ..... (6.10.1)

[B] is a band matrix with half band width equal to (m). {T} is a vector. {A} is a vector.

Having obtained the axial forces $T_{(j-1)(i)}$, [j =2,3, ...,m and i = 1,2, ..., n), the other forces and deformations of each layer can be determined.

6.4 Numerical Example

A cantilever multi-layered beam with n = 20, m = 15, span = 200 in., E = 3.0 x 10^6 lb/sq. in., A_{j-1} = 2 sq. in., $\ell_{j(j-1)}$ = 2 in., $h_{(i)}$ = 10 in., thickness = 1 in., k_i varies from 1000 to 1,000,000 lb/in., subjected to a uniformly distributed load p = 2 lb/in. A computer program was developed to get the forces and deformations of the layers. Fig. (6.3) shows the strain distribution across the layers in the panel nearest the fixed end. It may be noticed that when k = 1000, the multi-layered beam behaves as separate layers and when k = 1,000,000 it behaves as a homogeneous beam following the

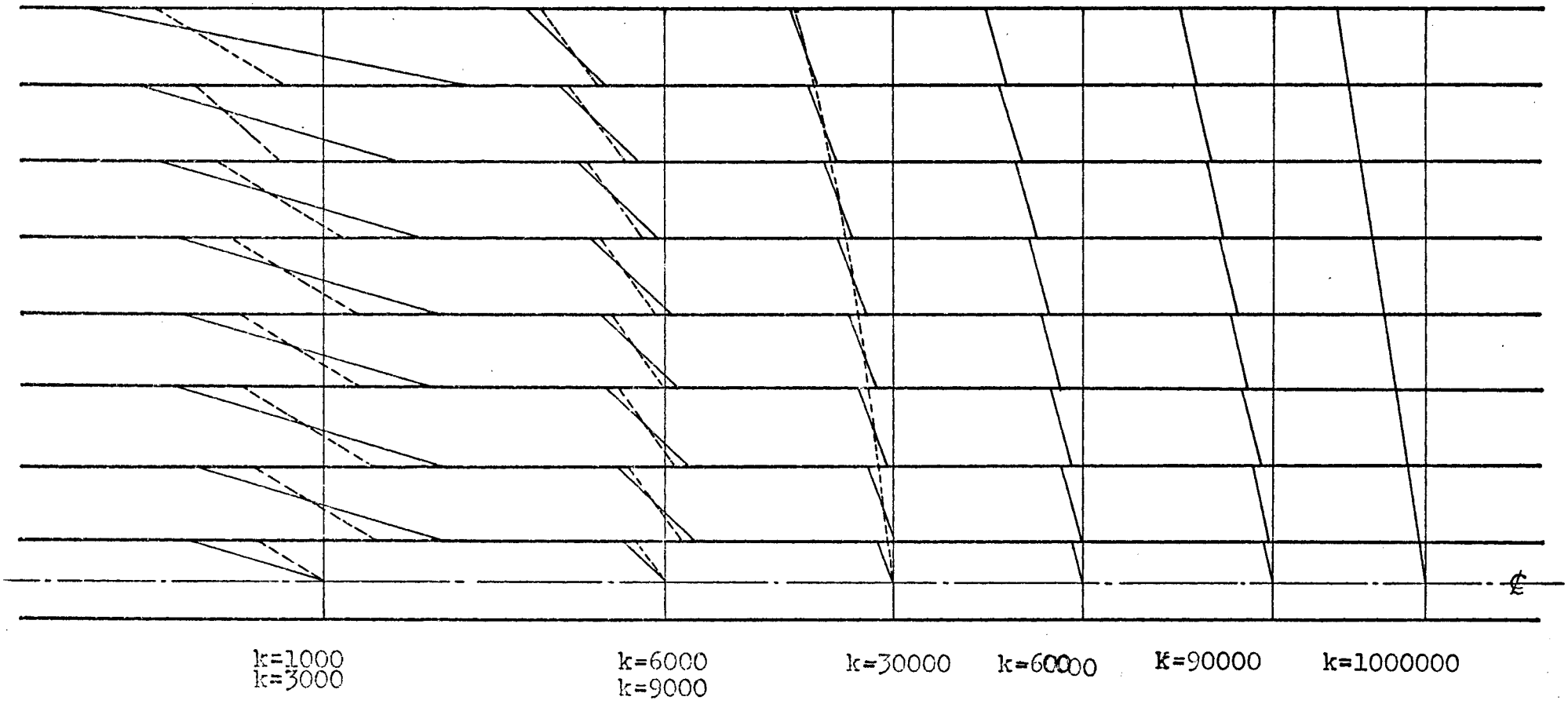

FIG. 6.3 STRAIN DISTRIBUTION AT BASE OF MULTI-LAYERED BEAM.

the simple bending theory.

6.5 Formulation of the Problem, Continuous Solution

Assuming the shear connection between the different layers as a continuous one, a continuous solution for the multi-layered beam can be developed.

Eq. (6.1) can be rewritten as,

$$\frac{d\gamma_i^{j(j-1)}}{dx} = \varepsilon_{j(j-1)} - \varepsilon_{(j-1)j} \tag{6.11}$$

Eq. (6.5) can be rewritten as,

$$q_i^{j(j-1)} h_{(i)} = k_i^{j(j-1)} \gamma_i^{j(j-1)} \tag{6.12}$$

Differentiating Eq. (6.12) once yields

$$\frac{d^2 T_{(j-1)(i)}}{dx} h_{(i)} = k_i^{j(j-1)} \cdot \frac{d\gamma_i^{j(j-1)}}{dx} \tag{6.13}$$

Substitution of Eqs, (6.13), (6.3) in Eq. (6.11) yields,

$$\frac{h_{(i)}}{k_i^{j(j-1)}} \frac{d^2 T_{(j-1)(i)}}{dx^2} - \frac{\ell_{j(j-1)}}{\Sigma EI} [T_{(1)(i)} \ell_{12} + T_{2(i)} \ell_{23} + \ldots\ldots$$

$$+ T_{(j-3)(i)} \ell_{(j-3)(j-2)}] + [\frac{1}{EA_{j-1}} - \frac{\ell_{j(j-1)} \ell_{(j-2)(j-1)}}{\Sigma EI}] T_{(j-2)(i)}$$

$$- [\frac{1}{EA_j} + \frac{1}{EA_{j-1}} + \frac{\ell^2_{j(j-1)}}{\Sigma EI}] T_{(j-1)(i)} + [\frac{1}{EA_i} - \frac{\ell_{j(j-1)} \ell_{j(j+1)}}{\Sigma EI}]$$

$$T_{(j)(i)} - \frac{\ell_{j(j-1)}}{\Sigma EI} [T_{(j+1)(i)} \ell_{(j+1)(j+2)} + \ldots\ldots + T_{(m-1)(i)} \ell_{(m-1)m}]$$

$$= - \frac{\ell_{j(j-1)}}{\Sigma EI} M_i \tag{6.14}$$

$$j = 2,3,4, \ldots, m$$

Eq. (6.14) represents the governing differential equation of the problem. For a multi-layered beam of m layers, there are (m-1) second order simultaneous differential equations, Eq. (6.14). The finite difference solution in section (6.3) can be considered a way of solving the (m-1) second order simultaneous differential equations (6.14).

6.6 Approximate Analysis of Multi-Piered Coupled Shear Walls

Considering a multi-piered coupled shear wall with m piers and assuming the point of contraflexure to be at mid-span of the connecting beams, the above analysis of multi-layered beams can be applied.

Equation (6.8) represents a finite difference equation for panel (i), (i=1,2,3,...,n), between two piers ($\dot{J}$) and ($\dot{J}$-1), ($\dot{J}$ = 2,3,4,...,m). For a coupled shear wall with n storeys and m piers connected together by m-1 connecting beams there are [n.(m-1)] such equations resulting in a set of [n.(m-1)] simultaneous finite difference equations.

The modulus of the connecting beams, $k_i^{\dot{J}(\dot{J}-1)}$ where ($\dot{J}$ = 2,3,...,m), can be found as:

$$k_i^{\dot{J}(\dot{J}-1)} = 1./\left[\frac{b^3_{\dot{J}(\dot{J}-1)}}{12E\, I_{b_{\dot{J}(\dot{J}-1)}}} + \frac{b_{\dot{J}(\dot{J}-1)}}{G\, A_{b_{\dot{J}(\dot{J}-1)}}}\right]$$

$$\dot{J} = 2,3,\ldots, m$$
$$i = 1,2,\ldots, n$$

where $b_{\dot{J}(\dot{J}-1)}$, $A_{b_{\dot{J}(\dot{J}-1)}}$, $I_{b_{\dot{J}(\dot{J}-1)}}$ represent the span, the reduced area and the moment of inertia of the connecting beam

between piers $\dot{J}$ and $(\dot{J}-1)$, $(\dot{J} = 2,3,\ldots,m)$.

6.6.1 Numerical Example

To illustrate the use of the theory, a coupled shear wall with 6 piers was analysed. The properties of the shear wall are, $h_{(i)} = 10$ ft., $H = 100$ ft., $b_{\dot{J}(\dot{J}-1)} = 5$ ft., $\ell_{\dot{J}(\dot{J}-1)} = 25$ ft., $d_{\dot{J}} = 20$ ft., $d_{b\dot{J}(\dot{J}-1)} = 2$ ft. and thickness 1 ft. under a uniformly distributed load of 2 kip/ft.

Figs. (6.4), (6.5) and (6.6) show the distribution of axial forces in the piers, the shearing forces in the connecting beams, the internal bending moments in the piers, the deflection of the piers and the strain distribution at the base of the coupled shear wall.

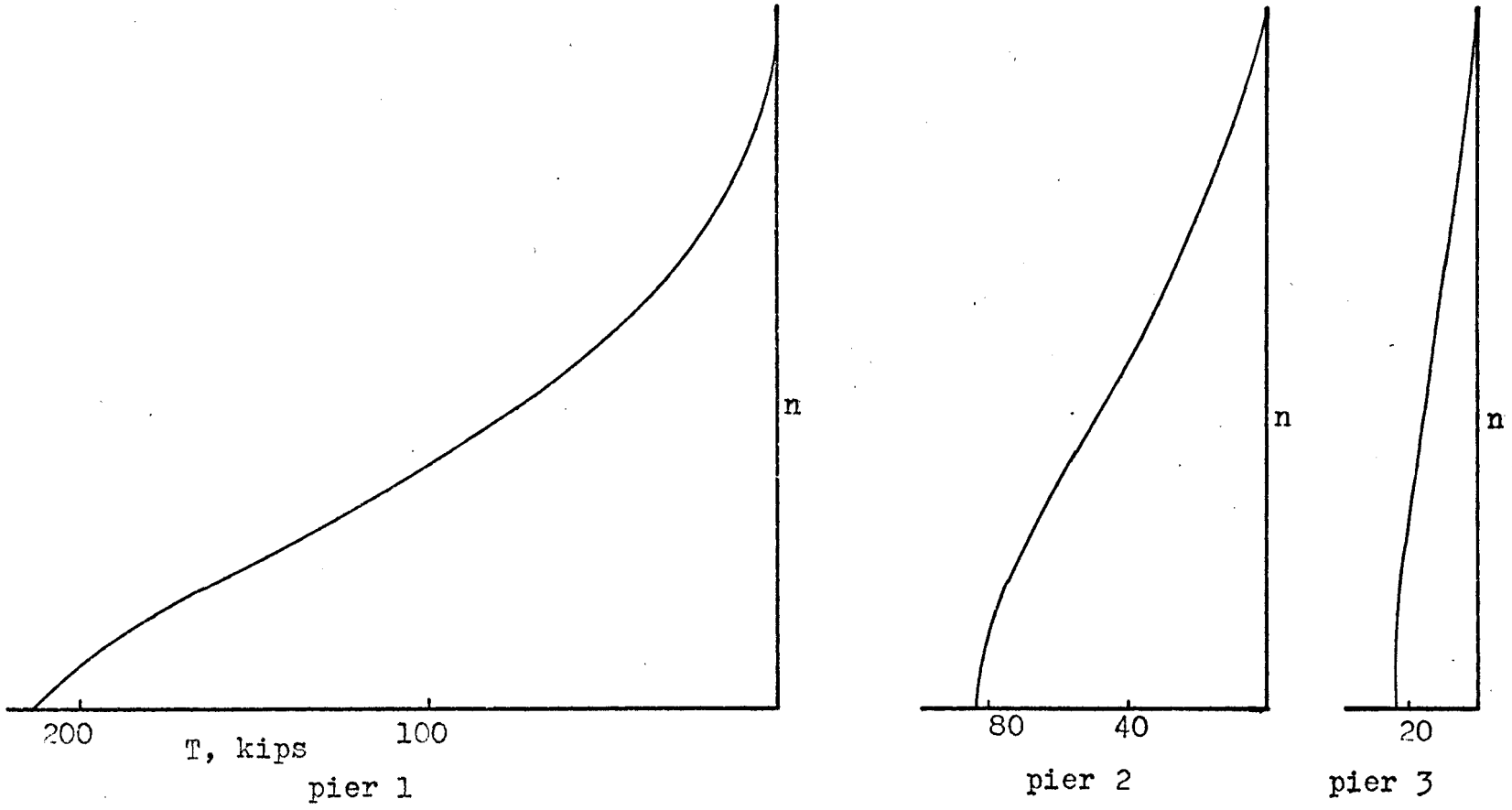

FIG. 6.4 "T" DIAGRAMS

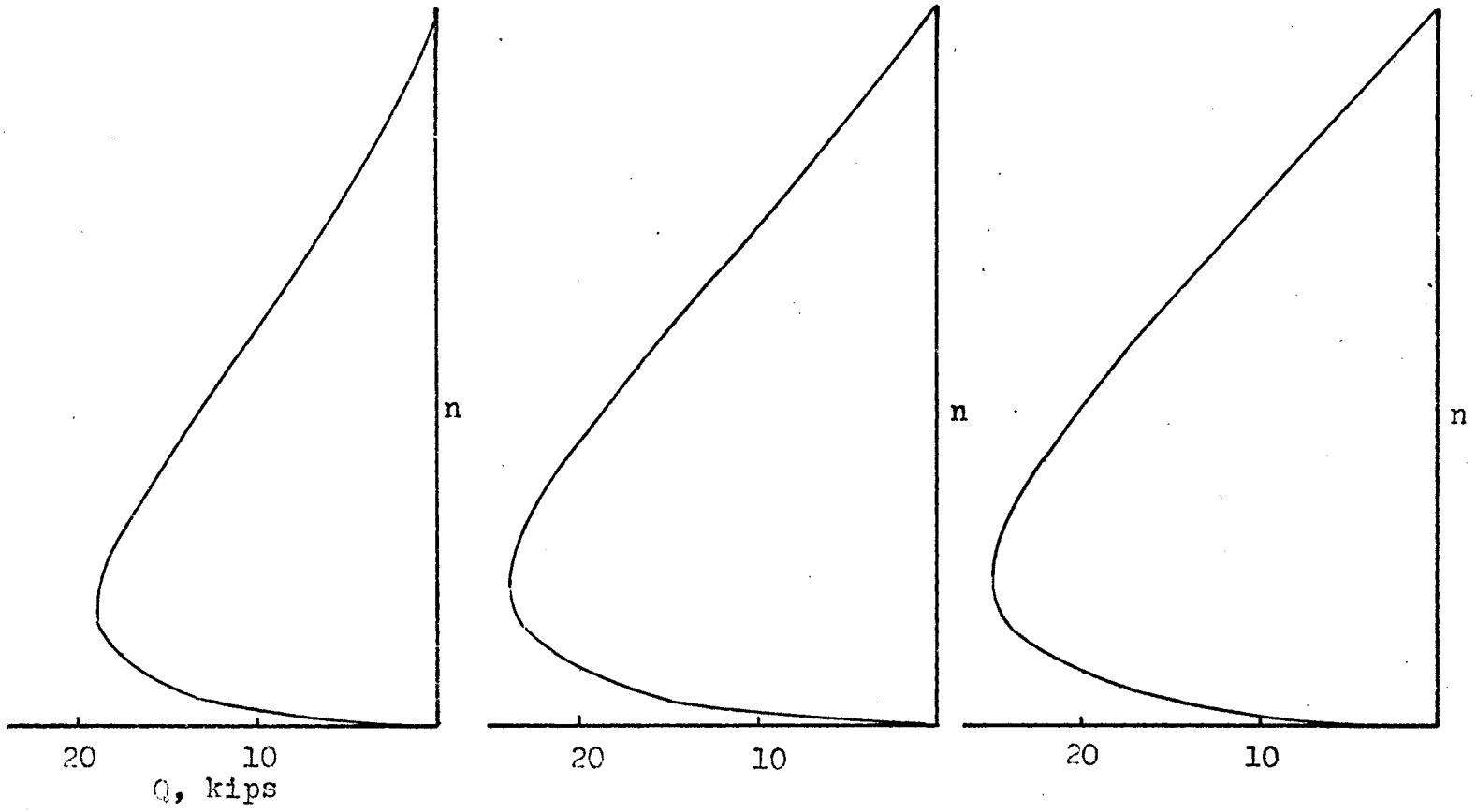

between piers 1&2 between piers 2&3 between piers 3&4

FIG. 6.5 "Q" DIAGRAMS

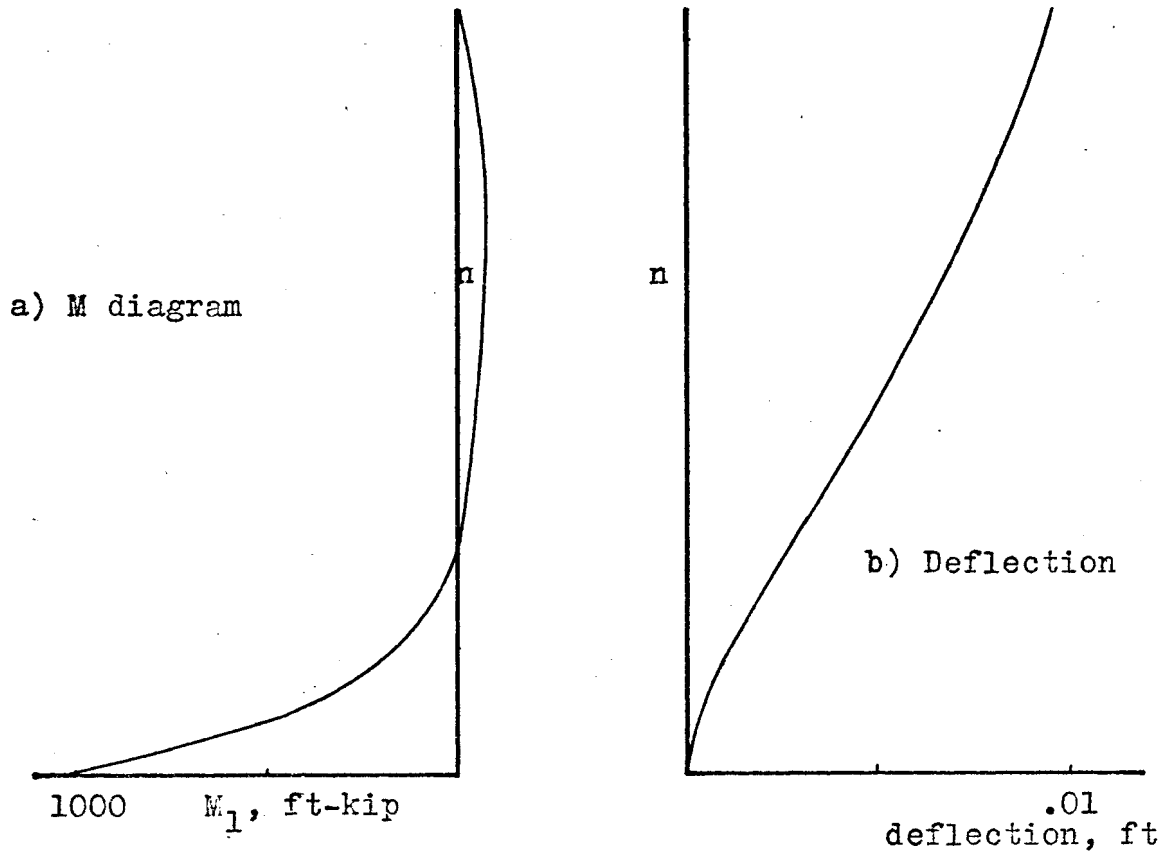

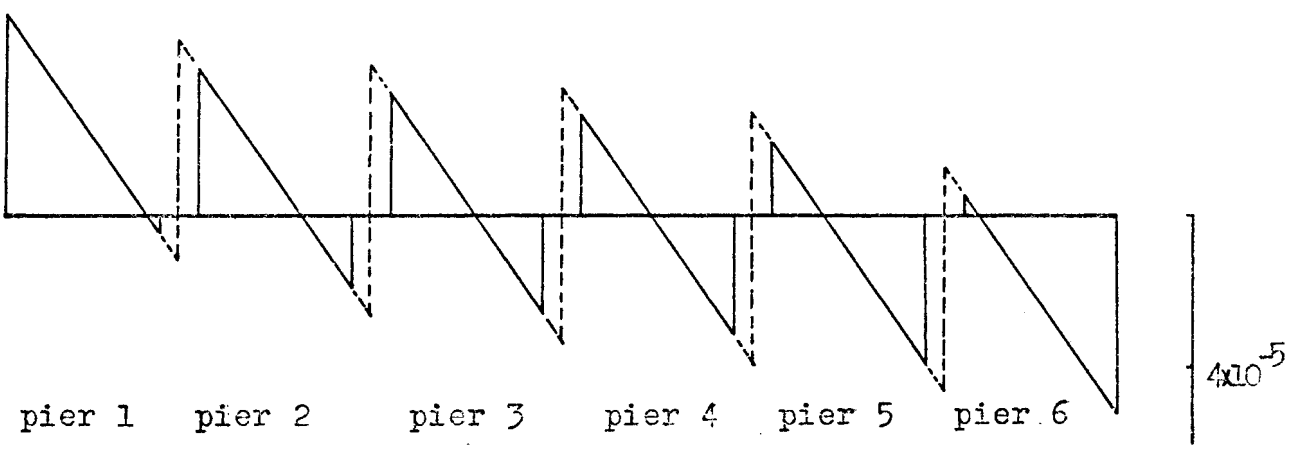

c) Strain distribution at the base accross the piers of the shear wall.

FIG. 6.6 M_1 , DEFLECTION AND STRAIN DISTRIBUTION AT BASE DIAGRAMS.

CHAPTER 7

COUPLED SHEAR WALLS WITH ELASTIC FOUNDATIONS

7.1 General

The majority of methods of analysis commonly used by engineers for the design of shear wall structures make the assumption that the structure is built into a rigid foundation. Such an assumption simplifies the mathematical analysis of the problem.

However, depending on the form of the structure and the particular soil conditions encountered, it may be considered desirable to estimate the effects of differential settlements produced by foundation movement. It is desirable to be able to estimate accuractely the influence of the foundation movement on the stress distribution and the overall deformation of the coupled shear wall. For this purpose, it is convenient to assume that the structure rests on elastic supports, which yield both vertically and rotationally under the action of axial forces and moments, respectively.

Coull, [13] in his recent paper in 1971, presents an analysis of a plane coupled shear wall resting on elastic supports. His analysis was based on the continuous connection method. Here, we develop the analysis of the plane coupled shear wall resting on elastic supports using the finite

difference method. This yields the solution of the problem in a simple way.

Coull made some mistakes in his paper. The solution of a coupled shear wall, based on the continuous method, are redeveloped and presented here, and the error by Coull pointed out.

7.2 Formulation of the Problem, Finite Difference Method

Consider the coupled shear wall shown in Fig. (7.1). For panel (i), the finite difference equation can be found as:

$$\frac{T_{(i-1)}}{k_i} - \left(\frac{1}{k_i} + \frac{1}{k_{i+1}} + \psi_{(i)} h_{(i)}\right) T_{(i)} + \frac{T_{(i+1)}}{k_{i+1}} = - \int_{h(i)} \zeta M \, dx \tag{7.1}$$

where

$$k_i = 1/\left[\frac{b^3}{12 E I_p} + \frac{b}{G A^*_b} \right]_i$$

$$\psi_{(i)} = \left[\frac{1}{E_1 A_1} + \frac{1}{E_2 A_2} + \frac{\ell^2}{\Sigma EI} \right]_{(i)} \tag{7.2}$$

$$\zeta = \frac{\ell^2}{\Sigma EI}$$

$$\Sigma EI = E_1 I_1 + E_2 I_2$$

M is the external applied bending moment at panel (i).

At the upper free end, the boundary condition is,

$$\text{At } x = 0, \quad T(0) = 0 \tag{7.3}$$

To get the boundary condition at the fixed end, two different forms of structure - foundation interaction will be considered.

7.2.1 Elastic Vertical Movement

Assume that the walls remain vertical, but, owing to

the elasticity of the foundations, a vertical displacement occurs which is directly proportional to the axial force at the base of the wall. The relative displacement γ_{n+1} at the base may be expressed as:

$$\gamma_{n+1} = K_{\gamma}\, T_{(n)} \quad .... \tag{7.4}$$

where K_{γ} is a constant depending on the foundation system used. For example, if the cross-sectional area of the two foundation systems are a_1 and a_2 with K_1 and K_2 the moduli of the subgrade reaction, the relative vertical displacement at the base becomes, Fig. (7.2),

$$\gamma_{n+1} = T_{(n)} \cdot \left(\frac{1}{k_1 a_1} + \frac{1}{k_2 a_2} \right) \quad .... \tag{7.5}$$

where $T_{(n)}$ is the axial force in panel (n) at the base.

Proceeding as in Chapter 2, the n simultaneous finite difference equations can be found as:

$$\begin{aligned}
&-\left(\frac{1}{k_1} + \frac{1}{k_2} + \psi_{(1)} h_{(1)} \right) T_{(1)} + \frac{T_{(2)}}{k_2} = -\int_{h(1)} \zeta\, M\, dx \\
&\frac{T_{(1)}}{k_2} - \left(\frac{1}{k_2} + \frac{1}{k_3} + \psi_{(2)} h_{(2)} \right) T_{(2)} + \frac{T_{(3)}}{k_3} = -\int_{h(2)} \zeta\, M\, dx \\
&\cdots\cdots \quad \cdots\cdots \quad \cdots\cdots \quad \cdots\cdots \quad \cdots\cdots\cdots \quad \cdots\cdots\cdots \\
&\frac{T_{(i-1)}}{k_i} - \left(\frac{1}{k_i} + \frac{1}{k_{i+1}} + \psi_{(i)} h_{(i)} \right) T_{(i)} + \frac{T_{(i+1)}}{k_{i+1}} = -\int_{h(i)} \zeta\, M\, dx \\
&\cdots\cdots \quad \cdots\cdots \quad \cdots\cdots \quad \cdots\cdots \quad \cdots\cdots\cdots \quad \cdots\cdots\cdots\cdots \\
&\frac{T_{(n-1)}}{k_n} - \left(\frac{1}{k_n} + \psi_{(n)} h_{(n)} + K_{\gamma} \right) T_{(n)} = -\int_{h(n)} \zeta\, M\, dx
\end{aligned} \tag{7.6}$$

The boundary conditions are

$$\text{At } x = 0 \qquad T(0) = 0 \tag{7.7}$$

$$\text{At } x = H \qquad \gamma_{n+1} = - T_{(n)} \cdot K_{\gamma} \cdot \tag{7.8}$$

7.2.2 Elastic Rotational Movement

Assume the foundations rotate under the influence of the imposed moments at the base of the walls. The base rotations for the two piers will be the same, θ, and proportional to the applied moment M_{iH} (i=1,2). The moment rotation relationship may be expressed as

$$\frac{dv}{dx} = \theta = K_{\theta} M_H \qquad \ldots\ldots \tag{7.9}$$

where K_{θ} is a constant which depends on the stiffness of the foundation system.

For example, if the applied moment is resisted by a linear pressure distribution on the base of the foundation slab, the edge displacement δ is given by, Fig. (7.4),

$$\delta = \frac{p}{K} = \frac{1}{K} \frac{M_H . d/2}{I} \qquad \ldots\ldots \tag{7.10}$$

where K is the modulus of the subgrade reaction, p is the edge pressure, and I is the second moment of area of the slab.

The rotation θ of the foundation is then given by

$$\theta = \frac{\delta}{d/2} = \frac{M_H}{K\ I} \tag{7.11}$$

The bending moment at the base of wall 1 is given by

$$M_{1H} = \frac{I_1}{I_1 + I_2} (M - T_{(n)} . \ell) \tag{7.12}$$

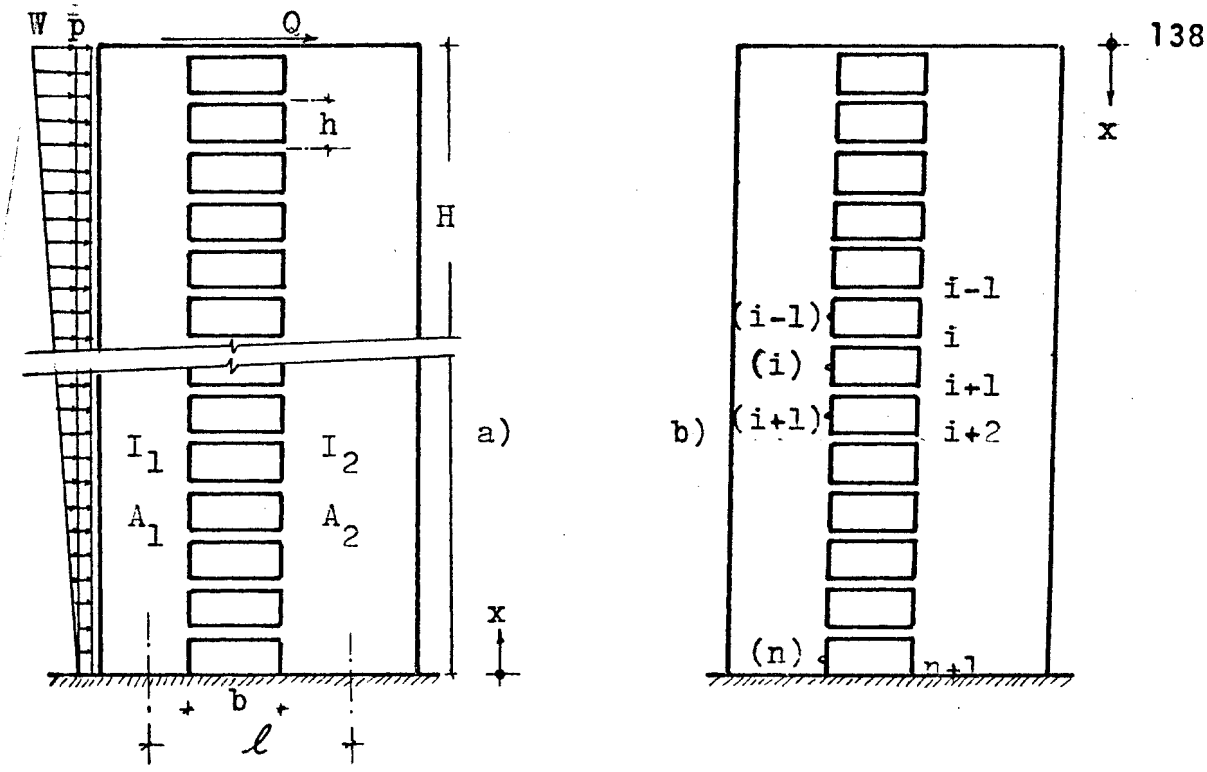

FIG. 7.1 COUPLED SHEAR WALL

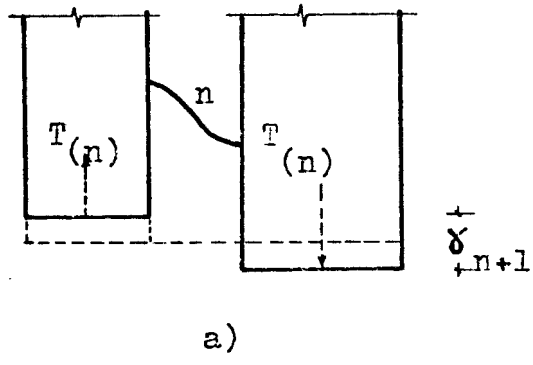

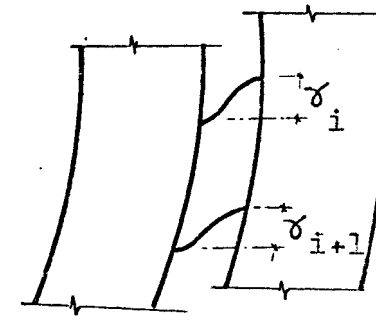

FIG. 7.3 SLIP OF THE CONNECTING BEAMS

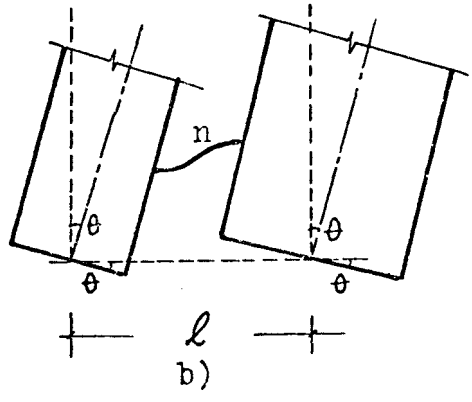

FIG. 7.2 VERTICAL AND ROTATIONAL SETTLEMENT AT BASE

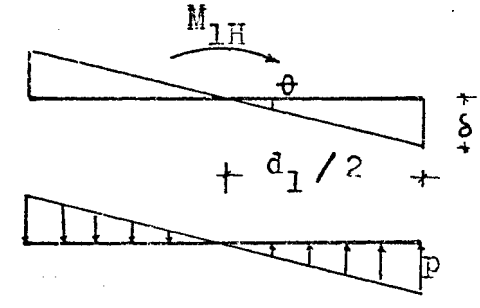

FIG. 7.4 REACTIVE PRESSURE DISTRIBUTION AND SETTLEMENT DUE TO IMPOSED MOMENT ON WALL 1.

The relative displacement at the base, γ_{n+1}, is equal to $\ell\theta$, i.e.

$$\gamma_{n+1} = \ell \frac{I_1}{I_1+I_2} K_{\theta 1} (M - T_{(n)}.\ell) \quad \ldots\ldots \quad (7.13)$$

Now the n simultaneous finite difference equations can be found as:

$$-\left(\frac{1}{k_1} + \frac{1}{k_2} + \psi_{(1)}h_{(1)}\right) T_{(1)} + \frac{T_{(2)}}{k_2} = -\int_{h(1)} \zeta M \, dx$$

$$\frac{T_{(1)}}{k_2} - \left(\frac{1}{k_2} + \frac{1}{k_3} + \psi_{(2)}h_{(2)}\right)T_{(2)} + \frac{T_{(3)}}{k_3} = -\int_{h(2)} \zeta M \, dx \quad (7.14)$$

$$\ldots\ldots \quad \ldots\ldots \quad \ldots\ldots \quad \ldots\ldots \quad \ldots\ldots \quad \ldots\ldots$$

$$\frac{T_{(i-1)}}{k_i} - \left(\frac{1}{k_i} + \frac{1}{k_{i+1}} + \psi_{(i)}h_{(i)}\right) T_{(i)} + \frac{T_{(i+1)}}{k_{i+1}} = -\int_{h(i)} \zeta M \, dx$$

$$\ldots\ldots \quad \ldots\ldots \quad \ldots\ldots \quad \ldots\ldots \quad \ldots\ldots \quad \ldots\ldots$$

$$\frac{T_{(n-1)}}{k_n} - \left(\frac{1}{k_n} + \psi_{(n)}h_{(n)} + \ell^2 \frac{I_1}{I_1+I_2} K_{\theta 1}\right) T_{(n)} = -\int_{h(n)} \zeta M \, dx - \ell \frac{I_1}{I_1+I_2}.K_{\theta 1}.M$$

The shear force in any connecting beam Q_i is obtained from,

$$Q_i = T_{(i)} - T_{(i-1)} \quad \ldots\ldots \quad (7.15)$$

The curvature in panel (i) is

$$\Phi_i = \frac{M - T_{(i)}.\ell}{\Sigma EI} \quad \ldots\ldots \quad (7.16)$$

The deformations of the coupled shear walls can be determined by numerical integration of the curvature and adding to them the linear effect of the rotational settlement at the base which has the values $[\theta.(H-x)]$.

The strain distribution at any section can be determined from the expressions mentioned in Chapter 2.

7.2.3 Elastic Vertical and Rotational Movement

If elastic vertical movement and rotational movement occurs simultaneously, the n simultaneous finite difference equations can be found as:

$$-\left(\frac{1}{k_1}+\frac{1}{k_2}+\psi_{(1)}h_{(1)}\right)T_{(1)}+\frac{T_{(2)}}{k_2}=-\int_{h(1)}\zeta\, M\, dx$$

$$\frac{T_{(1)}}{k_2}-\left(\frac{1}{k_2}+\frac{1}{k_3}+\psi_{(2)}h_{(2)}\right)T_{(2)}+\frac{T_{(3)}}{k_3}=-\int_{h(2)}\zeta\, M\, dx$$

.... (7.17)

$$\frac{T_{(i-1)}}{k_i}-\left(\frac{1}{k_i}+\frac{1}{k_{i+1}}+\psi_{(i)}h_{(i)}\right)T_{(i)}+\frac{T_{(i+1)}}{k_{i+1}}=-\int_{h(i)}\zeta\, M\, dx$$

....

$$\frac{T_{(n-1)}}{k_n}-\left(\frac{1}{k_n}+\psi_{(n)}h_{(n)}+K_\gamma+\ell^2\frac{I_1}{I_1+I_2}K_{\theta 1}\right)T_{(n)}=-\int_{h(n)}\zeta M dx-\ell\frac{I_1}{I_1+I_2}\cdot K_{\theta 1}\cdot M$$

The boundary conditions are,

At $x = 0$ $\quad T(0) = 0$

At $x = H$ $\quad \gamma_{n+1} = -T_{(n)}K_\gamma+\ell\frac{I_1}{I_1+I_2}K_{\theta 1}(M-T_{(n)}\cdot\ell)$ (7.18)

The above finite difference method is valid for analysing coupled shear walls with variable cross-sections resting on elastic foundations.

7.2.4 Example

To illustrate the use of the theoretical expressions, and to examine the influence of foundation settlement on the stresses and deflections in a system of coupled shear walls,

the example shown in section 2.2.4 is used.

Tables (7.1), (7.2) show the influence of a representative range of vertical and rotational foundation stiffness on the axial forces and moments at the base, and the maximum deflection at the top of the structure.

Figs. (7.5) and (7.6) show the influence of rotational and vertical stiffness on the axial forces and moments in the piers and the deflection of the piers.

As the vertical stiffness, K_γ, increases, the deflection of the shear wall and the internal moments in the piers increase while the axial forces in the piers decrease.

As the rotational stiffness, K_θ, increases, the deflection of the shear wall and the axial forces in the piers increase while the internal moments in the piers decrease.

Vertical compliance of the foundation is more significant than the rotational compliance of the foundation, both for stress and deflection considerations of the structure.

7.3 Formulation of the Problem, Continuous Connection Method

Consider the coupled shear wall shown in Fig. (7.1a), subjected to a concentrated load at the top Q, a distributed load of intensity p and a triangular load of intensity w at the top.

The governing differential equation can be found as,

$$\frac{d^2q}{dx^2} - \alpha^2 q = -\beta^2\{p(H-x) + \frac{w}{2H}(H^2 - x^2) + Q\} \qquad (7.19)$$

TABLE (7.1)

INFLUENCE OF VERTICAL STIFFNESS AND ROTATIONAL STIFFNESS
ON AXIAL FORCES AND BENDING MOMENTS AT BASE, AND DEFLECTION AT TOP

K_γ ft/lbx10^{-9}	K_{θ_1} rad./ ft-lbx10^{-12}	T_H lbx10^3	M_{H1} ft-lbx10^4	M_{H2} ft-lbx10^4	v_{max} ftx10^{-2}	γ_{n+1} ftx10^{-4}	θ radionsx10^{-6}	Strain ε_1 x10^{-4}	Strain ε_2 x10^{-4}
0	0	657	333	333	7.72	0	0	-1.476	.199
4	0	582	440	440	8.88	23.2	0	-1.672	-540
8	0	522	524	524	9.80	41.8	0	-1.828	.540
16	0	433	651	651	11.17	69.2	0	-2.059	1.216
0	.1	657	333	333	7.73	0	.33	-1.476	.197
0	1.0	660	329	329	7.74	0	3.3	-1.469	.185
0	4.0	668	316	316	7.79	0	12.7	-1.446	.146
0	12.0	688	288	288	7.97	0	37.5	-1.394	.055
0	100	789	144	144	8.43	0	144	-1.131	-.404
0	1000	874	24	24	9.10	0	240	-.910	-.791
4	.1	582	439	439	8.88	23.3	.44	-1.671	.539
8	1.0	526	519	519	9.85	42.1	5.19	-1.818	.795
16	4.0	448	629	629	11.43	71.7	25.17	-2.020	1.147

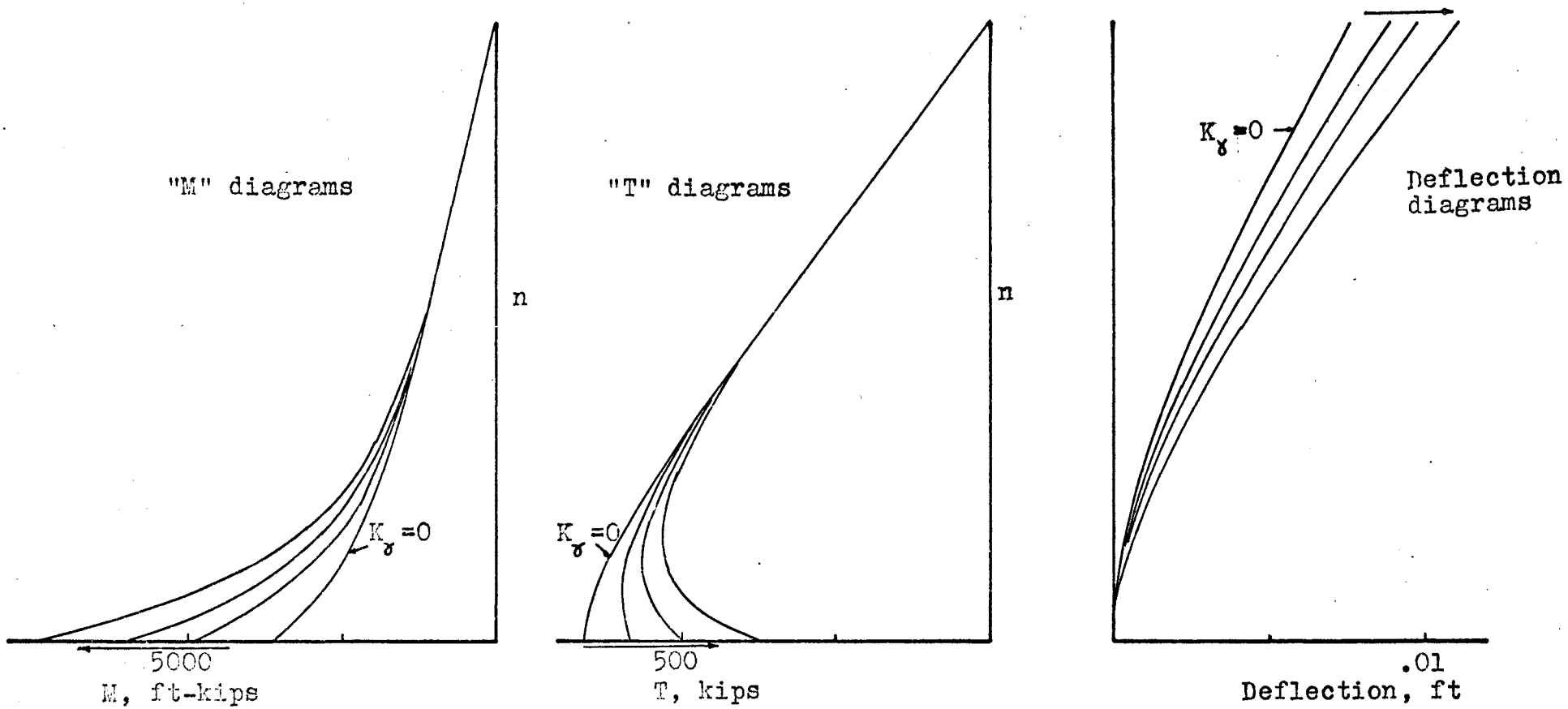

$$0 \leqslant K_\gamma \leqslant 16 \times 10^{-9} \text{ ft/lb}$$

FIG. 7.5 INFLUENCE OF VERTICAL STIFFNESS.

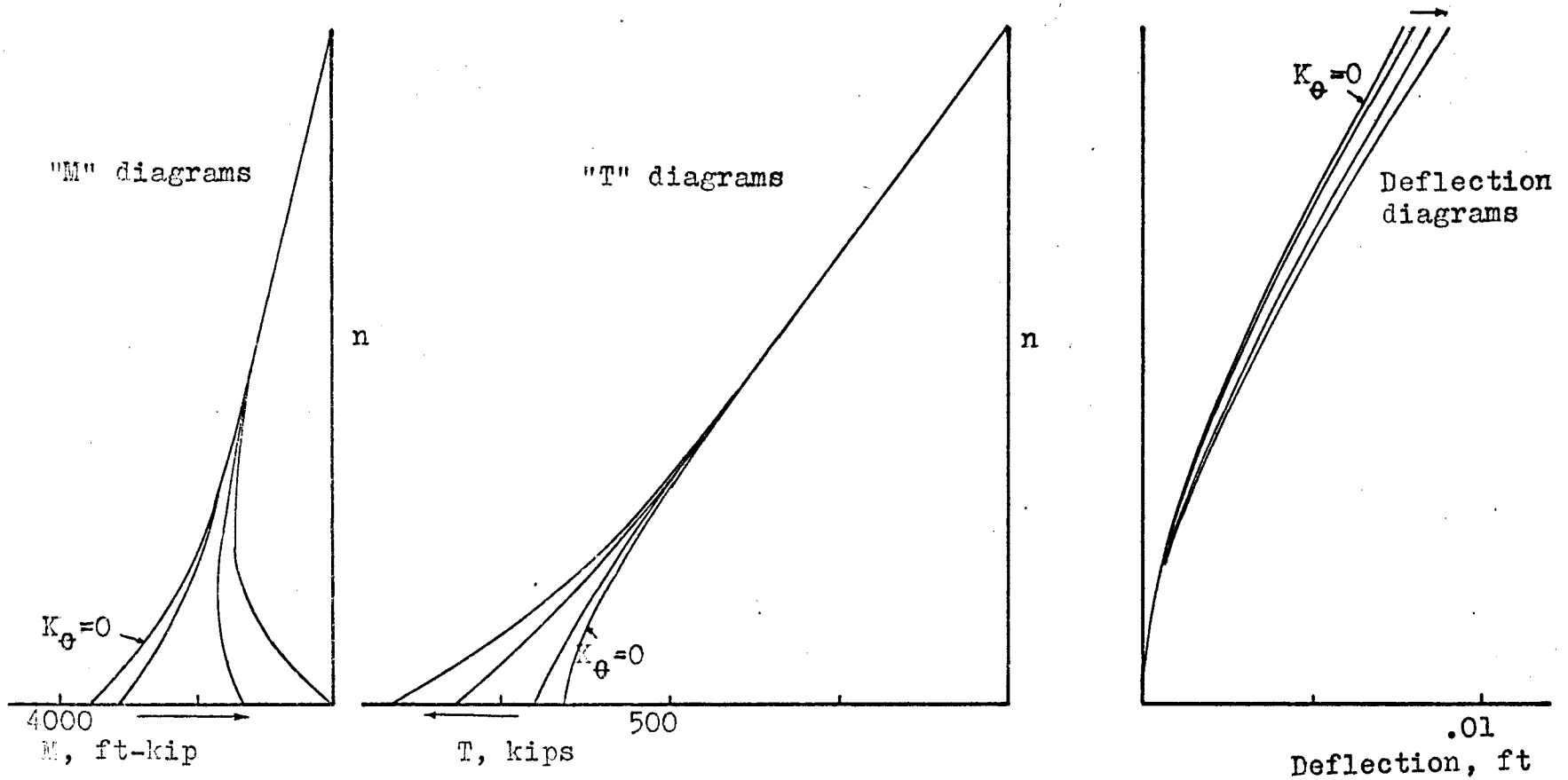

$0 \leqslant K_\theta \leqslant 1 \times 10^{-9}$ radians ft-lb

FIG. 7.6 INFLUENCE OF ROTATIONAL STIFFNESS.

where

$$\alpha^2 = \beta^2 \left\{\frac{AI}{A_1 A_2 \ell} + \ell\right\}$$

$$A = A_1 + A_2$$

$$I = I_1 + I_2 \qquad (7.20)$$

$$\beta^2 = \frac{12\, I_b\, \ell}{b^3\, h\, I}$$

The general solution of equation (7.19) is:

$$q = B_1 \cosh \alpha x + B_2 \sinh \alpha x + \frac{\beta^2}{\alpha^2}\left\{p(H-x) + \frac{\omega}{2H}\left(H^2 - x^2 - \frac{2}{\alpha^2}\right) + Q\right\} \qquad (7.21)$$

The axial force T at height x is:

$$T = \int_x^H q\, dx \qquad (7.22.1)$$

i.e.

$$T = \frac{1}{\alpha}\{B_1(\sinh \alpha H - \sinh \alpha x) + B_2(\cosh \alpha H - \cosh \alpha x)\}$$
$$+ \frac{\beta^2}{\alpha^2}(H-x)\left\{\frac{1}{2}p(H-x) + \frac{\omega}{6}\left[2H^2 - HX - x^2 - \frac{6}{\alpha^2}\right] + Q\right\} \qquad (7.22.2)$$

The axial force in the wall at foundation level is:

$$T_0 = \frac{1}{\alpha}[B_1 \sinh \alpha H + B_2(\cosh \alpha H - 1)]$$
$$+ \frac{\beta^2}{\alpha^2}\left[p\frac{H^2}{2} + \frac{\omega}{2H}\left(\frac{2}{3}H^3 - \frac{2H}{\alpha^2}\right) + QH\right] \qquad (7.22.3)$$

At the upper free end, the upper boundary conditions are:

$$\text{At } x = H, \quad \frac{dq}{dx} = 0 \qquad (7.23)$$

Two different forms of structure-foundation interaction will be considered.

7.3.1 Elastic Vertical Movement

The relative displacement γ at the base, Fig. (7.2.9) may be expressed as:

$$\gamma = K_\gamma T_0 \tag{7.24}$$

At any height x, the compatibility equation may be shown to be:

$$\ell \frac{dv}{dx} - \frac{qb^3h}{12EI_b} - \frac{1}{E}\left(\frac{1}{A_1} + \frac{1}{A_2}\right)_0 \int^x_\eta \int^H q(\lambda)\, d\lambda d\eta - \delta = 0 \tag{7.25}$$

where the four terms represents, respectively, the relative displacements due to the slopes of the walls, the deflections of the connecting beams, the vertical displacements due to axial deformations of the walls, and the relative vertical movement at the foundation.

From Eq. (7.25) since the slope is zero at the base, and the third term vanishes at x = 0, the lower boundary condition becomes

$$\text{At } x = 0,\ q = - K_v T_0 \tag{7.26.1}$$

where

$$K_v = \frac{12EI_b}{b^3h} \,.\, K_\gamma = \frac{EI}{\ell}\beta^2 K_\gamma \tag{7.26.2}$$

Substitution of Eq. (7.22.3), (7.26.1) and (7.23) into Eq. (7.21) yields the integration constants, a correction of Coull's expression,

$$B_1 = -\frac{1}{\Delta_1}\frac{\beta^2}{\alpha^2}\{[pH + \frac{\omega}{2H}(H^2 - \frac{2}{\alpha^2}) + Q] + K_v[\frac{p+\omega}{\alpha^2 \cosh\alpha H}(\cosh\alpha H - 1)$$

$$+ p\frac{H^2}{2} + \frac{\omega}{2H}(\frac{2}{3}H^3 - \frac{2H}{\alpha^2}) + QH]\} \qquad (7.27.1)$$

$$B_2 = \frac{\beta^2}{\alpha^3}\frac{p+\omega}{\cosh\alpha H} - B_1 \tanh \alpha H$$

where

$$\Delta_1 = 1 + \frac{K_v}{\alpha}\tanh \alpha H$$

7.3.2 Elastic Rotational Movement

The moment-rotation relationship may be expressed as:

$$\frac{dv}{dx} = \theta = K_\theta M_0 \qquad (7.28)$$

The bending moment at the base of wall 1 is given by:

$$M_{10} = \frac{I_1}{I}(\overline{M} - T_0 \ell) \qquad (7.29.1)$$

where $\overline{M}$ is the static moment at foundation level, given by:

$$\overline{M} = \frac{1}{2}pH^2 + \frac{1}{3}\omega H^2 + QH \qquad (7.29.2)$$

The relative displacement at the base is equal to $\ell\theta$, and thus the lower boundary conditions become, using Eq. (7.25), a correction of Coull's expression,

$$\text{At } x = 0,\ q = K_r(\overline{M} - T_0\ell) \qquad (7.30)$$

where

$$K_r = \frac{12EI_b}{b^3h}\ell\ \frac{I_1}{I}K_{\theta_1}$$

Substituion of Eq. (7.30), (7.29.2), (7.23) and (7.22.3) into Eq. (7.21) yields the integration constants, a correction of Coull's expression,

$$B_1 = \frac{1}{\Delta_2}\{K_r \bar{M} - \frac{\beta^2}{\alpha^2}[pH + \frac{\omega}{2H}(H^2 - \frac{2}{\alpha^2}) + Q]$$

$$- K_r \ell \frac{\beta^2}{\alpha^2}[\frac{p + \omega}{\alpha^2 \cosh \alpha H}(\cosh \alpha H - 1) + \frac{pH^2}{2} + \frac{\omega}{2H}$$

$$(\frac{2H^3}{3} - \frac{2H}{\alpha^2}) + QH]\}$$

$$B_2 = \frac{\beta^2}{\alpha^3} \frac{p + \omega}{\cosh \alpha H} - B_1 \tanh \alpha H \qquad (7.31)$$

where

$$\Delta_2 = 1 + \frac{K_r \ell}{\alpha} \tanh \alpha H$$

7.3.3 Elastic Vertical and Rotational Movement

If elastic vertical movement and elastic rotational movement occurs simultaneously, the lower boundary conditions become:

$$\text{At } x = 0,\ q = - K_V T_0 + K_r (\bar{M} - T_0 \ell) \qquad (7.32)$$

Substitution of Eq. (7.22.3), (7.32) and (7.23) into Eq. (7.21) yields the integration constants:

$$B_1 = \frac{1}{\Delta}\{K_r \bar{M} - \frac{\beta^2}{\alpha^2}[pH + \frac{\omega}{2H}(H^2 - \frac{2}{\alpha^2}) + Q]$$

$$- (K_V + K_r \ell) \frac{\beta^2}{\alpha^2}[\frac{p + \omega}{\alpha^2 \cosh \alpha H}(\cosh \alpha H - 1) + \frac{pH^2}{2}$$

$$+ \frac{\omega}{2H}(\frac{2H^3}{3} - \frac{2H}{\alpha^2}) + QH]\} \qquad (7.33)$$

$$B_2 = \frac{\beta^2}{\alpha^3} \frac{p + \omega}{\cosh \alpha H} - B_1 \tanh \alpha H$$

where

$$\Delta = 1 + \frac{K_V}{\alpha} \tanh \alpha H + \frac{K_r \ell}{\alpha} \tanh \alpha H$$

Once the integration constants have been determined, the distribution of forces and displacements throughout the structure may be determined.

The axial forces T at height x can be determined from Eq. (7.22.2)

The bending moments in the walls become:

$$M_1 = \frac{I_1}{I}\{\frac{1}{2}p(H-x)^2 + \frac{1}{6}\frac{\omega}{H}(H-x)^2(2H+x) + p(H-x) - T\ell\}$$

$$M_2 = \frac{I_2}{I}\{\frac{1}{2}p(H-x)^2 + \frac{1}{6}\frac{\omega}{H}(H-x)^2(2H+x) + p(H-x) - T\ell\} \quad (7.34)$$

On integrating Eq. (7.25) and putting in the boundary conditions at the base, the deflection becomes:

$$v = \frac{1}{EI}[(1 - \frac{\ell\beta^2}{\alpha^2})\{\frac{1}{24}p(6H^2x^2 - 4Hx^3 + x^4) + \frac{1}{120}\frac{\omega}{H}(20H^3x^2 - 10H^2x^3 + x^5) + \frac{1}{6}Q(3Hx^2 - x^3)\} + \frac{1}{6}\ell\frac{\beta^2}{\alpha^4}\frac{\omega}{H}(3Hx^2 - x^3) - \frac{\ell}{\alpha}B_1(\frac{x^2}{2}\sinh\alpha H - \frac{1}{\alpha^2}\sinh\alpha H + \frac{1}{\alpha}x) - \frac{\ell}{\alpha}B_2(\frac{x^2}{2}\cosh\alpha H - \frac{1}{\alpha^2}\cosh\alpha x + \frac{1}{\alpha^2})] + \theta x \quad (7.35)$$

The last term θx represents the deflections at any level due to the rotation θ of the foundation, where θ is defined as:

$$\theta = K_{\theta_1}\frac{I_1}{I}(\bar{M} - T_0\ell) \quad (7.36)$$

The maximum deflection at the top of the structure becomes, at x = H:

$$v_{MAX} = \frac{1}{EI}\left[\left(1 - \ell\frac{\beta^2}{\alpha^2}\right)\left\{\frac{1}{8}pH^4 + \frac{11}{120}\omega H^5 + \frac{1}{3}QH^3\right\}\right.$$

$$+ \frac{1}{3}\ell\frac{\beta^2}{\alpha^4}\omega H^2 - \frac{\ell}{\alpha}\left(\frac{H^2}{2} - \frac{1}{\alpha^2}\right)(B_1 \sinh \alpha H + B_2 \cosh \alpha H)$$

$$\left. - \frac{\ell}{\alpha^2}\left(B_1 H + \frac{B_2}{\alpha}\right)\right] + \theta H \qquad (7.37)$$

Figs. (7.7), (7.8) and (7.9) and Tables (7.2) and (7.3) show the insluence of vertical and rotational stiffness on deflection at the top, bending moments and axial forces in the piers at the base of the coupled shear wall, using the properties of the example employed by Coull (13).

TABLE (7.2)

INFLUENCE OF VERTICAL STIFFNESS ON AXIAL FORCES AND BENDING MOMENTS AT BASE, AND DEFLECTION AT TOP

K_v, ft^{-1}	K_γ, $ft/lb \times 10^{-9}$	T_0, $lb \times 10^3$	M_{10}, $ft\text{-}lb \times 10^4$	M_{20}, $ft\text{-}lb \times 10^4$	v_{max} $ft \times 10^{-2}$	γ $in. \times 10^{-2}$
0	0	349	176	595	1.984	0
0.01	4.39	272	232	785	2.473	14.4
0.02	8.78	223	268	906	2.786	23.5
0.04	17.57	164	312	1052	3.163	34.6

TABLE (7.3)

INFLUENCE OF ROTATIONAL STIFFNESS ON AXIAL FORCES AND BENDING MOMENTS AT BASE, AND DEFLECTION AT TOP

K_v	$K_{\theta 1}$ radians/ $ft\text{-}lb \times 10^{-12}$	T_0, $lb \times 10^3$	M_{10}, $ft\text{-}lb \times 10^4$	M_{20}, $ft \times lb \times 10^4$	v_{max}, $ft \times 10^{-2}$	θ, $deg. \times 10^{-3}$
0	0	349.2	176.1	594.8	1.984	0
2×10^{-6}	0.121	349.6	175.8	593.8	1.986	.012
2×10^{-5}	1.210	353.4	173.0	584.3	1.997	.120
7×10^{-5}	4.22	363.5	165.6	559.5	2.029	.401
2×10^{-4}	12.10	386.0	149.2	503.8	2.098	1.034

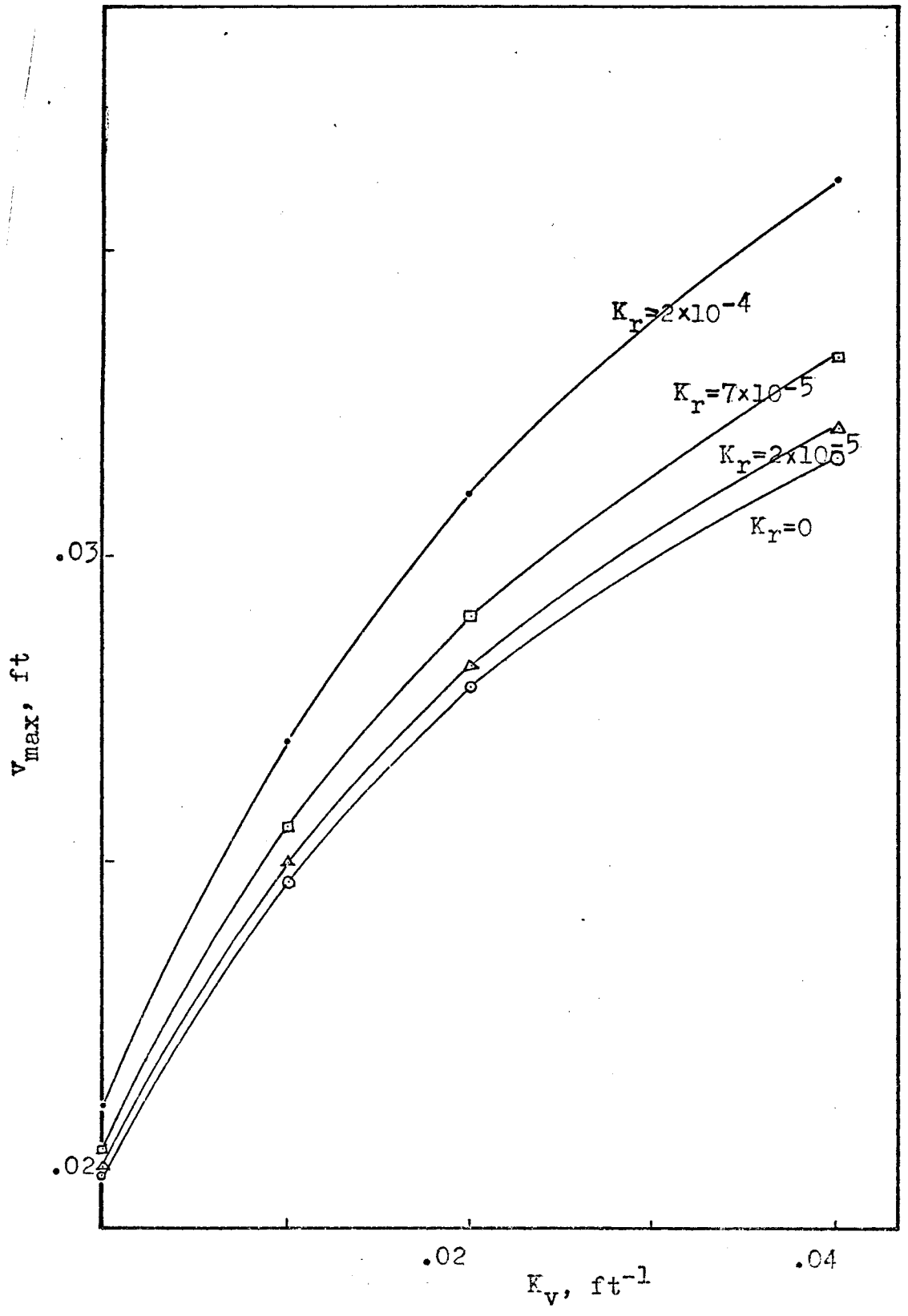

FIG. 7.7 INFLUENCE OF VERTICAL AND ROTATIONAL STIFFNESS ON DEFLECTION AT TOP

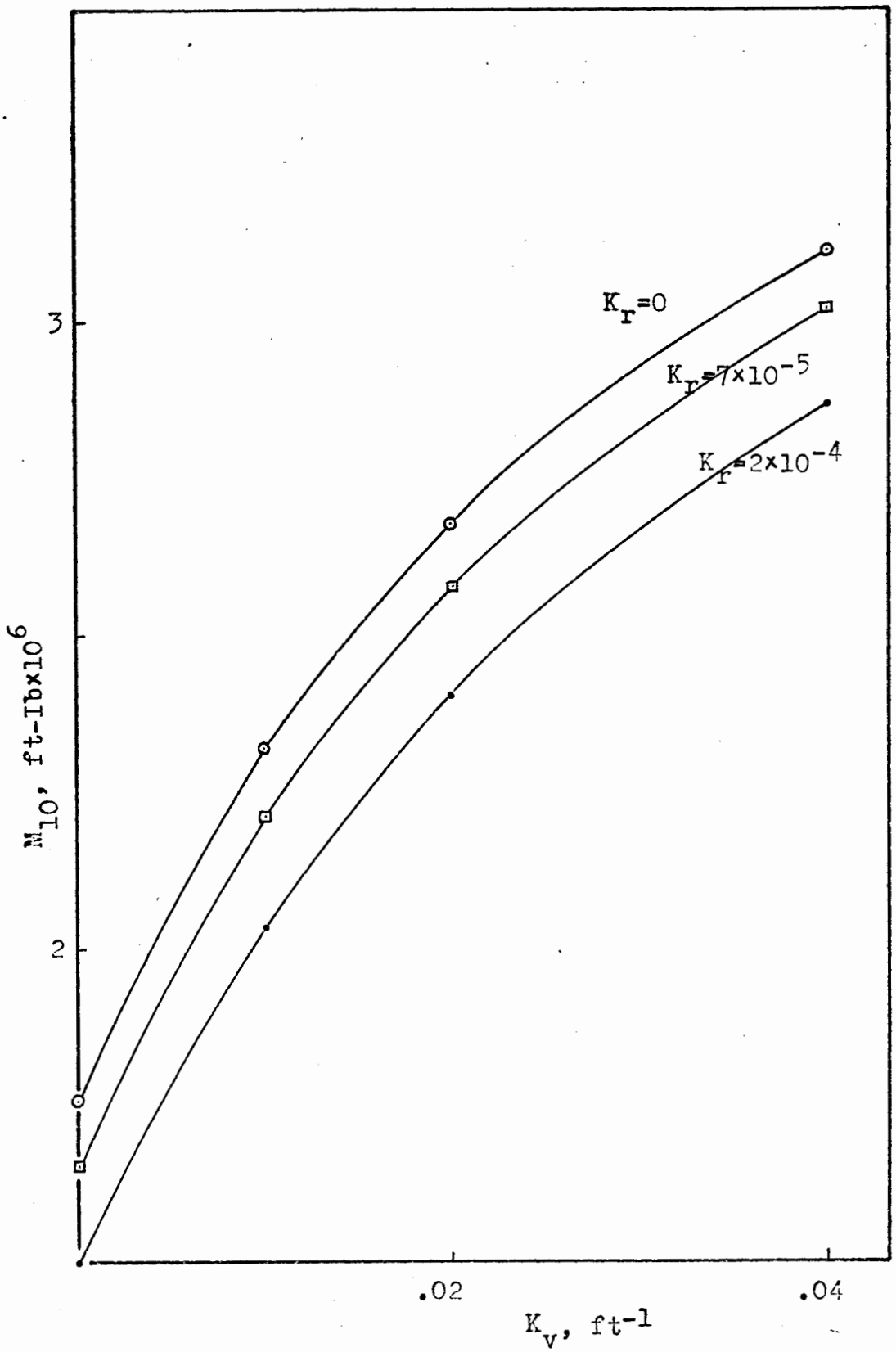

FIG. 7.8 INFLUENCE OF VERTICAL AND ROTATIONAL STIFFNESS ON BENDING MOMENTS AT BASE.

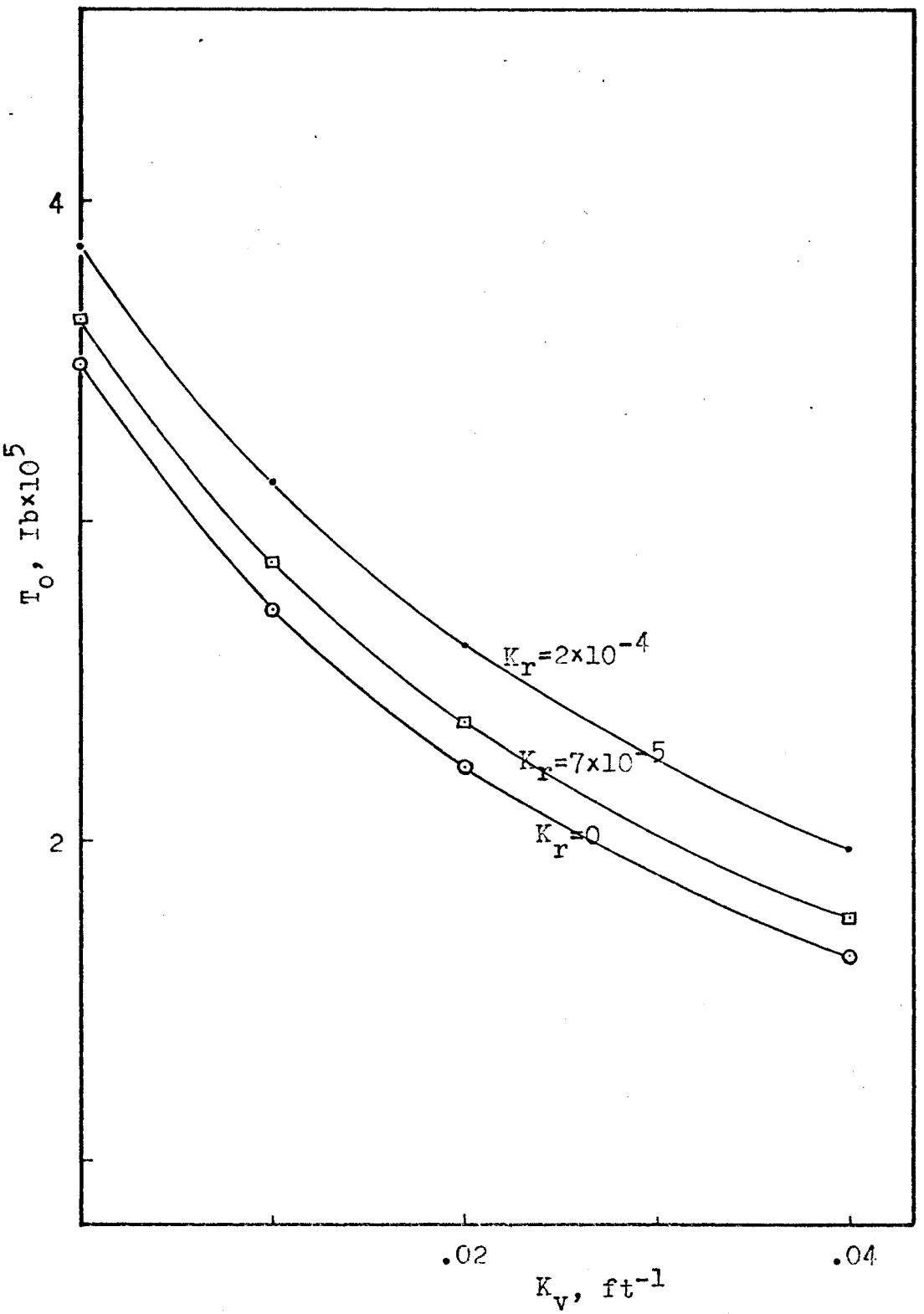

FIG. 7.9 INFLUENCE OF VERTICAL AND ROTATIONAL STIFFNESS ON AXIAL FORCES AT BASE.

CHAPTER 8

SUMMARY

8.1 Conclusions

A static analysis of Coupled Shear Walls with constant cross-section or with variable cross-section with abrupt change in cross-section at one or several levels was presented. The Coupled shear walls may be built into a rigid foundation or supported on elastic foundations, with elastic or inelastic connecting beams.

The following conclusions are made on this work:

1. A simple method for analysing coupled shear walls, the finite difference method, treats the coupled shear walls as two piers connected together by a system of discrete connecting beams. This method, over the continuous connection method, can treat coupled shear walls where the storey height, the properties of the piers and the stiffness of the connecting beams may be varied over the entire height of the building. It can treat a coupled shear wall with an abrupt change in cross-section at one or several levels and with it resting on rigid or elastic foundations, in a more convenient form and with fewer mathematical expressions than the continuous connection method. The finite difference method can treat

actual coupled shear walls of reinforced concrete as far as it can take into account different properties of the piers and the connecting beams at different horizontal levels.

Small capacity computers can be used to get the solution of the coupled shear walls using the finite difference method.

2. Whatever the type of connection at the top of the coupled shear wall, the internal forces in the lower parts of the wall, which usually become critical in design, are not affected.

3. A continuous solution of coupled shear walls with variable cross-section was achieved using the principles of the minimum of the total potential. The continuous connection solution was verified using the finite element method assuming the problem as a plane stress boundary value problem.

4. To illustrate the advantage of the finite difference method, a coupled shear wall with high bottom storey, which was solved before using the finite element method as a plane stress boundary value problem, is analysed. The agreement between the forces and deformations obtained by the two methods was good.

5. For moderate height coupled shear walls, the agreement between the forces and deformations obtained by the finite difference method as well as the continuous connection method and the finite element method starts for interaction coefficients $\alpha H > 8.0$ for $H/d = 8.5$ and $\alpha H > 12.0$ for $H/d = 12.0$. For smaller interaction coefficients, the two methods give

larger forces and defection in comparison with the finite element method.

6. The coupled shear wall behaves as a homogeneous cantilever when the interaction coefficient $\alpha H > 14.0$, corresponding to a value $1/c > 20.0$ for composite beams.

7. The coupled shear walls behave as two separate cantilevers under the applied load when the interaction coefficient $\alpha H < 0.5$.

8. An approximate analysis of multi-pierced coupled shear wall, assuming that the cross-beams deflect with a point of contraflexure at mid-span, was achieved. The finite difference solution for the problem was presented. It can take into account any configuration of the multi-pierced coupled shear wall.

9. For coupled shear walls with elastic foundations, as the vertical stiffness, K_γ, increases, the deflection of the model and the internal moments in the piers increase, while the axial forces in the piers decrease. As the rotational stiffness, K_θ, increases, the deflection of the model and the axial forces in the piers increase, while the internal moments in the piers decrease.

The vertical movement of the foundation is more significant than the rotational movement of the foundation, both for stress and deflection considerations of the structure.

8.2 Suggestions for Further Work

The concept of analysing the inelastic behaviour of composite beams may be used to analyse the inelastic behaviour of coupled shear walls. For a reinforced concrete shear wall the actual properties of the piers and the connecting beams at different horizontal levels, the tension allowed in concrete and the gravity load at different horizontal levels may be taken into account.